

## Efectis Nederland report

### 2008-Efectis-R0425

# Effects of water mist on real large tunnel fires: Experimental determination of BLEVE-risk and tenability during growth and suppression

Efectis Nederland BV  
Centre for Fire Safety  
Lange Kleiweg 5  
Postbus 1090  
2280 CB Rijswijk

[www.efectis.nl](http://www.efectis.nl)

T 015 276 34 80

F 015 276 30 25

E [nederland@efectis.com](mailto:nederland@efectis.com)



Date June 2008

Author(s) Ir. A.D. Lemaire  
Ir. V.J.A. Meeussen

Number of pages 55  
Number of appendices 3

Sponsor	TNO Bouw en Ondergrond	Bouwdienst Rijkswaterstaat
	P.O. Box 49 2600 AA DELFT	P.O. Box 20000 3502 LA UTRECHT

Project name Meting van BLEVE en leefbaarheid  
Project number 2007461

All rights reserved.

No part of this publications may be reproduced and/or published by print, photoprint, microfilm or any others means without the previous written consent of Efectis.

In case this report was drafted on instructions, the rights and obligations of contracting parties are subject to either the Standard Conditions for Research Instructions given to TNO, or the relevant agreement concluded between the contracting parties. Submitting the report for inspection to parties who have a direct interest is permitted.

© 2008 Efectis Nederland BV: a TNO company

This report is issued by Efectis Nederland BV (previously TNO Centre for Fire Research). Efectis Nederland BV and her sister company Efectis France are full subsidiaries of Efectis Holding SAS since 1 January 2008, in which the Dutch TNO and the French CTICM participate. The activities of the TNO Centre for Fire Research were privatized in Efectis Nederland BV since 1<sup>st</sup> July 2006. This is in response to international developments and requests by customers. In order to be able to give a better answer to the customer's request and offer a more comprehensive service of high quality and a wider range of facilities, the international collaboration has been further expanded. This is done with highly experienced partners in fire safety in Norway (Sintef-NBL), Spain (Afiti-Licof), Germany (IFT), USA (South West Research Institute) and China (TFRI). Further information can be found on our website.

# Contents

<b>1</b>	<b>Introduction .....</b>	<b>4</b>
<b>2</b>	<b>Background of the BLEVE- and tenability tests .....</b>	<b>5</b>
2.1	Principles of the test-methods .....	5
2.1.1	Principle of Bleve Tests .....	5
2.1.2	Principle of tenability tests .....	5
2.2	Location, description and geometry of the test-tunnel .....	5
2.3	Location of the Efectis instrumentation .....	6
2.3.1	The coordinate reference system .....	6
2.3.2	The time reference system.....	6
2.3.3	Tenability measurements.....	6
2.4	Location of fire load and location of the water mist system.....	7
2.5	Description of the five test-scenarios .....	9
2.5.1	Overview of tests.....	9
<b>3</b>	<b>The BLEVE-tests.....</b>	<b>10</b>
3.1	Assessment method and data required.....	10
3.2	Measurement system and instrumentation .....	11
3.2.1	The test tank .....	11
3.2.2	Sensors .....	12
3.2.3	Layout of sensors.....	13
3.2.4	Data acquisition system.....	15
3.3	Presentation and discussion of test results.....	16
3.3.1	Presentation of all measured data .....	16
3.3.2	Discussion: measured temperatures around the tank.....	22
3.3.3	Discussion: measured temperatures of the tank wall.....	23
3.3.4	Discussion: measured heat fluxes.....	23
3.4	Assessment of BLEVE risk from test results .....	24
3.5	Conclusion.....	24
<b>4</b>	<b>The tenability-tests .....</b>	<b>25</b>
4.1	The criteria for tenability.....	25
4.2	The measurement-system and instrumentation .....	25
4.2.1	Three main types of measurements were performed during the tests: .....	25
4.2.2	Location of the sensors.....	26
4.2.3	Modification of the system during the tests.....	27
4.3	Test results of verification test 1 on 13-12-2007, a 50 MW solid fire.....	28
4.3.1	Location: 20 m downstream .....	28
4.3.2	Location: 40 and 50 m downstream .....	29
4.3.3	Location: 100 m downstream .....	30
4.3.4	Location: 300 m downstream .....	31
4.4	Test results of verification test 2 on 19 December 2007, a 100 m <sup>2</sup> pool fire .....	32
4.4.1	Location: 20 m downstream.....	32
4.4.2	Location: 40 m and 50 m downstream .....	33
4.4.3	Location: 100 m downstream .....	34
4.4.4	Location: 300m downstream .....	35
4.5	Test results of Performance test 1 on 9 January 2008, a 100 m <sup>2</sup> pool fire .....	36
4.5.1	Location: 20 m downstream .....	36
4.5.2	Location: 40 m and 50 m downstream .....	36

4.5.3	Location: 100 m downstream .....	37
4.5.4	Location: 300 m downstream .....	38
4.6	Test results of performance test 2 on 14 January 2008, a 100 m <sup>2</sup> pool fire.....	39
4.6.1	Location: 20 m downstream .....	39
4.6.2	Location: 40 and 50 m downstream .....	39
4.6.3	Location: 100 m downstream .....	40
4.6.4	Location: 300 m downstream .....	41
4.7	Test results of Performance test 3 on 17 January 2008, a 200 MW solid fire.....	42
4.7.1	Location: 20 m downstream .....	42
4.7.2	Location: 40 m and 50 m downstream .....	42
4.7.3	Location: 100 m downstream .....	43
4.7.4	Location: 300 m downstream .....	44
4.8	Discussion of the test results .....	45
4.8.1	The test environment and assessment of data.....	45
4.9	Preliminary evaluation of tenability-data .....	45
4.9.1	Background: .....	45
4.9.2	Evaluation method.....	45
4.9.3	Evaluation of verification test 1 .....	47
4.9.4	Evaluation of verification test 2 .....	48
4.9.5	Evaluation of performance test 1 .....	49
4.9.6	Evaluation of performance test 2.....	50
4.9.7	Evaluation of performance test 3.....	51
4.10	Conclusions .....	52
4.11	Recommendations .....	52
<b>5</b>	<b>References .....</b>	<b>54</b>
<b>6</b>	<b>Acknowledgements.....</b>	<b>55</b>
<b>Appendices</b>		
A Technical information measurement equipment		
B Presentation of measured data on the test tank		
C Indicative measurement of vision distance in “cold” test		

# 1 Introduction

Large scale tunnel fire tests were carried out in December 2007 and January 2008 in the Runehamar Tunnel in Andalsnes, Norway. The fire scenarios used consisted of pool fires and solid fuel fires each with a nominal rate of heat release of up to 200 MW. The prime objective of these tests was to determine the suppression and extinguishing effect of a water mist system on fully developed fires. The tests were carried out by SINTEF NBL and Aquasys upon request of Rijkswaterstaat, the department within the Ministry of Public Works of The Netherlands that is also responsible for tunnel safety. The system was intended to be similar to the design that is being installed in the Dutch Roer- and Swalmen tunnels in The Netherlands.

Rijkswaterstaat decided in July 2007 that these tests should also serve as a unique opportunity to obtain experimental data on the risk of a BLEVE in the area immediately downwind of the fire, and also to perform measurements on the tenability conditions along the first few hundreds of meters downwind of the fire.

Accordingly, Efectis in combination with TNO were asked to submit designs of suitable measuring methods and to carry out the necessary measurements during the fire tests.

In December 2007 and January 2008 five tests were carried out, using both solid fire loads and fire pools. The largest solid fire load consisted of 720 pallets, configured to represent a loaded heavy goods vehicle. The fire pool consisted of diesel fuel and had a surface area of 100 m<sup>2</sup>. The fire loads were designed to be similar to the ones used in previous tests for Rijkswaterstaat in 2005, and (for the solid fire load) to one of the UPTUN-tests in 2003.

This report focuses exclusively on the BLEVE-risk and on the tenability conditions. It does not deal with the effectiveness of the extinguishing system. It gives an overview of the data that were collected in a systematic way, and it gives some conclusions. We thank NBL and Aquasys for the use of some of their data.

The report is structured to give in chapter two, the background common to both the BLEVE- tests and the tenability-tests, such as the general test objectives, the test location, tunnel description, geometry, the location of fire load and the location of the water mist system.

Chapter three describes the BLEVE-measurements in terms of the predictive model used, the required experimental data, the measurement system and the experimental results that were obtained.

In chapter four, the tenability-measurements are described in terms of the required experimental data, the measurement system and the experimental results that were obtained.

## 2 Background of the BLEVE- and tenability tests

### 2.1 Principles of the test-methods

#### 2.1.1 Principle of Bleve Tests

The principle of the BLEVE-test was to actually measure the thermal behaviour of a water filled LPG tank near the fire and to predict the risk of a BLEVE from this thermal behaviour. The use of a full-size LPG-tank as test-object would ensure that the flow of air and water mist around the tank, the absorption of radiation, the condensation of water vapour on the outer surface and even the run-off of water from the surface should conform to reality as closely as possible.

The measurements were targeted to predict the BLEVE risk for a reference tank filled with LPG for 10% of its maximum capacity. According to an extensive simulation study this filling percentage will give the highest risk of a BLEVE. See Ref [1] and [2]. The test tank was filled with water for 5% of its volume to achieve the best similarity with the thermodynamic behaviour of LPG. This described in Ref [4]. The test tank was equipped with extensive instrumentation to measure wall temperatures, inside and outside air temperatures as well as heat fluxes from the environment through the tank wall into the water.

#### 2.1.2 Principle of tenability tests

The tenability-tests consisted of measuring temperatures and CO-concentrations as prime indicators. In addition, visibility was measured as well, because this factor may influence the time during which occupants can be exposed to the primary threats.

### 2.2 Location, description and geometry of the test-tunnel

All tests described were done in the Runehamar tunnel near Andalsnes in Norway. The location of the test site and entrance to the tunnel are shown in Figure 2.1. The overall layout and cross section of the tunnel with main dimensions are shown in Figure 2.2 and Figure 2.3.

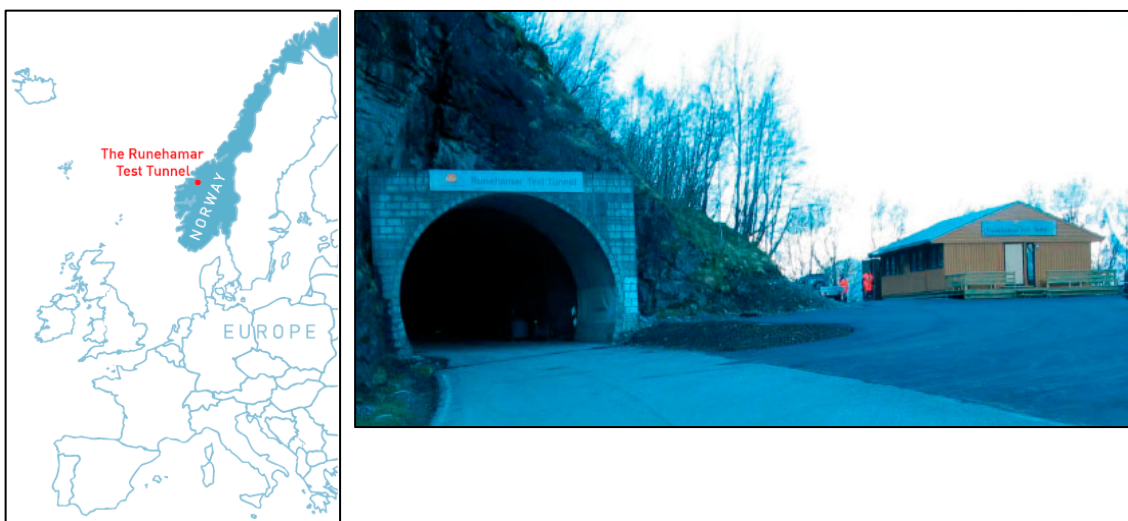


Figure 2.1 Location of test-site, and entrance of the tunnel.

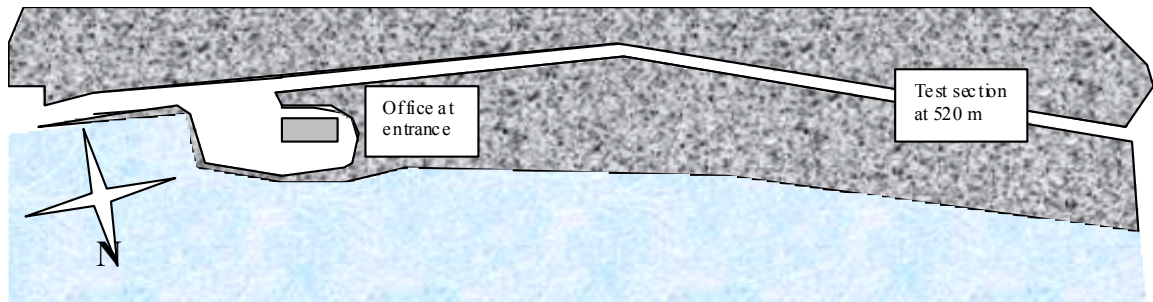


Figure 2.2. Overall lay-out. The total length of the tunnel is 1650 m.

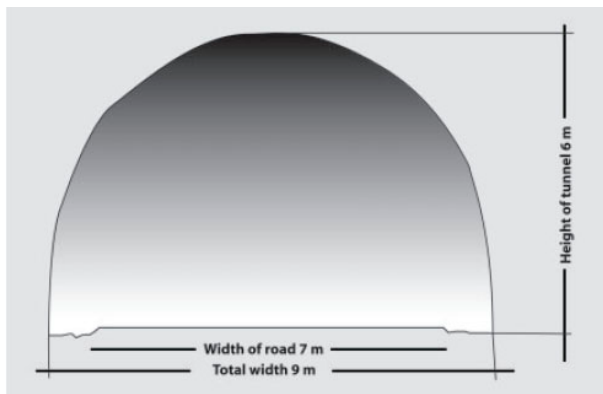


Figure 2.3 Cross-section of the tunnel

## 2.3 Location of the Efectis instrumentation

### 2.3.1 *The coordinate reference system*

A common reference system was agreed by all parties prior to the tests. In this reference system, in the tunnel, the downwind (i.e. the western) face of the fire load is set at 0 meters, and all positions downwind have a positive coordinate. Note: the ventilation direction in all drawings is from left to right (from east to west), and the tunnel entrance is always on the left hand (western) side.

The reference coordinates are illustrated in Figure 2.4 and Figure 2.5: the test-tank is positioned between + 6 m and +12 m. For any position across the tunnel, the North edge of the hard road surface was set at 0 m, this coordinate increasing to about 8 m on the South edge of the hard road surface. The exact location and orientation of the test-tank is illustrated in Figure 2.5.

### 2.3.2 *The time reference system*

All participants in the project have used Central European Time (CET) to synchronize their datalogging and imaging systems. Actions such as ignition and activating the water mist system were timed using CET.

### 2.3.3 *Tenability measurements*

In order to evaluate tenability conditions, measurements of temperature, relative humidity, CO-concentration and vision distance were carried out at 4 locations shown in the Figure 2.4 .

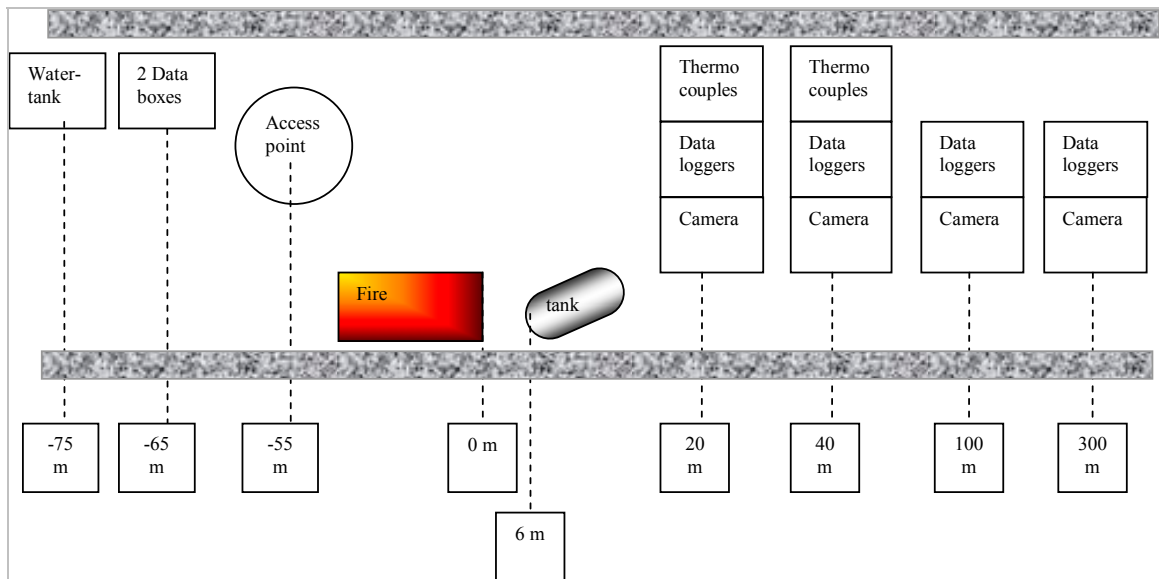


Figure 2.4. Main components of the Efectis network in the tunnel. Coordinates refer to the position along the length of the tunnel. The water tank provided cooling water through a 100 m long duct to the radiation sensors mounted on the tank. The data boxes contained a PC and two dataloggers each. Thermo-couple signals from the tank and from the positions at 20 m and 40 m travelled through underground cables to the data boxes. There they were digitized and logged, and transmitted by Ethernet to the access point. From there they were transmitted to the main building by glass fibre connection.

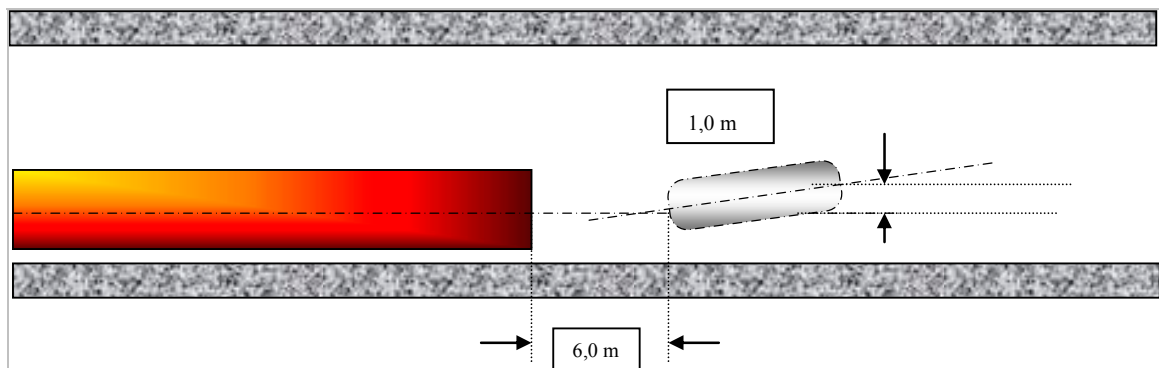


Figure 2.5. Location of the test-tank in relation to the fire load. Note: the figure shows the solid fire load on the right lane. The liquid fire load (diesel pool) was positioned in the middle of the tunnel, i.e. on both lanes.

## 2.4 Location of fire load and location of the water mist system

The fire loads were positioned within the section of the tunnel that is protected with a heat-resistant lining. This section is about 100 m long, and centred at 520 m from the tunnel entrance. The edge of the fire load was always positioned at 0 m, i.e. the closest distance to the tank was always 6 m. The solid fuel fire load (180 or 720 stacked pallets, simulating a truckload) was situated between +0.5 m and +2.5 m across the tunnel. The 100 m<sup>2</sup> diesel pool was situated in the middle of the tunnel and was 25 m long and 4 m wide.

The water mist-system consisted of three sections as shown. Together the sections are 75m long and run from - 50 m to + 25 m.

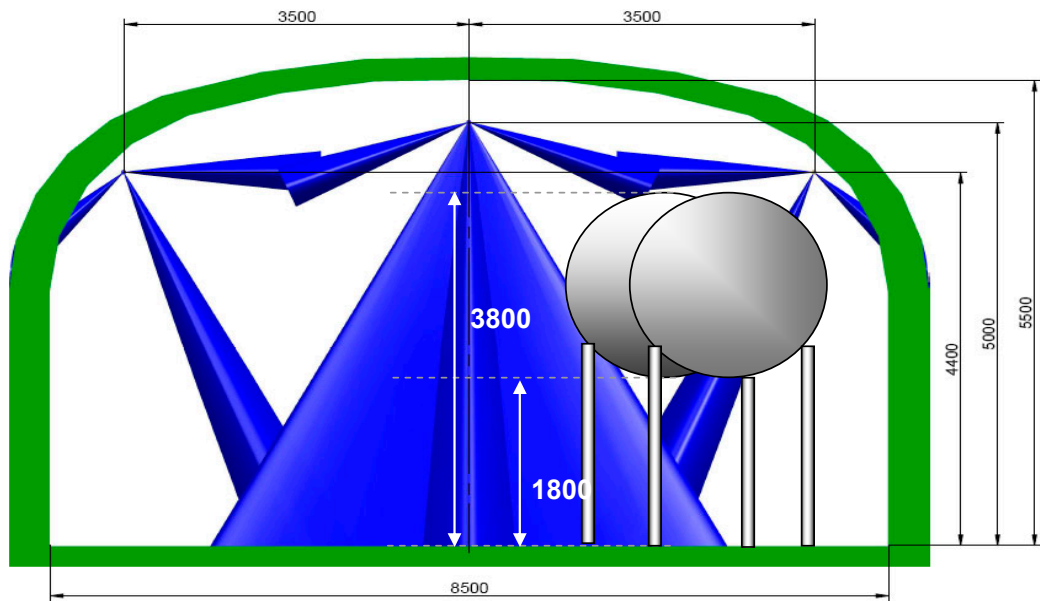
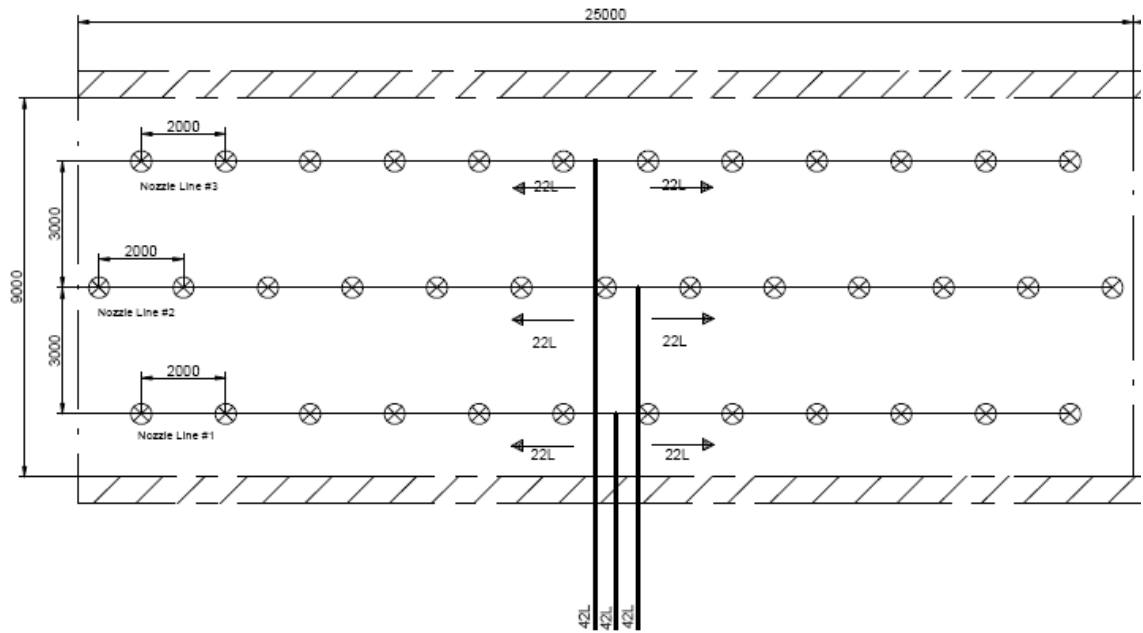


Figure 2.6. One of the three sections of the water mist-system in top view. Together, the sections are 75 m long, and run from - 50 m to + 25 m. Bottom: a cross-section of the tunnel showing the location of the nozzles and the intended spray pattern and the approximate position of the tank.



## 2.5 Description of the five test-scenarios

### 2.5.1 Overview of tests

Eight full-scale tests of fire suppression with the water mist system were performed by SINTEF NBL. The BLEVE-risk and tenability measurements presented in this report were performed by Efectis NL in the latter five of these full-scale tests. The BLEVE simulation tank and measurement equipment were installed after the third full-scale test.

The main characteristics of the five tests are given in Table 2.1

Table 2.1 Main characteristics of the latter five fire tests with BLEVE-risk and tenability measurements

IDENTIFICATION OF TEST			SCENARIO		
Nr and date 1)	Full name	Abbreviation	Fire load	Additives	Nominal HRR <sup>2)</sup>
4, 13 dec 2007	Verification Test 1	VerTest1	Solid (180 pallets)	1% AFFF	50 MW
5, 19 dec 2007	Verification Test 2	VerTest2	Pool 100 m <sup>2</sup>	1% AFFF	200 MW
6, 9 jan 2008	Performance Test 1	PerTest1	Pool 100 m <sup>2</sup>	No additives	200 MW
7, 14 jan 2008	Performance Test 2	PerTest2	Pool 100 m <sup>2</sup>	1% Bioversal	200 MW
8, 17 jan 2008	Performance Test 3	PerTest3	Solid (720 pallets)	No additives	200 MW

<sup>1)</sup> According to Ref. [3]

<sup>2)</sup> HRR = Heat Release Rate

The actual conditions during the tests are given in Table 2.2. The tests were carried out in December 2007 and January 2008.

Table 2.2 Actual conditions of the five fire tests with BLEVE-risk and tenability measurements according to Ref. [3].

Test	SCENARIO		ACTUAL CONDITIONS			
	Fire load	Additives	Initial ventilation speed	Activation time of suppression	Aproximate burning period	Max. HRR
			m/s	s (after ignition)	s	MW
VerTest1	Solid (180 p.)	1% AFFF	3.7	335	1140	
VerTest2	Pool <sup>1)</sup> 100 m <sup>2</sup>	1% AFFF	4.0	96	150	
PerTest1	Pool <sup>2)</sup> 100 m <sup>2</sup>	no additives	4.0	125	180 ?	
PerTest2	Pool <sup>1)</sup> 100 m <sup>2</sup>	1% Bioversal	4	160	420	
PerTest3	Solid (720 p.)	no additives	4	439	2100	

<sup>1)</sup> Fuel layer thickness = 40 mm; <sup>2)</sup> Fuel layer thickness = 70 mm

An extensive description of the fire loads and water mist-system, as well as the measured water flows, ventilation conditions and Heat Release Rates during the tests is given in Ref. [3].

## 3 The BLEVE-tests

### 3.1 Assessment method and data required

A method was developed to assess the risk of a “warm” or heat induced BLEVE (as opposed to a “cold” BLEVE caused by mechanical damage) of a reference LPG tank filled with LPG from thermal measurements on a full-size test tank filled with water. The method was based on the models developed by Solico [1], [2] for an extensive simulation study on the risk of a BLEVE due to a rupture of a LPG tanker (filled with LPG) involved in a tunnel fire. A full description and motivation of the method is given in Ref. [4] Hereafter the method is described briefly.

According to the theory the rupture of the tank will depend on the stress in the tank shell and not on the stress in the end caps (= front and rear side) of the tank. The method therefore determines:

- the rise of the actual stress in the shell (wall) of the reference LPG tank due to pressure built up in the tank;
- the decline of the maximum stress that the shell can resist due to the heating up of the shell.

As long as the actual stress remains well below the maximum stress the risk on a BLEVE is considered negligible.

In order to determine the actual and maximum stresses the method requires the temperature distribution of the outside and inside surface of the tank wall and the heat fluxes into the ‘wet’ part (belly) of the tank. These quantities are directly measured on the test tank and considered representative for the reference tank in the same fire environment.

The maximum allowable stress is calculated from the maximum temperature measured on the outside surface of the test tank using the strength properties of the reference tank.

The actual stress is calculated from the dimensions of the reference tank shell and the LPG vapour pressure inside the reference tank. This pressure follows directly from the LPG temperature and the thermo physical properties of the LPG mixture. The LPG temperature is calculated from the heat fluxes towards the LPG liquid coming from the ‘wetted’ and ‘non wetted’<sup>1</sup> parts of the wall of the reference tank.

The heat fluxes from the ‘wetted’ part of the tank (the belly) are directly measured on the test tank. The heat fluxes from the ‘non wetted’ tank wall are calculated from the temperatures measured on the inside surface of the test tank. The determination of the heat fluxes is visualised in Figure 3.1.

---

<sup>1</sup> The ‘wetted’ and ‘non-wetted’ parts of the tank wall are those parts of the wall directly in contact with the liquid respectively vapour phase of the fluid inside the tank.

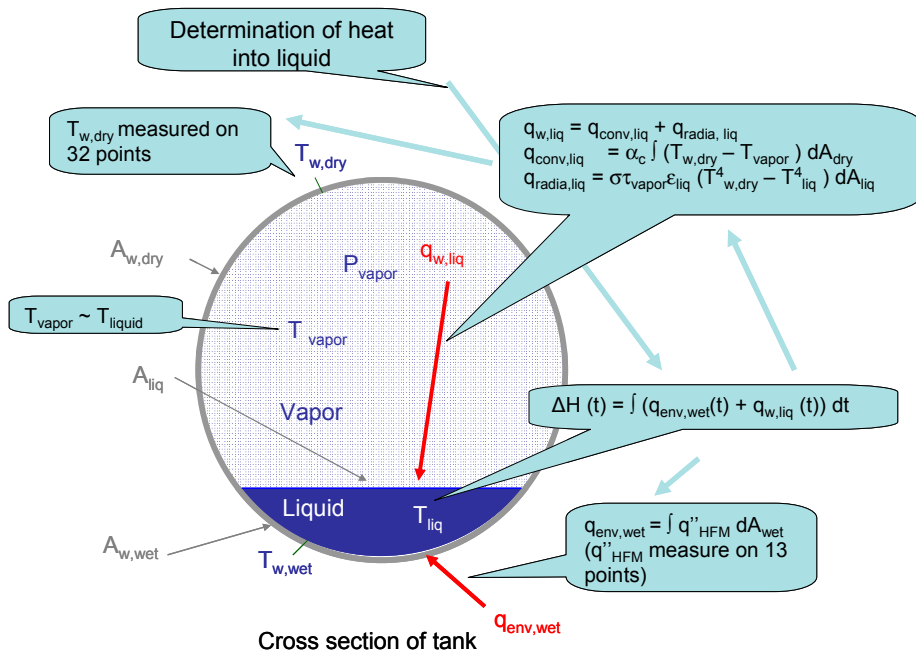


Figure 3.1 Determination of the heat fluxes into the liquid of the tank. Ref. [4].

### 3.2 Measurement system and instrumentation

#### 3.2.1 The test tank

The test tank consisted of a full-size LPG-tank, filled with water for 5% of its volume. The tank is shown in Figure 3.2.

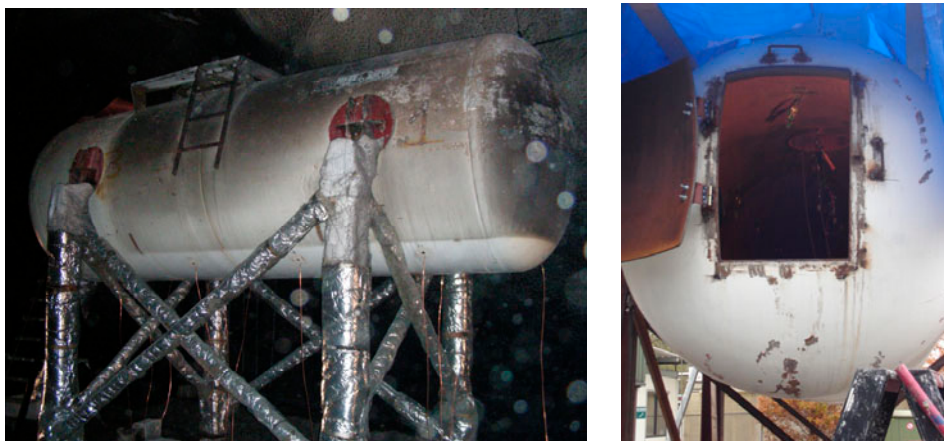


Figure 3.2 The test tank in the tunnel and the access door that was cut in the end wall. The supporting structure was designed and built to ensure that the top side of the test-tank was at 3.8 m above the road surface, similar to the height assumed in the Solico-model. The picture at the left shows the structure wrapped in protection against heat, after the first verification test.

For practical reasons the test-tank (length 6m, diameter 2.2m) was smaller than the reference tank (length 12.0m, diameter 2.5m). The smaller diameter of the test-tank corresponds well with the fact that the test-tunnel has a somewhat smaller cross-section than the reference tunnel. The shorter length of the test-tank will cause a quicker rise in LPG temperature and thus a higher probability of a BLEVE. The wall thickness is 8.8 mm as compared to 10 mm for the reference tank. This will lead to somewhat higher wall temperatures and is an acceptable conservative approach. The thermal properties of the steel are equivalent to those in the reference tank studied in Ref. [1] and [2].

The tank was mounted on a steel construction. The construction itself was fire protected with mineral wool. Special attention was given to the fire protection of the section of the data cables between the test tank and the road surface by using a high internal thermal mass in combination with extensive insulation.

### 3.2.2 Sensors

Heat flux-sensors were installed in holes that were drilled in the lower tank wall. The receiving surface of the sensors was carefully mounted exactly flush with the outer tank wall with a clearance of less than 0.2 mm. The heat-flux sensors were cooled by water supplied from a main hose outside the tank. The main hose was connected to smaller copper tubes inside the tank leading to the heat flux-sensors. The tubes were insulated with mineral wool to prevent heating up of the cooling water. The cooling water was discharged via copper tubes mounted through the ‘belly’ of the tank. See Figure 3.3. Technical information about the heat flux-sensors used is given in Appendix A.

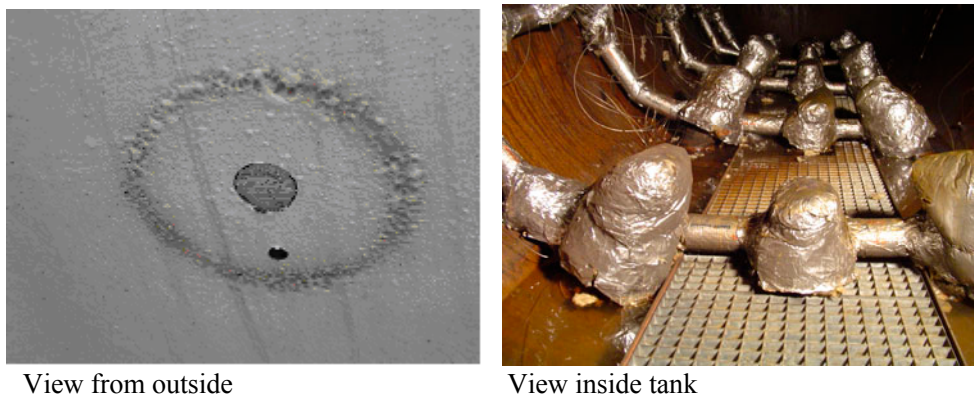


Figure 3.3 Mounting of heat flux-sensor in the tank wall and insulation of the water cooling inside the tank.

The heat flux-sensors measure the heat flux into the ‘wetted’ part of the tank without taking into account the ‘heat resistance’ of the water layer inside the tank. This is closer to the real situation, because the ‘heat resistance’ of the LPG liquid in the reference tank will be less than the ‘heat resistance’ of the water layer in the test tank. The measured heat fluxes will be somewhat higher than in reality. This is an acceptable conservative approach. See also Ref.[4].

Mantle thermocouples with a diameter of 1.5 mm were mounted on the tank wall to measure the inside and outside surface temperatures. They also protruded from the tank wall to measure the outside air temperatures 0.10 m from the tank shell. The thermocouples were connected inside the tank to thermocouple extension wires. The extension wires, the signal wires connected to the heat flux sensors and the hose for the cooling water supply were bundled and led through one fire protected tube at the rear side of the tank. This tube was put in a trench under the tunnel road (near the tunnel wall) and connected to the data-acquisition system in the data boxes at -65 m. (See Figure 2.4).

The instrumentation of the test tank was completed, connected to the data acquisition system and fully tested at the site of Efectis NL. See also Figure 3.4.

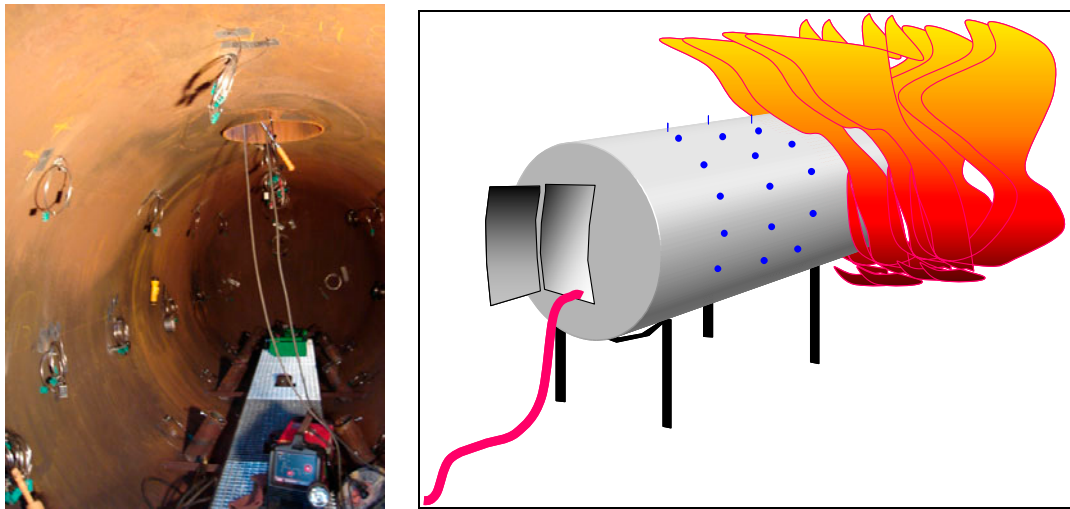


Figure 3.4 Interior of the tank during installation of thermocouples and configuration during a test.



Figure 3.5 The actual test-tank after completing the installation in the Runehamar tunnel

### 3.2.3

#### *Layout of sensors*

The planned lay-out and labeling of the heat flux sensors and thermocouples is shown in Figure 3.6.

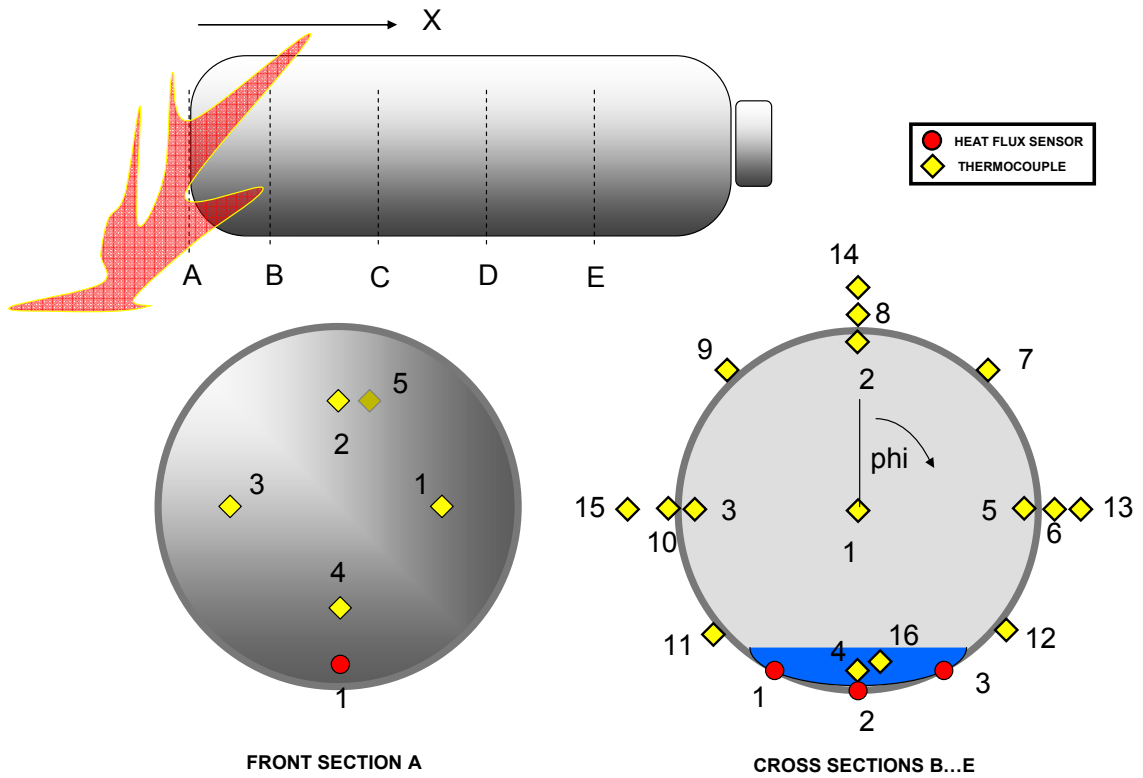


Figure 3.6 Lay out and labelling of heat flux sensors and thermocouples. In this figure the right side of the tank (labels 6, 13 e.g.) is facing the right wall of the tunnel and the left side of the tank (labels 10, 15 e.g.) is facing the middle of the tunnel.

The actual layout of the sensors was slightly different due to the presence of the connections to the mounting frame and the manhole. The actual positions are shown in Table 3.1 in polar coordinates.

Table 3.1 Actual lay out of the sensors in sections B ... E in polar coordinates. Bold printed positions are deviated from the planned positions.

Pos	Type	nr	Section B		Section C		Section D		Section E	
			x <sup>1)</sup> (m)	phi <sup>2)</sup> (deg)	x (m)	phi (deg)	x (m)	phi (deg)	x (m)	phi (deg)
Outside	RAD	1	1.03	-30	2.13	-30	3.30	-30	4.46	-30
Outside	RAD	2	1.03	0	2.13	0	3.30	0	4.46	0
Outside	RAD	3	1.03	30	2.13	30	3.30	30	4.46	30
In-vapour	TK	1	1.03	0	2.13	0	3.30	0	4.46	0
Inside	TK	2	1.03	0	2.13	0	<b>3.12</b>	0	4.46	0
Inside	TK	3	1.03	-90	2.13	-90	3.30	-90	<b>4.08</b>	-90
Inside	TK	4	1.03	180	2.13	180	3.30	180	4.46	180
Inside	TK	5	1.03	90	2.13	90	3.30	90	<b>4.08</b>	90
Outside	TK	6	1.03	90	2.13	90	3.30	90	<b>4.08</b>	90
Outside	TK	7	1.03	45	2.13	45	3.30	45	4.46	45
Outside	TK	8	1.03	0	2.13	0	<b>3.12</b>	0	4.46	0
Outside	TK	9	1.03	-45	2.13	-45	3.30	-45	4.46	-45
Outside	TK	10	1.03	-90	2.13	-90	3.30	-90	<b>4.08</b>	-90
Outside	TK	11	1.03	-135	2.13	-135	3.30	-135	4.46	-135
Outside	TK	12	1.03	135	2.13	135	3.30	135	4.46	135
Outside	TK	13	1.03	90	2.13	90	3.30	90	<b>4.08</b>	90
Env. air	TK	14	1.03	0	2.13	0	<b>3.12</b>	0	4.46	0
Env. air	TK	15	1.03	-90	2.13	-90	3.30	-90	<b>4.08</b>	-90
In-water	TK	16	1.03	180	2.13	180	3.30	180	4.46	180

<sup>1)</sup> x-coordinate along tank axis from front side of tank facing the fire

<sup>2)</sup> phi-coordinate = 0 deg on top of tank and 90 deg on right side of tank facing the tunnel wall.

The sensors were installed in 5 sections A...E.

Section A is the front side of the tank, facing the fire. It consists of 1 heat flux sensor, 4 thermocouples on the outside surface and 1 thermocouple on the inside surface.

Sections B...E are cross-sections of the tank, spaced at about 1.2 m. Each of these sections consists of: 3 heat flux sensors, 3 thermocouples in the outside air temperature, 7 thermocouples on the outside surface, 3 thermocouples on the inside surface, 1 thermocouple in the water vapor inside the tank and 1 thermocouple in the water in side the tank.

The total number of sensors used was:

- 13 heat flux meters in the lower section of the tank
- 12 thermocouples at 10 cm outside the tank wall
- 32 thermocouples on the “non-wetted” wall outside
- 13 thermocouples on the “non-wetted” wall inside
- 4 thermocouples along the tank axis
- 4 thermocouples in liquid (water) at the bottom of the tank.

### 3.2.4 Data acquisition system

The data acquisition system consisted of 2 Agilent HP-3970 data loggers, each placed in one data box. Each data logger was connected to a laptop (also in the box). See also Figure 2.4. All sensors belonging to section A, C, E were connected to one data logger and the remaining sensors to the other data logger. Data loss due to power failure was prevented with a UPS system in the box. The laptops were connected to the glass fiber Ethernet network in the tunnel and controlled via remote desk top

control on 2 laptops (one for each data logger) in the office near the tunnel. A NAS back-up system was connected to the network.

The data was acquired with Agilent VEE software adapted to Efectis NL special needs. The sample interval was 10 s.

Before each test, the connection, proper labeling and proper working of each thermocouple and heat flux sensor were tested by heating each sensor with a lighter and checking the signal on the data-acquisition system.

Technical details about the data-acquisition system are given in Appendix A.

### 3.3 Presentation and discussion of test results

#### 3.3.1 *Presentation of all measured data*

The measured data for all tests are presented in Figure 3.7 till Figure 3.11. Each Figure presents the complete data set of one test. The measured temperatures and heat fluxes are presented in graphs as function of time for the relevant test period. The time = 0s at ignition of the fire.

The upper left graph of each Figure shows the temperatures of the water (halfway height) in the tank.

The remaining graphs present data measured on a specific section per graph. Each row of graphs presents data belonging to the same cross section, starting with section A in the upper row till section E in the lower row. Each column of graphs presents data of one specific type. Starting from left to right the following data are presented: the outside air temperature (measured 10 cm from the tank shell), the outside wall temperature, the inside wall temperature and the heat flux into the 'wetted' tank wall.

In the upper left corner of each graphs a coloured cross section (or face) of the tank is shown with the tunnel wall. The colours of the cross section correspond with the colours of the symbols and lines in the graph. E.g. position B12 (orange) is on the lower right part of the tank.

The same graphs are shown in a larger size in Appendix B.



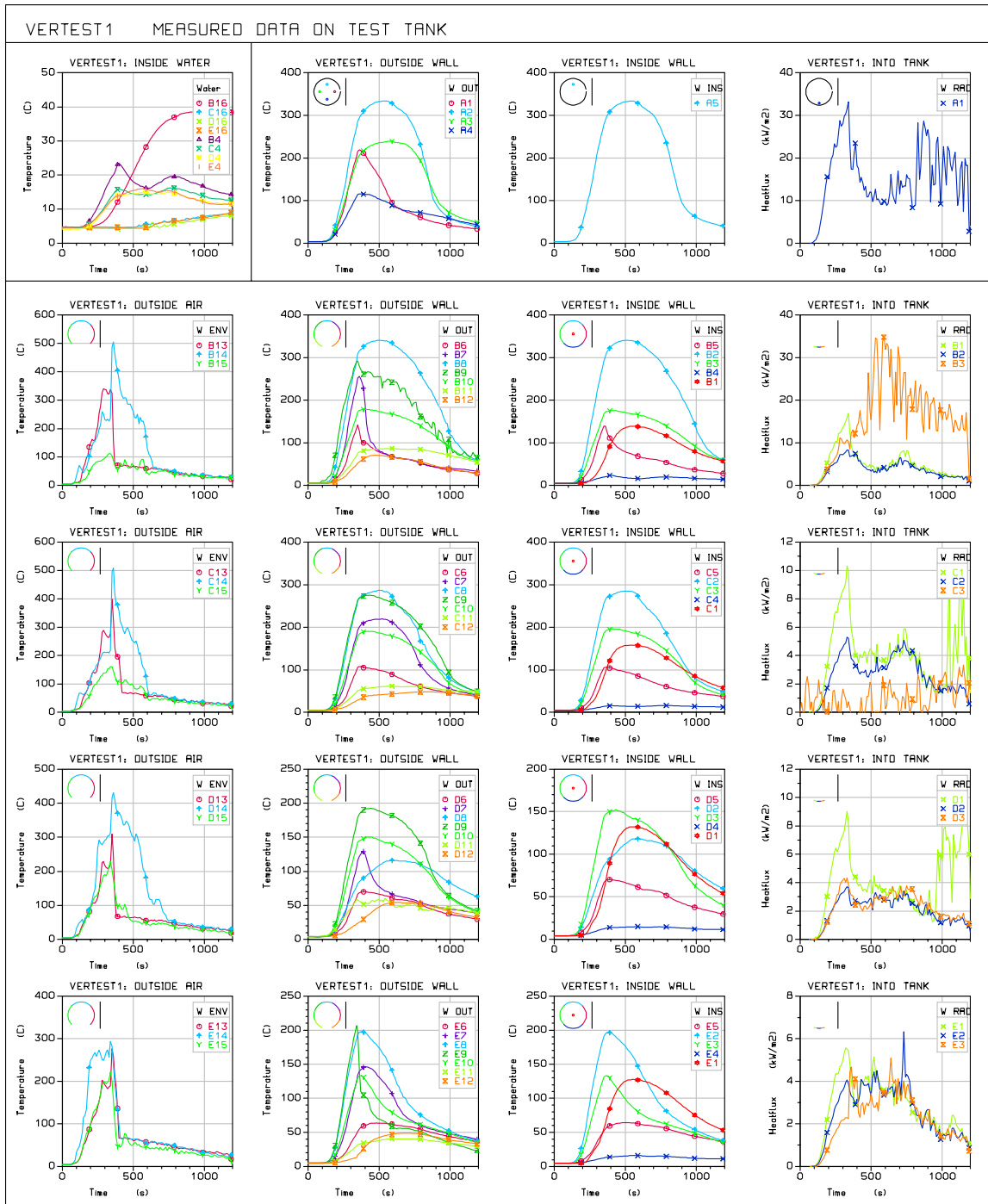


Figure 3.7 VerTest 1: measured data on test tank

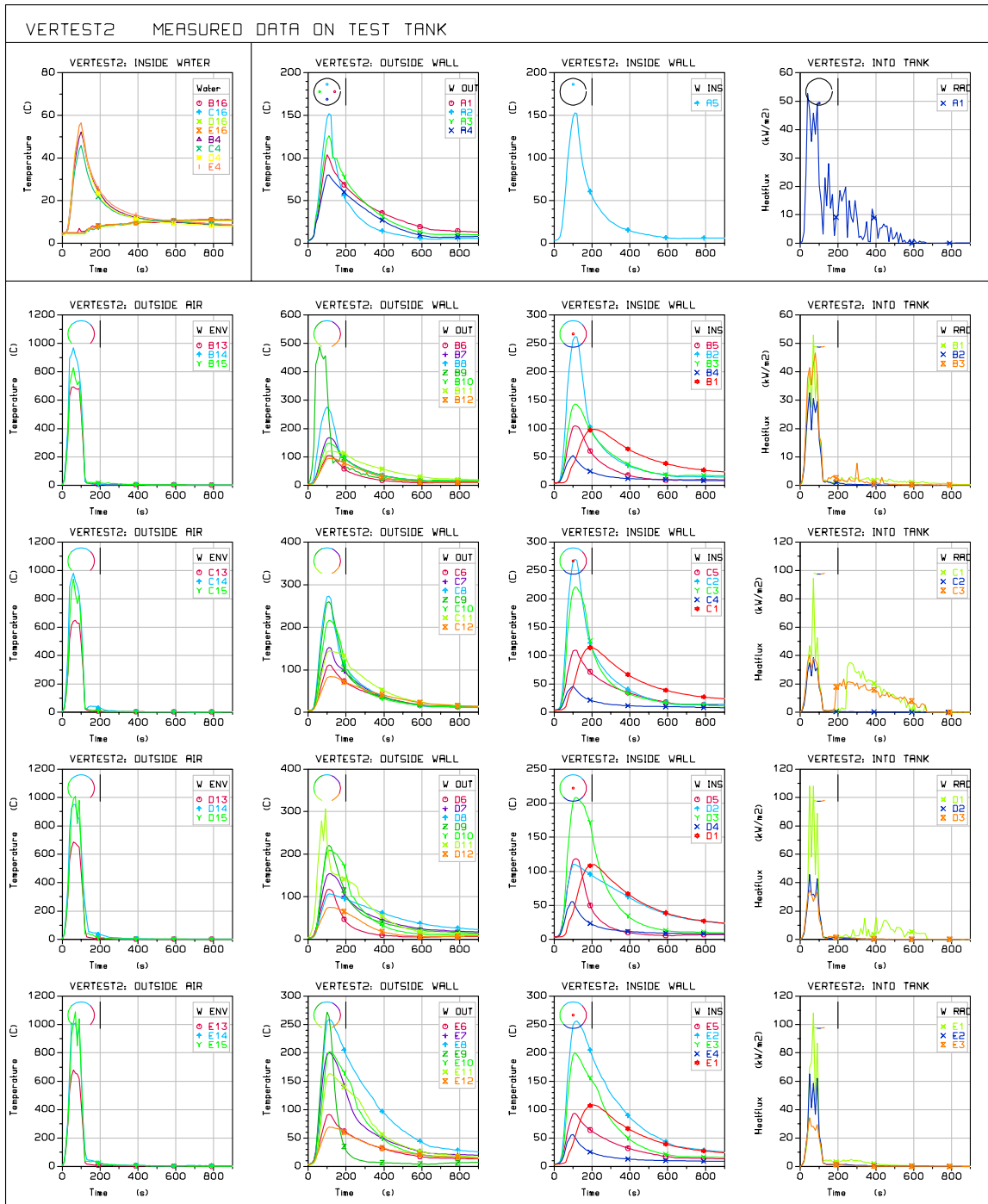


Figure 3.8 VerTest 2: measured data on test tank

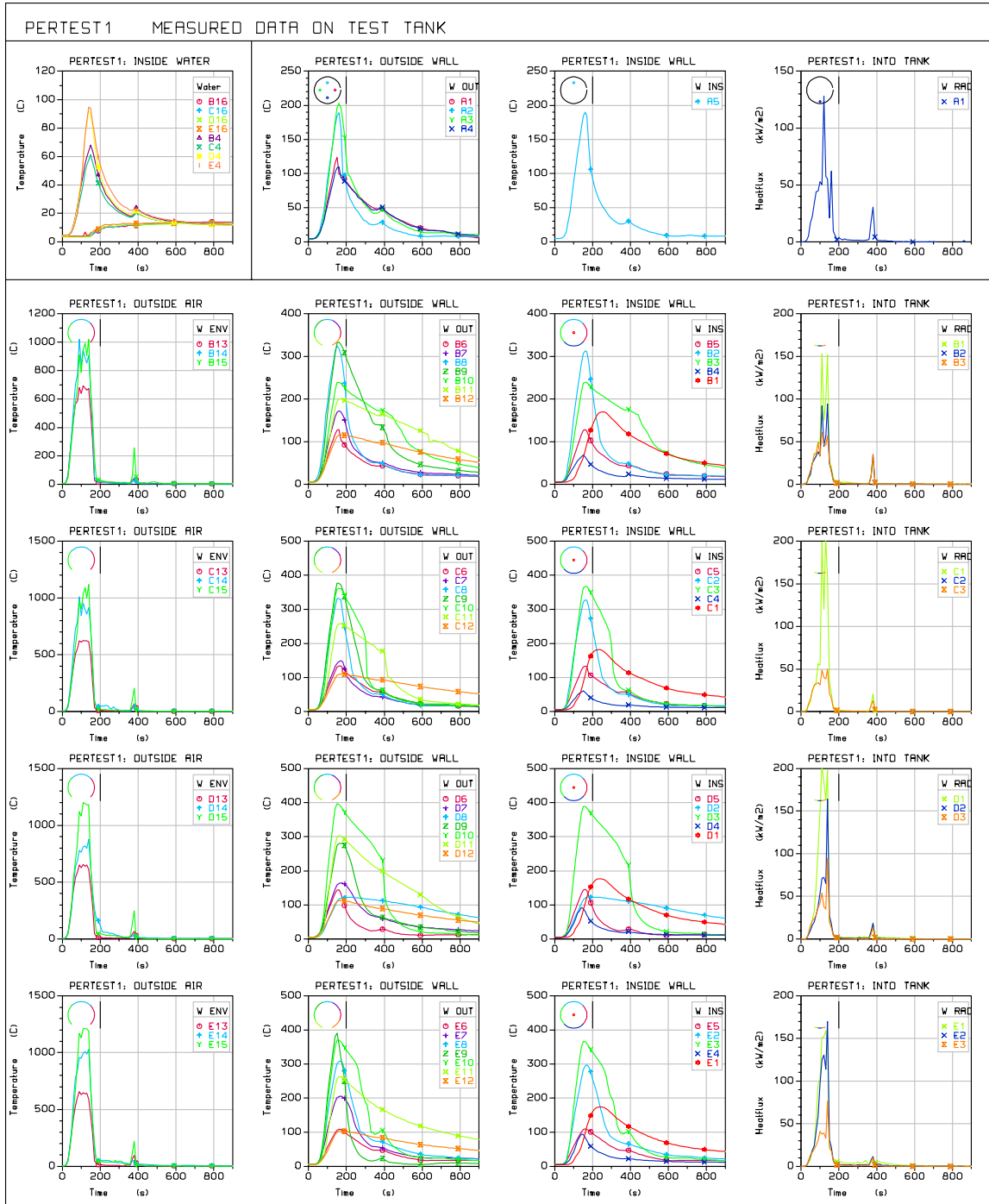


Figure 3.9 PerTest 1: measured data on test tank

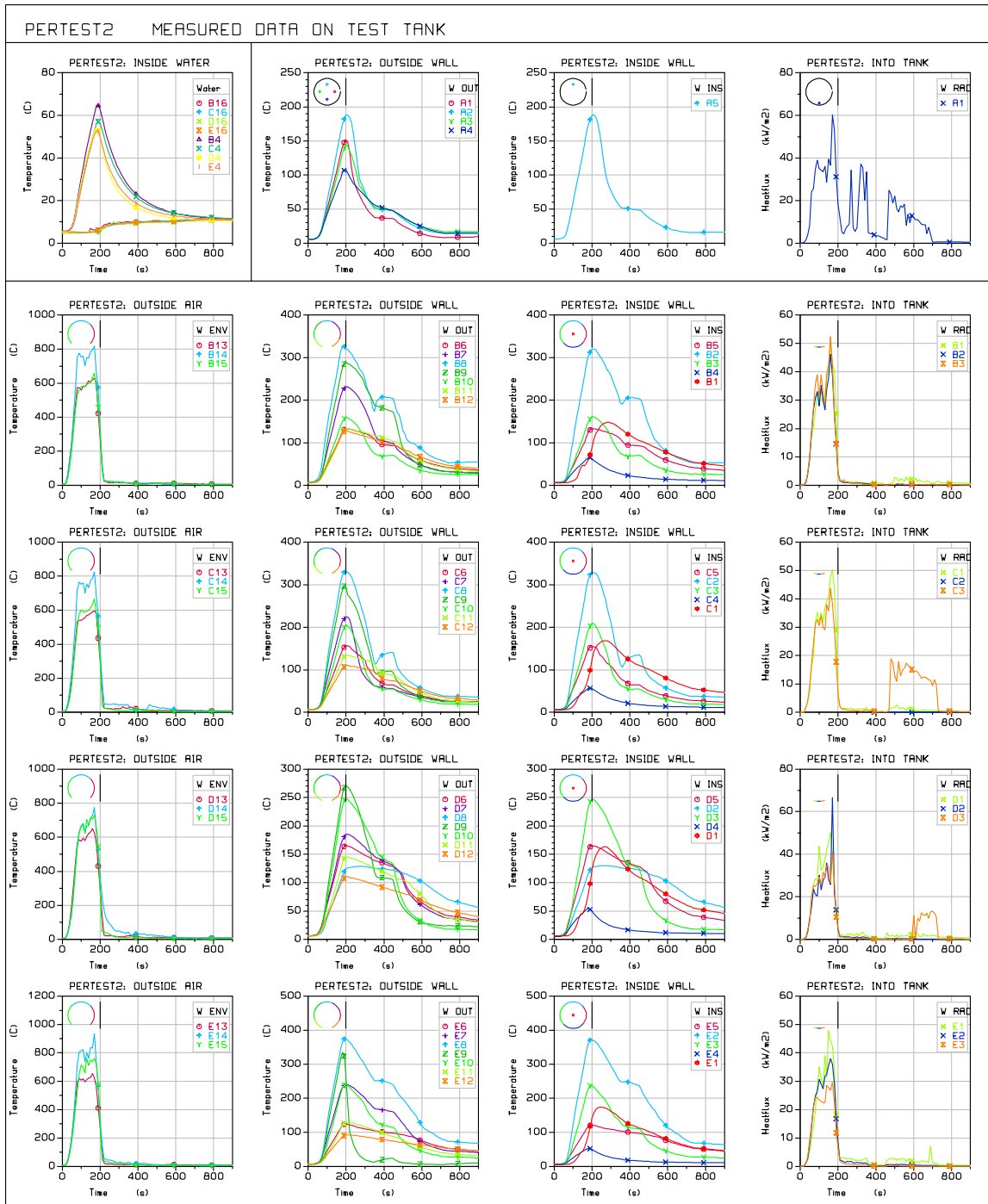


Figure 3.10 PerTest 2: measured data on test tank

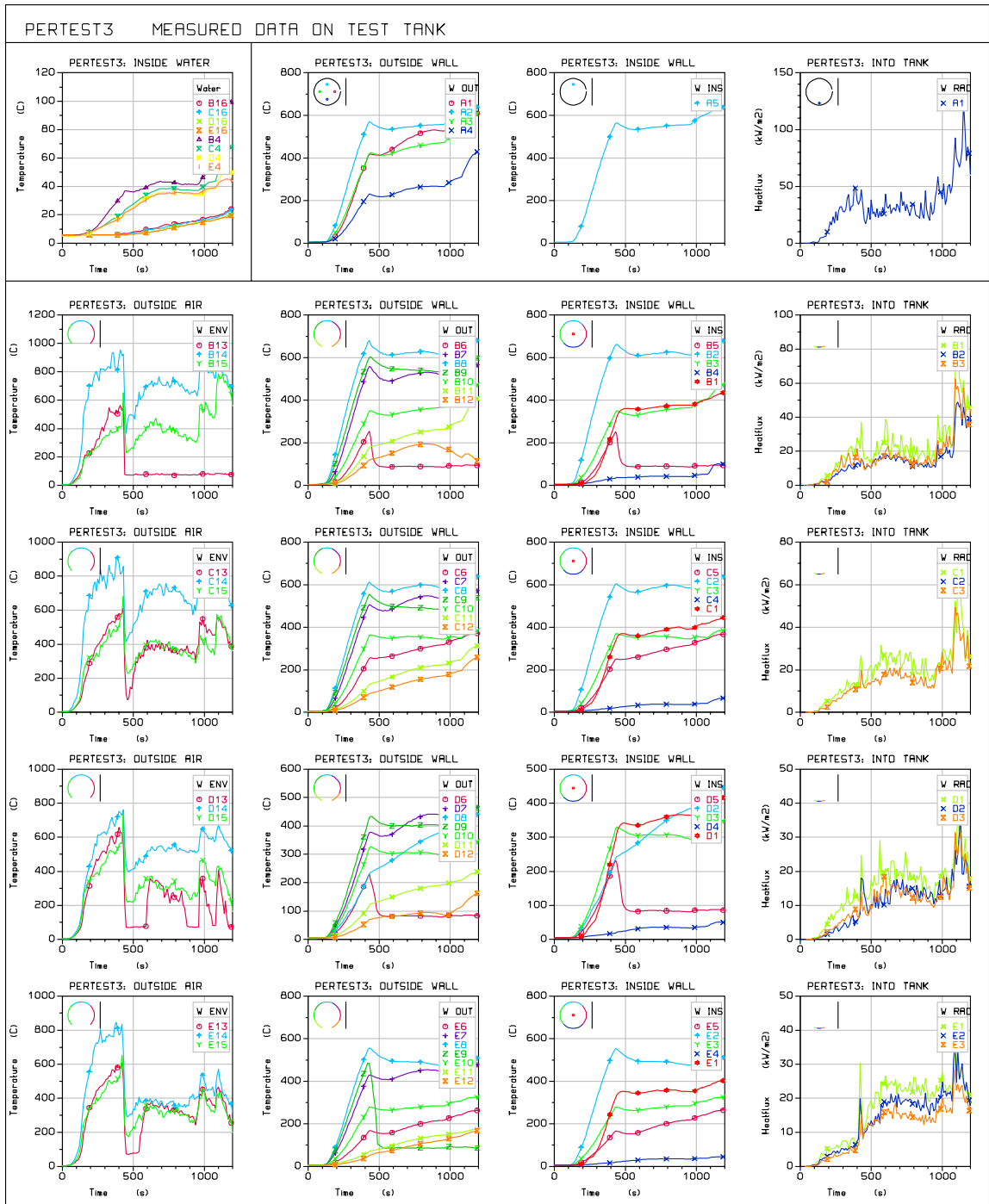


Figure 3.11 PerTest 3: measured data on test tank

3.3.2 Discussion: measured temperatures around the tank

Measured temperatures near the outer surface of the tank (0.10 m from the tank shell) are shown in Figure 3.12. The graph left shows the average of the 12 air temperatures measured over a period of 900 s after ignition of the fire. The sharp decrease of the air temperature is caused by the switching on of the water mist system. In the pool fire tests (VerTest2 and PerTest1 & 2) the fire was extinguished or significantly reduced within 60 s by the water mist, resulting in a temperature drop below 40 °C. In the tests with the solid fire (VerTest1 and PerTest3) the fire was not extinguished but controlled by the system. In PerTest3, seeking the limits of the system, the mean air temperature stayed around 400 °C (after an initial drop to 220 °C) and the maximum air temperature around 700 °C (after an initial drop to 400 °C).

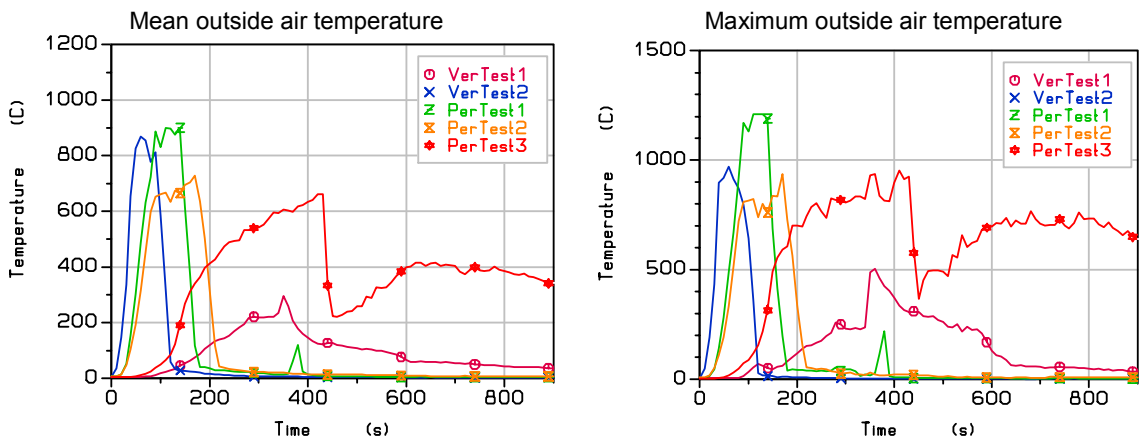


Figure 3.12 Mean and maximum temperature of the air surrounding the test tank

The position of the maximum temperature depended on the fire source as explained below.

Firstly, in the pool fire tests the (left) side of the tank facing the middle of the tunnel was exposed to higher temperatures than the other (right) side. This was partly caused by the symmetric position of the pool in the tunnel in contrast to the non-symmetric position (on the right lane) of the tank and partly by the non-parallel position of the tank with respect to the tunnel walls. In the solid fire tests the thermal exposure of the tank sides was more symmetrically, due to the fact that both the tank and fire source were positioned on the right lane.

Secondly, in the pool fire tests the lower and middle part of the tank were exposed to the highest temperatures. In the solid fire tests on the other hand the highest exposure occurred on top of the tank. This can be explained by the higher position of the solid fuel with respect to the pool.

Finally, in the pool fire tests the exposure to the highest temperatures was more towards the end of the tank (Section D and E) whereas in the solid fire tests this maximum was more at the beginning (Section A and B). This difference was most probably caused by the different distances between the base of the fire and the tank. In the pool fire the minimum distance to the tank was almost immediately attained due to the fast spread of the fire over the total fuel bed. With the solid fire the initial distance was larger, because of the more slowly fire spread from the rear of the pallet pile (where the fire was ignited) to the front (facing the tank) of the pile. See also Ref. [3].

Clearly in all tests except “VerTest1” a significant part of the tank was immersed in flames. With the pool fires the flames were lower and more to the left side of the tank. With the solid fires the flames

were higher and more symmetrical surrounding the top part of the tank. The reason for this difference is the position and height of the base of the fire source with respect to the tank position.

### 3.3.3 Discussion: measured temperatures of the tank wall

The maximum temperature of the tank wall is shown in Figure 3.13 for each test, but now for a period of 1800s. The maximum wall temperatures were in the same area as the maximum air temperatures around the tank. Clearly the wall temperatures follow the surrounding air temperatures, but with a time delay caused by the thermal inertia of the wall. The highest temperature (about 600°C) occurred in the solid fire test “PerTest3” where the fire was only to a certain extent controlled by the water mist system.

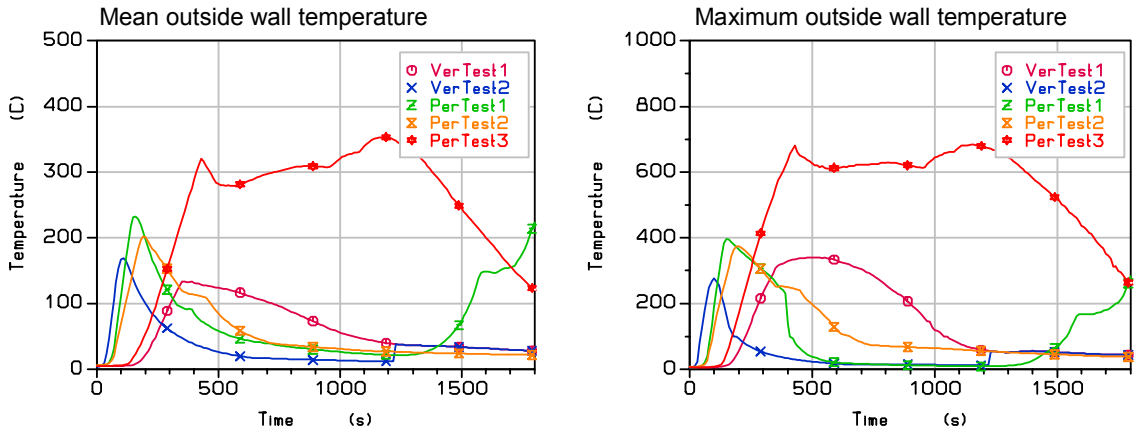


Figure 3.13 Mean and maximum temperature of the outside surface of the tank shell. Note: the increase of temperature in PerTest 1 is caused by the after burning of the fuel and is not a part of the official test.

### 3.3.4 Discussion: measured heat fluxes

Measured heat fluxes from the tunnel environment into the ‘belly’ of the tank in contact with the water in the tank are shown in Figure 3.14.

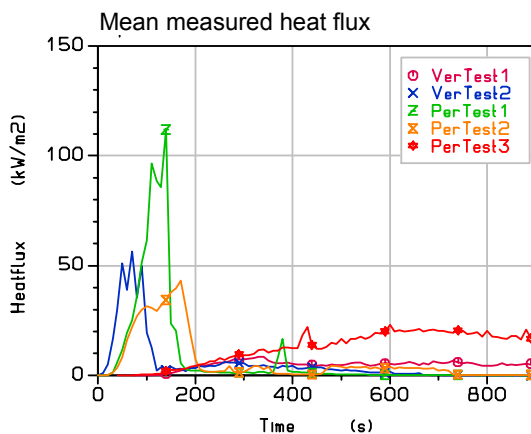


Figure 3.14 Mean heat flux into the ‘wetted’ part of the test tank

The figure shows the weighted mean value of all 13 heat flux meters. The highest heat fluxes occurred in the pool fire tests where the tank is more heated from below as in the solid fire tests. The high peak in ‘PerTest1’ is probably due to the somewhat higher ventilation velocity during that test.

The heat fluxes due to the solid fires are much lower, because of the higher position of the flames, as already explained in Section 4.3.1. Even in “PerTest3” the mean heat flux remains below 20 kW/m<sup>2</sup>.

### 3.4 Assessment of BLEVE risk from test results

Figure 3.15 shows the (LPG vapour) pressure rise inside the reference LPG tank calculated with the simple method described in Section 3.1 based on the measured heat fluxes shown in Figure 3.14 and the maximum outside tank wall temperatures shown in Figure 3.13. The highest pressure rise will occur in “PerTest3”. The highest rise in tensile stress in the tank wall will therefore also occur in “PerTest3”. This is shown in Figure 3.16 under the label “TS-LPG”. Figure 3.16 also shows the decline of the maximum stress that the tank wall would be able to resist for each test.

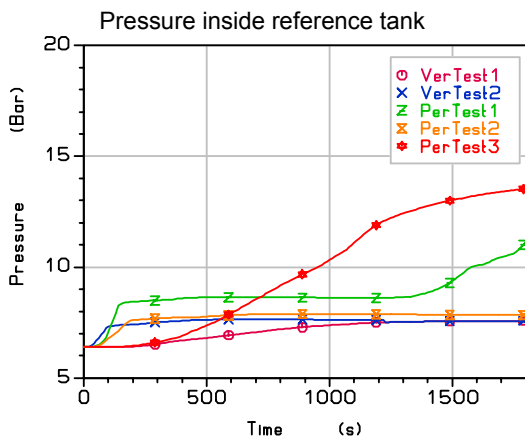


Figure 3.15 Calculated pressure rise in reference tank

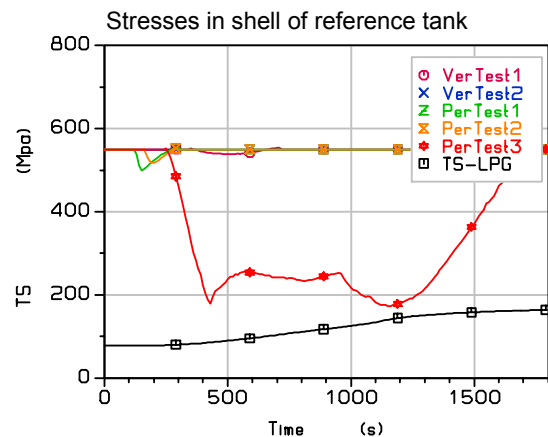


Figure 3.16 Calculated maximum allowable stress for all tests and actual stress (TS-LPG) for PerTest3 in the reference

Clearly the only critical situation will occur in “PerTest3” where a sharp decrease of the maximum allowable stress occurs due the high tank wall temperature at the top of the tank in Section B. The critical situation begins after about 400s and lasts until about 1300s. The pressure rise due to the heating up of the LPG is less important.

### 3.5 Conclusion

Only in “PerTest3”, a test with a solid fire seeking the limits of the water mist system, a serious risk of a BLEVE will occur due to a possible rupture of the tank. In all other tests the fire was extinguished or controlled fast enough to prevent heating up of the tank wall above a critical temperature of about 600 °C. Quick detection and extinguishment of the fire is in particular important with a pool fire, due to the fast increase of the temperature around the tank to about 1000 °C.

The effect of the pressure increase of the LPG due to the heating up of the LPG was less important.



## 4 The tenability-tests

### 4.1 The criteria for tenability

During previous large scale tests as performed in the Runehamar-tunnel in 2003 and 2005, temperature-data were collected at large distances (about 1 km downstream) as part of data to measure the rate of heat release. At that distance, cooling has already caused loss of stratification, and conditions are likely to be very different from those closer to the fire.

The parameters that have the most important influence on the chance of surviving a fire are the thermal effects due to the heat transfer to the human body, and the toxic effects of combustion products, in combination with the duration of exposure. [5]

The heat transfer of the environment to the human body is governed by convection of hot air, by radiation from flames or hot smoke, and by evaporation or condensation. For this latter mechanism the relative humidity plays a very important role. For example, in a sauna the relative humidity is only about 30%, and an air temperature of about 80°C can be endured for many minutes, because the skin is cooled by rapid evaporation of sweat. In a very moist atmosphere however, an air temperature as low as 50°C can be painful immediately and eventually lead to skin burns, also in the respiratory tract. Ideally, in order to predict the heat transfer to the human skin and body more accurately, separate measurements of each parameter would be required. Even then, the actual risk to persons depends strongly on factors like clothing and physical stress. In the evaluation of the tests described in this report it is assumed that an air temperature of 70 °C presents an acute danger, and that a temperature of 50 °C presents an acute danger after 5 minutes duration of exposure. The criteria are set at these levels taking into account that fairly high humidity can be expected during a real incident, due to water introduced by the extinguishing system, but also because of the water vapour produced by the fire itself.

The main toxic effects can be expected from gases like carbon monoxide, hydrogen cyanide and hydrogen chloride. In the tests described here, the fire loads consisted almost exclusively of carbohydrates (cellulose) and hydrocarbons (diesel, plastics). Carbon monoxide is the main toxic gas produced in these tests, and the CO concentration in the local atmosphere is regarded as the decisive criterion. In the evaluation of these tests it is assumed that a CO concentration of 500 ppm presents an acute danger, and that a CO concentration of 250 ppm presents acute danger after 5 minute. duration.

The duration of exposure to the thermal and toxic effects is determined by the time it takes to reach a safe location, and this time, in turn, is strongly influenced by local visibility.

The current tests should yield information about tenability in the area of a few hundred meters downwind of the fire. Therefore it was decided to install sensors at a relevant height (between 0.6 m and 2.0 m), and at a range of distances from the fire: 20 m, 40 m, 100 m and 300 m.

### 4.2 The measurement-system and instrumentation

#### 4.2.1 *Three main types of measurements were performed during the tests:*

1. Temperature, using thermocouples, plate thermocouples and semiconductor sensors that measured both temperature and relative humidity. In the tests, provisions were made to protect the semiconductor sensors against temperatures higher than about 70 degrees C. This meant that higher temperatures could not be measured with these sensors.
2. CO-concentration, using semiconductor sensors.
3. Vision distance, using camera's and LED beacons at a range of distances (5m, 7m, 10m, 15m, 20m and 30m) from the camera.

#### 4.2.2 *Location of the sensors*

At 20 m, on the south side of the tunnel, a set of two thermocouples (at heights of 0.6 m and 1.6 m) and one plate-thermocouple (at a height of 1.6 m) was installed. The plate thermocouple was installed facing the fire load and tilted 45 degrees backward to receive radiation also from the hot smoke near the ceiling. The sensors were connected to the on-line measurement network. At 20 m, on the north side of the tunnel, a semiconductor sensor was installed. This was a stand-alone data logger that measured both temperature and relative humidity. Also on the north side, a stand-alone data logger was installed that measured the concentration of carbon monoxide. Again, on the north side, a stand-alone camera was installed at a height of 0.6 m that looked downstream towards a line of six beacons with LED-lamps. The beacons were also installed along the north edge of the road surface, and mounted at distances from the camera of 5, 7, 10, 15, 20 and 30 m.

At 40 m, on the south side of the tunnel, a set of two thermocouples (at heights of 0.6 m and 1.6 m) and one plate-thermocouple (at a height of 1.6 m) was installed. The plate thermocouple was installed facing the fire load and tilted 60 degrees backward to receive radiation also from the hot smoke near the ceiling. The sensors were connected to the on-line measurement network.

At 50 m, on the north side of the tunnel, a semiconductor sensor was installed at a height of 0.6 m. This was a stand-alone data logger that measured both temperature and relative humidity. Also on the north side, a stand-alone data logger was installed at a height of 0.6 m that measured the concentration of carbon monoxide. Again, on the north side, a stand-alone camera was installed at a height of 0.6 m that looked downstream towards a line of six beacons with LED-lamps. The beacons were also installed along the north edge of the road surface, and mounted at distances from the camera of 5, 7, 10, 15, 20 and 30 m respectively.

At 100 m, on the north side of the tunnel, the following sensors were installed: A CO-logger at 1.2 m height, and temperature/relative humidity loggers at 0.6 m and 1.6 m height. On the north side, a stand-alone camera was installed at a height of 0.6 m that looked downstream towards a line of six beacons with LED-lamps. The beacons were also installed along the north edge of the road surface, and mounted at distances from the camera of 5, 7, 10, 15, 20 and 30 m respectively.

At 300 m, on the south side of the tunnel, a temperature/relative humidity logger, a CO-logger and a camera and associated beacons were installed. At 300 m the sensors were installed at the south side rather than the north side because all transport to NBL installations further downstream used a track on the north side, and it was considered safer for the equipment to be installed away from the traffic. Due to the long distance from the fire, it is virtually certain that there was no significant difference between conditions on both sides.

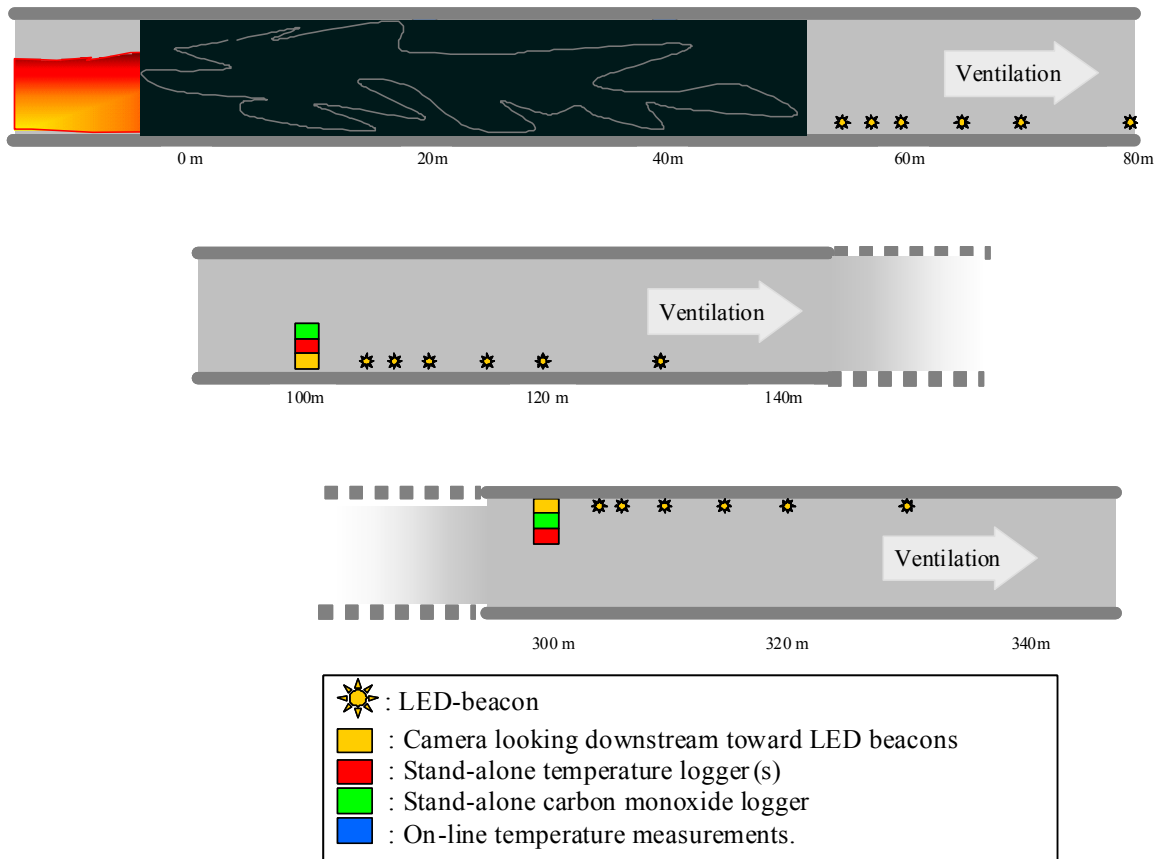


Figure 4.1. Location of main components of the tenability-measurements. The figures below each length represent de length-coordinate along the tunnel in m. Note: Contrary to convention, North is in the downward direction in this schematic drawing..

As the series of tests proceeded, the following modifications were made to the measurement system:

#### 4.2.3 Modification of the system during the tests

After the verification test 1 of 13-12-2007, the conditions at 20 m turned out to be so severe that all LED beacons at this location were destroyed by the effects of heat and subsequent rapid cooling by the water spray. In addition, the loggers for temperature and CO-concentration at this location were destroyed by the ingress of water, despite protective measures.

In the verification test 2 of 19-12-2007, therefore, the camera and beacons were omitted at 20 m, and the protection of the data loggers was revised. They were mounted in holes drilled into concrete blocks. This resulted in satisfactory CO-measurements, but in very slow response of the temperature loggers.

In the performance test 1 of 9-01-2008, the temperature loggers at 20 m and 50 m were omitted, and the poor time response of the temperature loggers at 100 m and 300 m had to be accepted for this test.

In the test 2 of 14-01-2008, two stand-alone temperature loggers of a new type with 4 thermocouple-channels each were installed at 100 m and 300 m, and proved to be fully functional.

These loggers were also used in the performance test 3 on 17-01-2008 with good results.

### 4.3 Test results of verification test 1 on 13-12-2007, a 50 MW solid fire

#### 4.3.1 Location: 20 m downstream

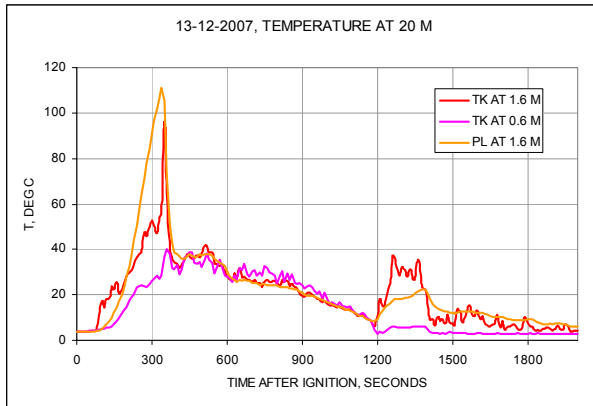


Figure 4.1 Temperatures at 20 m measured on-line. TK signifies a mantle thermocouple and PL a plate thermocouple with increased radiation sensitivity. The height in m. above the road surface is given.

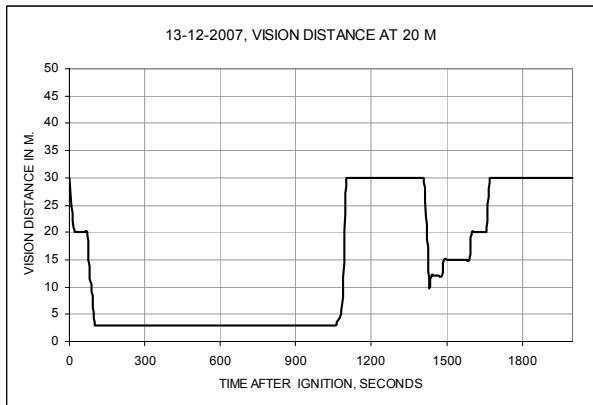


Figure 4.2 Vision distance measured from 20 m in downstream direction.



Stills from the video that were used to determine visibility. From left to right: before, during and after the test. Note the reflection of the beacons in the flooded road surface after the test.

No temperature or CO-readings from the stand-alone dataloggers were obtained at 20 m due to the fact that the dataloggers were irreparably damaged, despite protective measures, by a combination of heat, soot and ingress of water.

4.3.2 Location: 40 and 50 m downstream

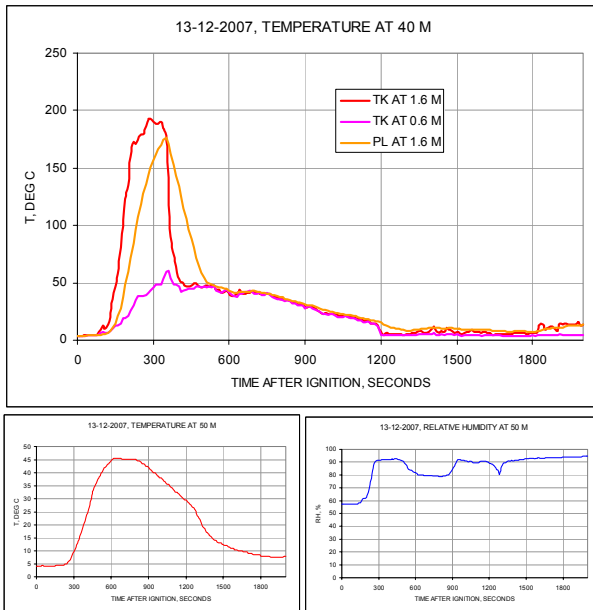


Figure 4.3 Top: temperatures measured on-line with thermocouples. Bottom: temperature and relative humidity measured at 0.6 m height with stand-alone semiconductor sensor. The temperature readings are discussed in 4.8.1

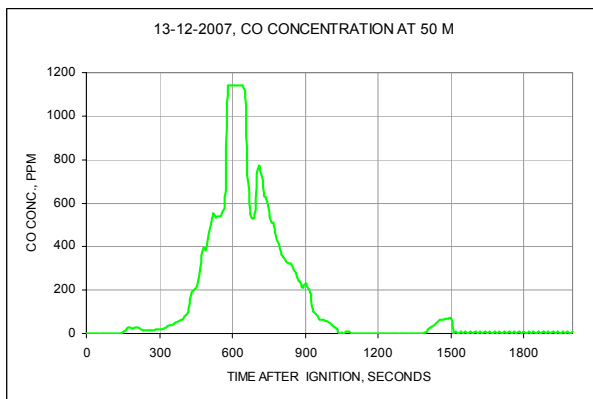


Figure 4.4 CO concentration measured at 0.6 m height with stand-alone semiconductor sensor.

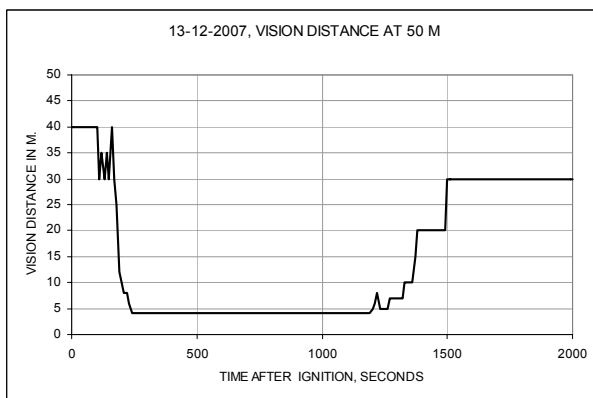


Figure 4.5. Vision distance measured in downstream direction

4.3.3 Location: 100 m downstream

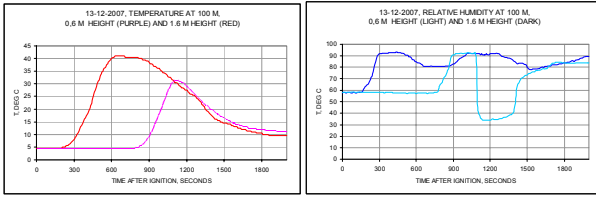


Figure 4.6 Temperatures and relative humidities measured with semiconductor sensors.

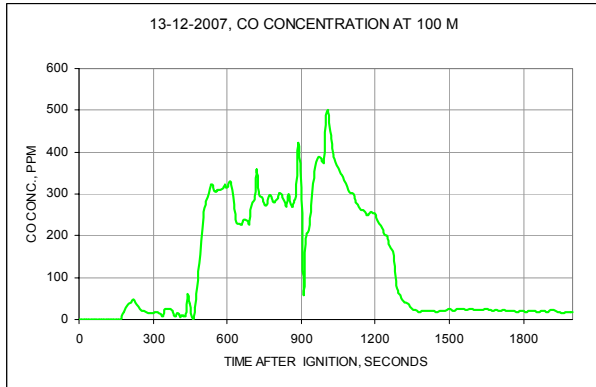


Figure 4.7 CO concentration

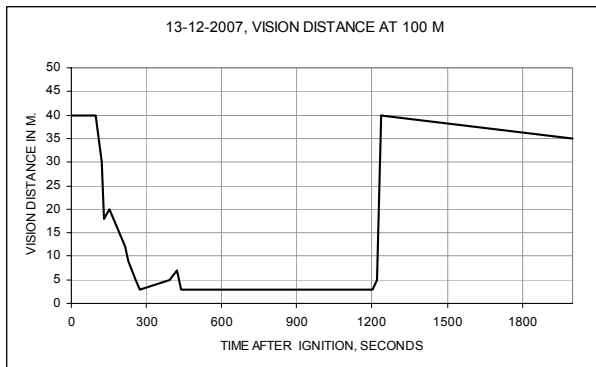


Figure 4.8 Vision distance measured in downstream direction

4.3.4 Location: 300 m downstream

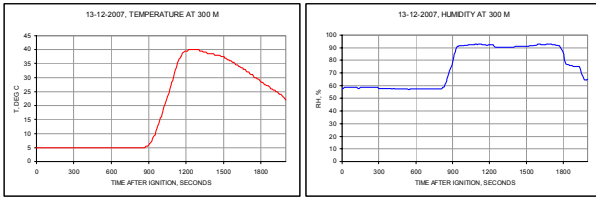


Figure 4.9 Temperature and relative humidity measured at 0.6 m height with semiconductor sensor. The temperature readings are discussed in 4.8.1

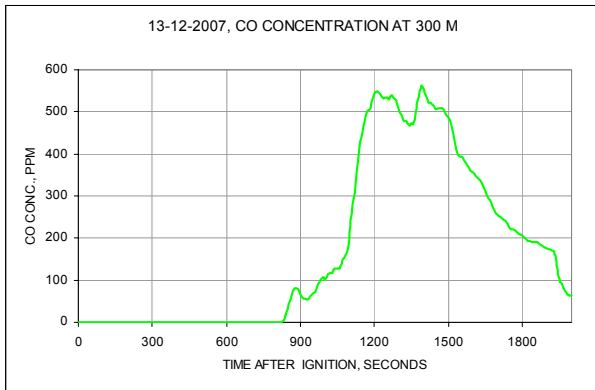


Figure 4.10 CO concentration

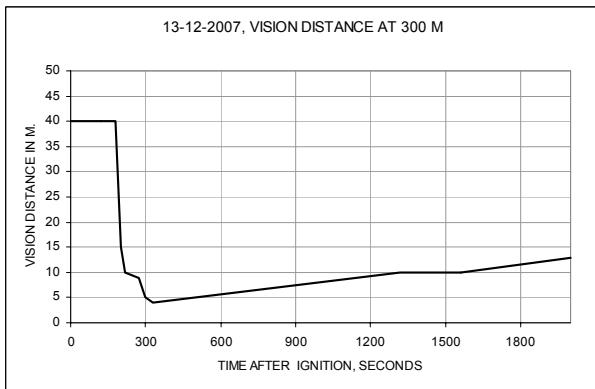


Figure 4.11 Vision distance measured in downstream direction

#### 4.4 Test results of verification test 2 on 19 December 2007, a 100 m<sup>2</sup> pool fire

##### 4.4.1 Location: 20 m downstream

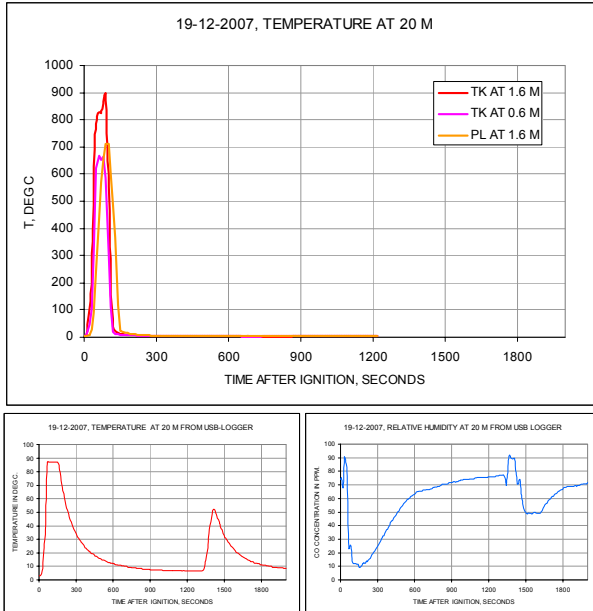


Figure 4.12 Top: temperatures measured with thermocouples. Bottom: temperature and relative humidity measured at 0.6 m height with semiconductor sensor. The temperature readings are discussed in 4.8.1

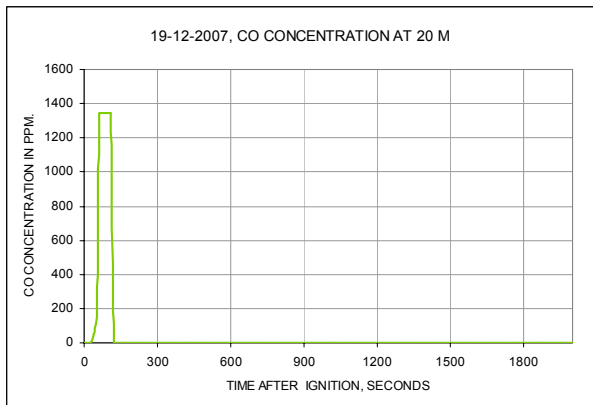


Figure 4.13 CO concentration measured with semiconductor sensor at 0.6 m

No visibility could be measured at 20 m due to the fact that all the protective glass covers of the beacons were destroyed by the direct spray of cold water from the extinguishing system.



4.4.2 Location: 40 m and 50 m downstream

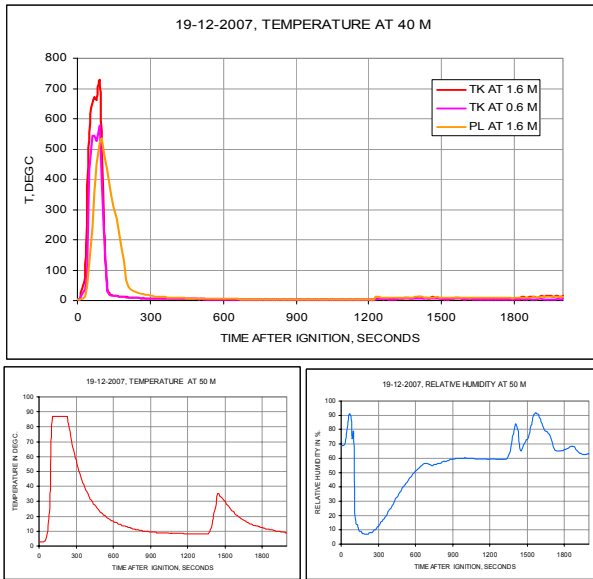


Figure 4.14 Top: temperatures measured with thermocouples. Bottom: temperature and relative humidity measured at 0.6 m height with semiconductor sensor. The temperature readings are discussed in 4.8.1

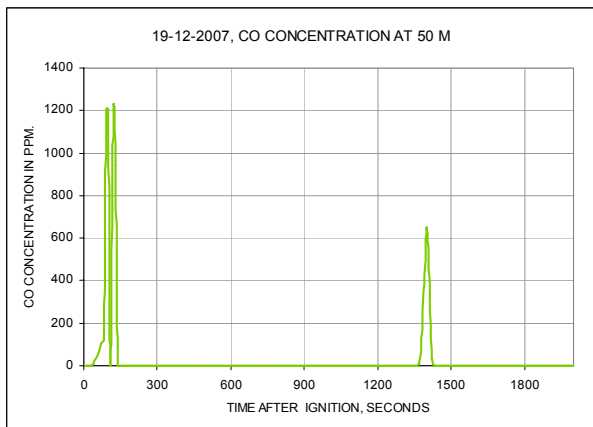


Figure 4.15 CO concentration measured with semiconductor sensor at 0.6 m

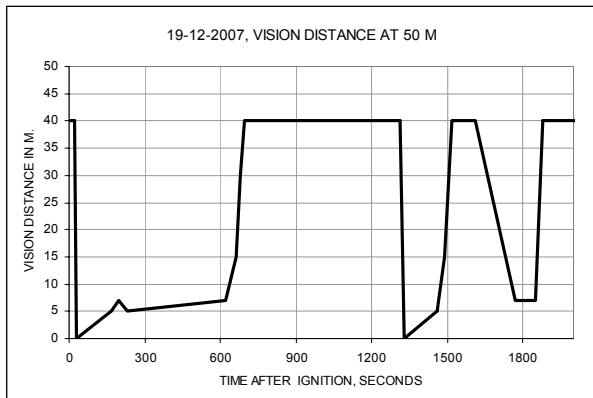


Figure 4.16 Vision distance measured in downstream direction

4.4.3 Location: 100 m downstream

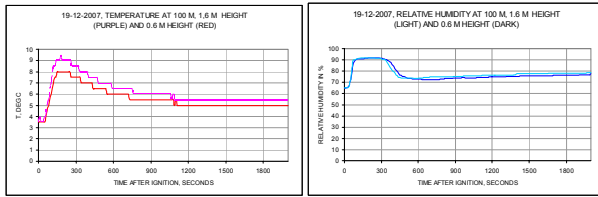


Figure 4.17 Temperatures and relative humidities, measured with semiconductor sensors at 1.2 m height. The temperature rise is very small, and is recorded by both sensors. It is also consistent with the readings at 300 m.

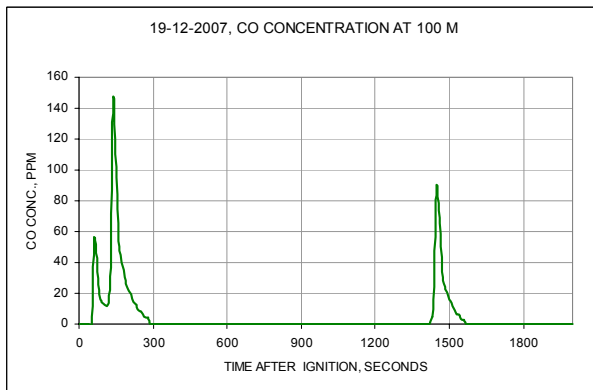


Figure 4.18 CO concentration measured with semiconductor sensors at 1.2 m

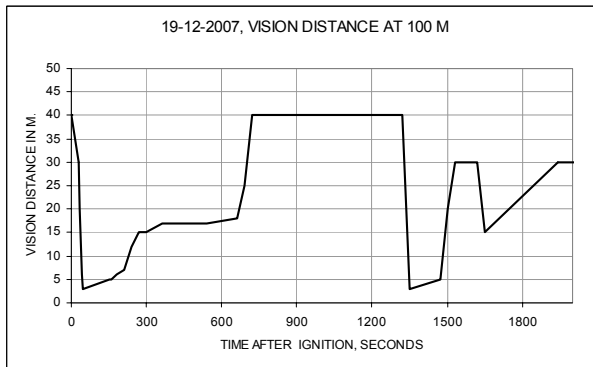


Figure 4.19 Vision distance measured in downstream direction

4.4.4 Location: 300m downstream

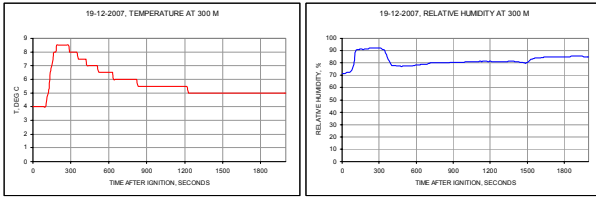


Figure 4.20 Temperatures and relative humidities, measured with semiconductor sensors at 1.2 m height.

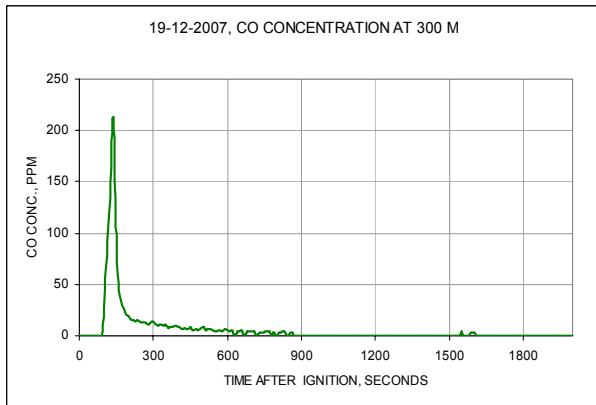


Figure 4.21 CO concentration measured with semiconductor sensors at 1.2 m

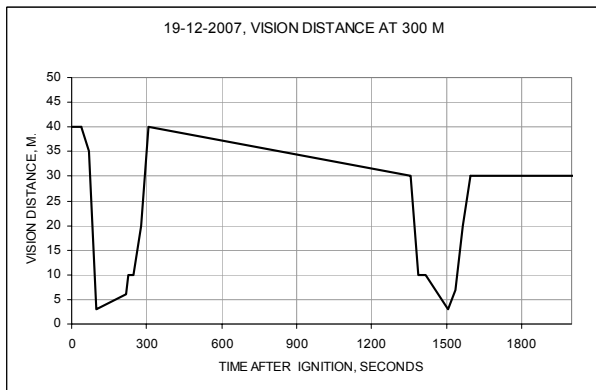


Figure 4.22 Vision distance measured from in downstream direction

## 4.5 Test results of Performance test 1 on 9 January 2008, a 100 m<sup>2</sup> pool fire

### 4.5.1 Location: 20 m downstream

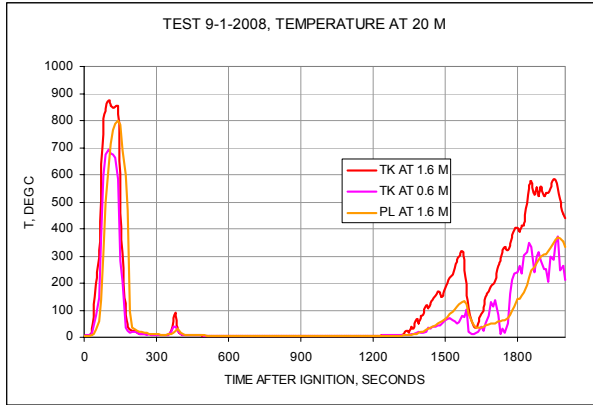


Figure 4.23. Temperatures measured with thermocouples. The rise after 1300 s. is caused by burning-off of excess fuel.

### 4.5.2 Location: 40 m and 50 m downstream

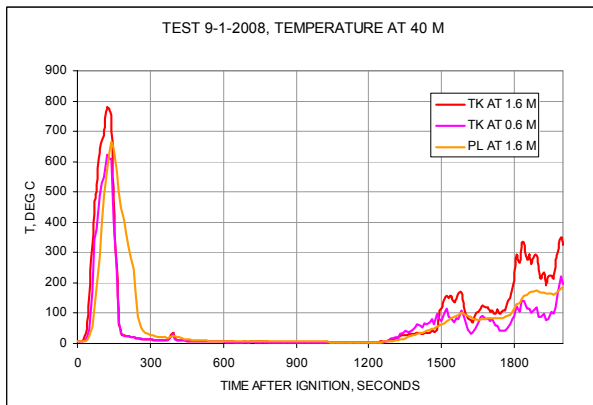


Figure 4.24 Temperatures measured with thermocouples

No useful CO data have been collected at 50 m due to ingress of water in the sensor.  
Due to a technical fault no visibility data have been collected.

4.5.3 Location: 100 m downstream

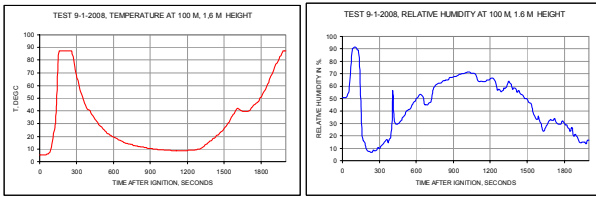


Figure 4.25 Temperature and relative humidity, measured with semiconductor sensors at 1.2 m height

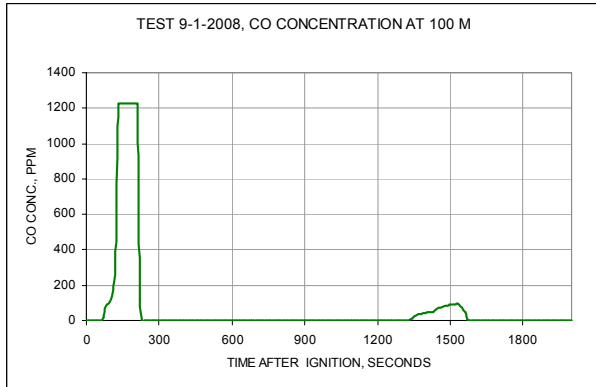


Figure 4.26 CO concentration, measured with semiconductor sensors at 1.2 m height

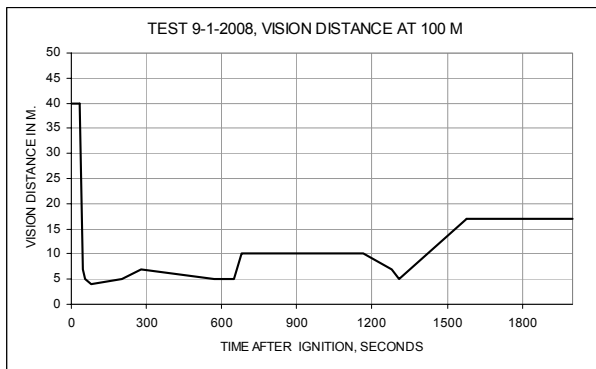


Figure 4.27 Vision distance measured in downstream direction

4.5.4 Location: 300 m downstream

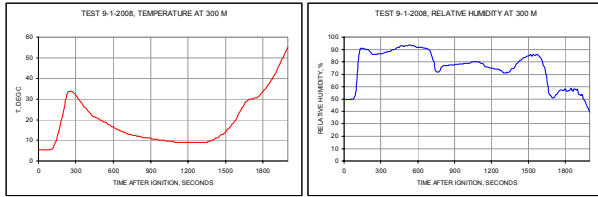


Figure 4.28 Temperatures, measured with semiconductor sensors at 1.2 m height

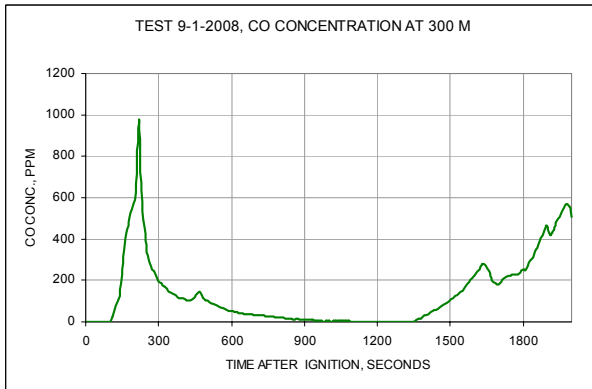


Figure 4.29 CO concentration, measured with semiconductor sensors at 1.2 m height

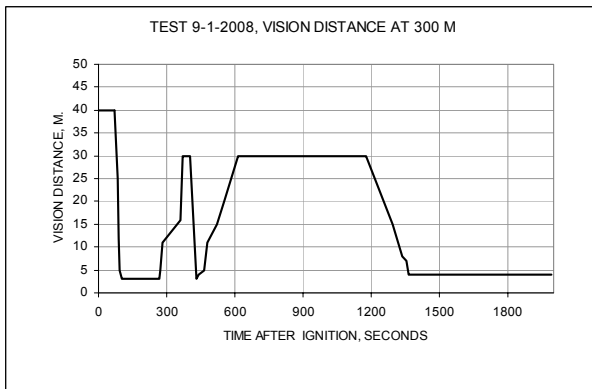


Figure 4.30 Vision distance measured in downstream direction

#### 4.6 Test results of performance test 2 on 14 January 2008, a 100 m<sup>2</sup> pool fire

##### 4.6.1 Location: 20 m downstream

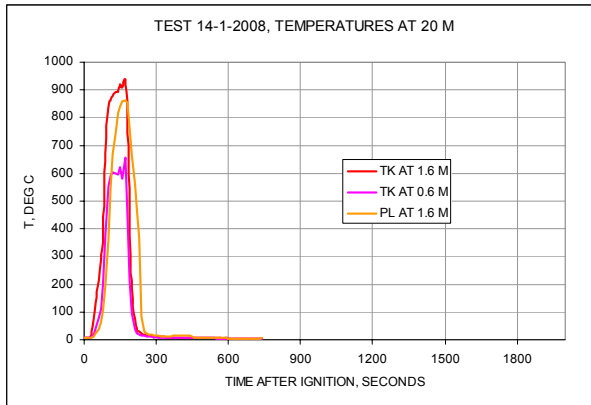


Figure 4.31 Temperatures measured with thermocouples

##### 4.6.2 Location: 40 and 50 m downstream

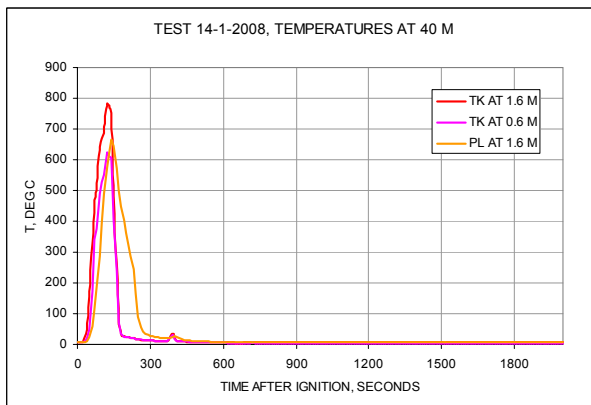


Figure 4.32 Temperatures measured with thermocouples

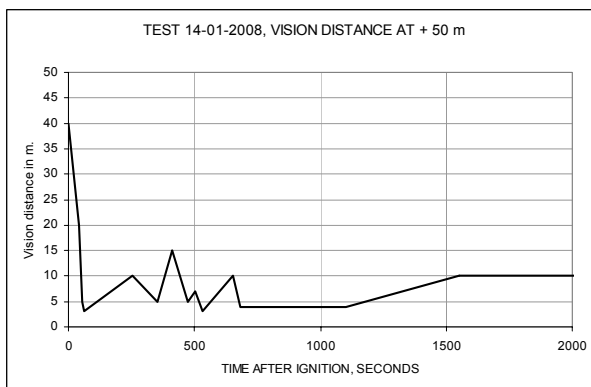


Figure 4.33 Vision distance measured in downstream direction

4.6.3 Location: 100 m downstream

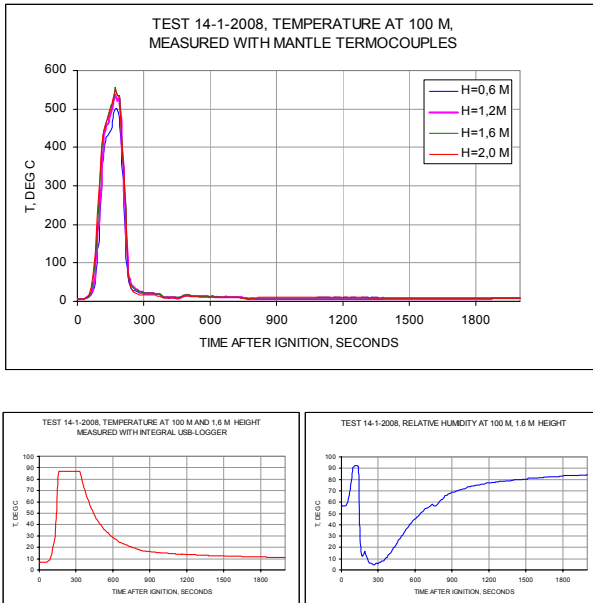


Figure 4.34 Top: temperatures measured with thermocouples. Bottom: temperature and relative humidity measured with semiconductor sensors at 1.2 m height.

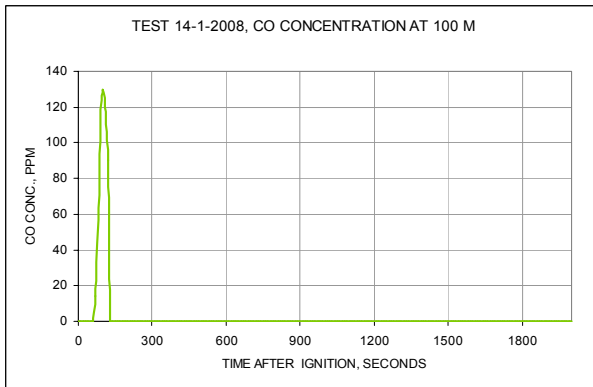


Figure 4.35 CO concentration measured with semiconductor sensor at 1.2 m height.

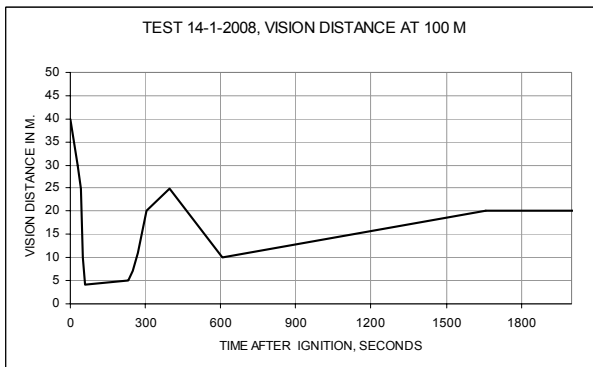


Figure 4.36 Vision distance measured in downstream direction



4.6.4 Location: 300 m downstream

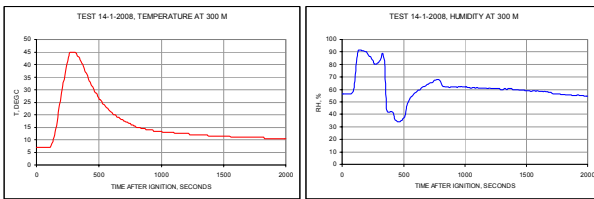
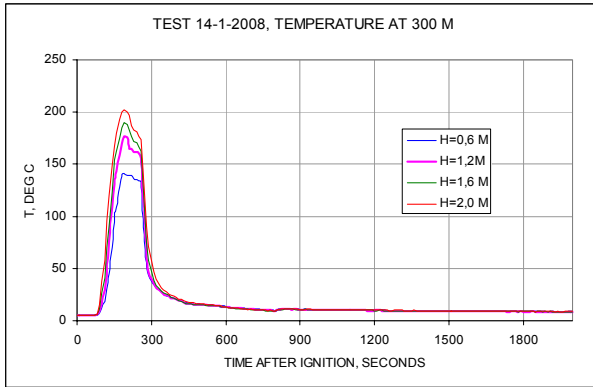


Figure 4.37 Top: temperatures measured with thermocouples. Bottom: temperature and relative humidity measured with semiconductor sensors at 1.2 m height.

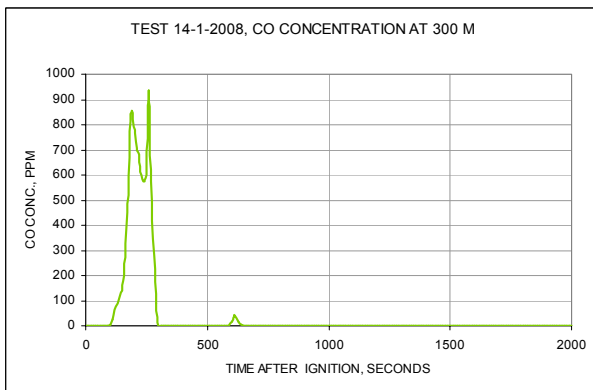


Figure 4.38 CO concentration measured with semiconductor sensor at 1.2 m height.

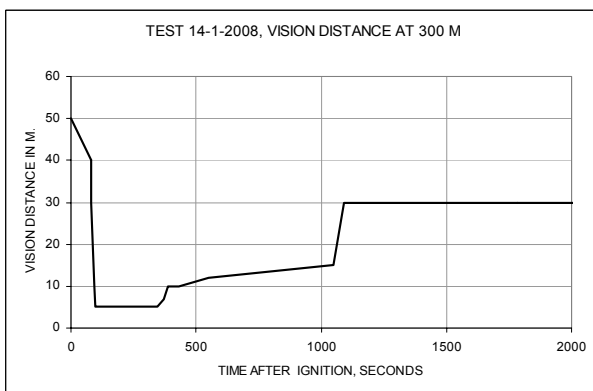


Figure 4.39 Vision distance measured in downstream direction

## 4.7 Test results of Performance test 3 on 17 January 2008, a 200 MW solid fire

### 4.7.1 Location: 20 m downstream

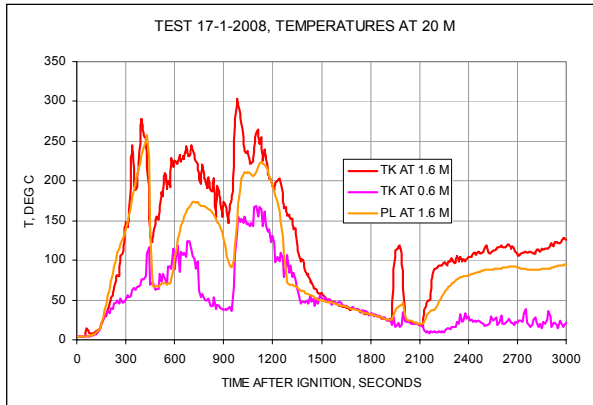


Figure 4.40 Temperatures measured with thermocouples

### 4.7.2 Location: 40 m and 50 m downstream

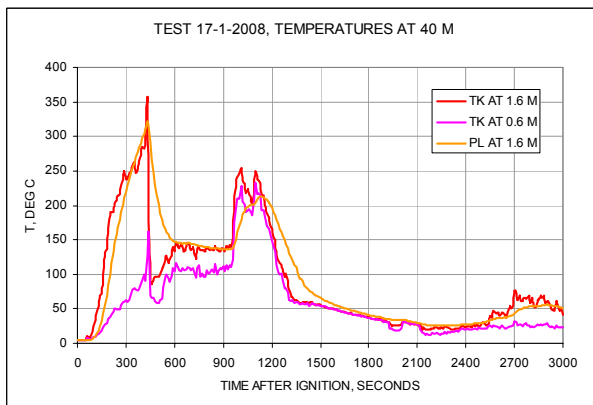


Figure 4.41 Temperatures measured with thermocouples

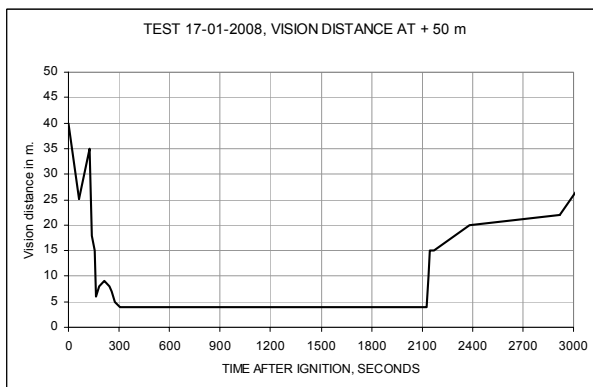


Figure 4.42 Vision distance measured in downstream direction

4.7.3 Location: 100 m downstream

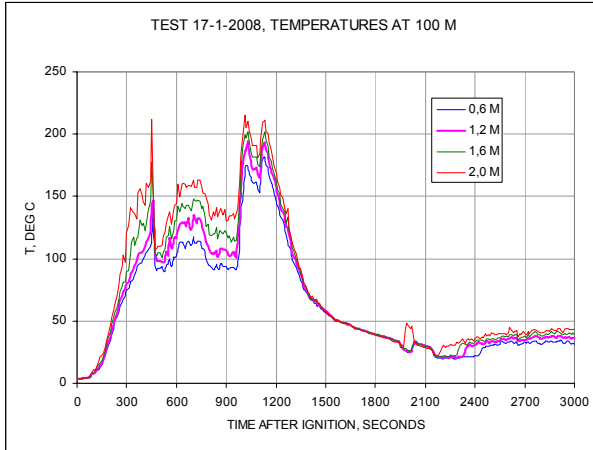


Figure 4.43 Temperatures measured with thermocouples

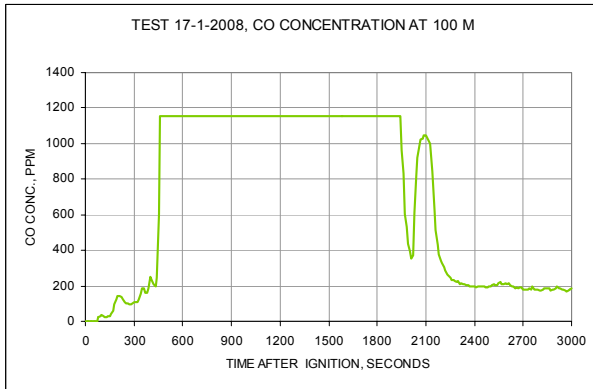


Figure 4.44 CO concentration measured with semiconductor sensor at 1.2 m height.

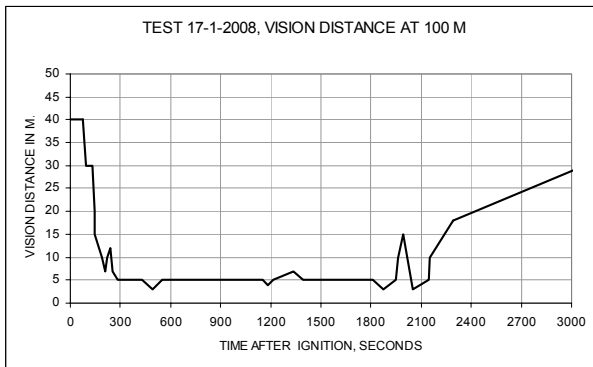


Figure 4.45 Vision distance measured in downstream direction

4.7.4 Location: 300 m downstream

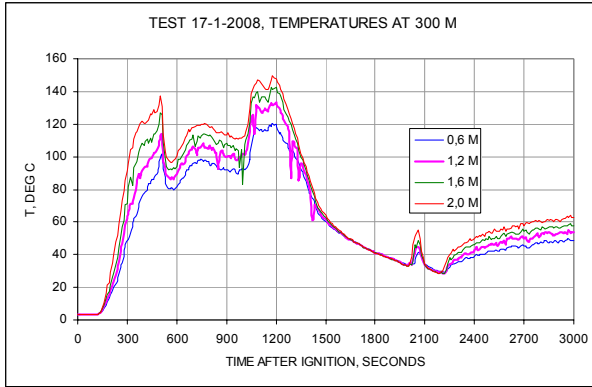


Figure 4.46 Temperatures measured with thermocouples

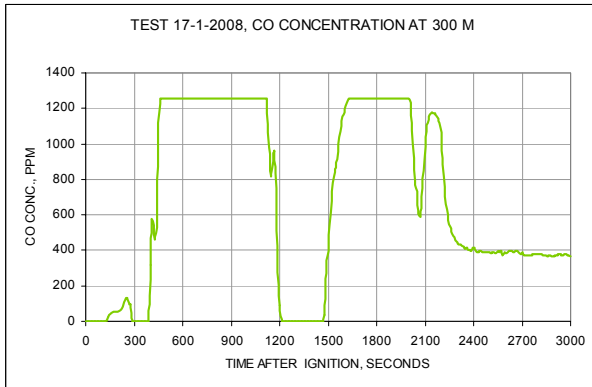


Figure 4.47 CO concentration measured with semiconductor sensor at 1.2 m height. The “dip” between 1200 s and 1500 s. is probably an instrument error, due to ingress of water

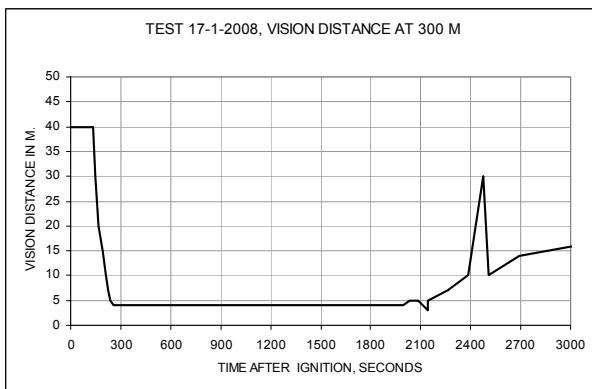


Figure 4.48 Vision distance measured in downstream direction

## 4.8 Discussion of the test results

### 4.8.1 *The test environment and assessment of data*

The conditions downstream during the actual fire test were very severe. High temperatures, a very high moisture content, condensation of steam and sudden cooling by the water mist system had to be dealt with. Due to these very severe conditions, not all measurements have yielded useful results.

The semiconductor data loggers that recorded temperature and relative humidity turned out to have a very slow response (as opposed to the thermocouples that were installed at 20 m and 40 m). This slow response is at least partially due to the substantial protection against water and high temperatures that was needed to shield these loggers. Accordingly, the temperature measurements done with the semiconductor sensors are treated with due caution. Their temperature readings are considerably lower and later than the readings from thermocouples. The value of the temperature readings from the semiconductor instruments was later examined by lab tests. These confirmed the slow response of the loggers alone (with a 95% time of more than 2 minutes). The response will have slowed even more by the massive thermal protection of the sensors required in the tunnel tests.

The carbon monoxide loggers have a much quicker response time, and have, in general, yielded reliable data. A general problem with the electrochemical sensors that are used for gas-analysis is that they have a limited temperature range, and also that their measurement range is limited. Further, the soot that is emitted during the fire test penetrates quite easily into electronic circuitry where it can cause malfunction because of its conductive properties. This has caused sensor failures on two occasions, despite the specially designed protective measures.

## 4.9 Preliminary evaluation of tenability-data

### 4.9.1 *Background:*

The large amount of information in the preceding graphs requires fairly basic criteria to make an assessment of the tenability conditions that occur downwind, during and after a fire. The three threats, heat, carbon monoxide and poor visibility each have their specific effects and there can be significant synergy between them.

### 4.9.2 *Evaluation method*

For temperatures, we have assumed the following safety limits in our initial evaluation

- Up to 50 °C is tenable indefinitely. (hereafter characterized as Green)
- 50 to 70 °C is tenable for 5 minutes. (hereafter characterized as Yellow)
- Above 70 °C is immediately life-threatening. (hereafter characterized as Red)

The general influence of high relative humidity on the effect of high temperatures is taken into account, and has led to the above limits. In setting the above temperature limits, a relatively high humidity (60 - 100 %) is assumed that corresponds with the activation of a sprinkler- or watermist-system, as already described in 4.1.

For carbon monoxide concentration the following values are used:

- Up to 250 ppm is tenable indefinitely. (Green)
- Up to 500 ppm is tenable for 5 minutes. (Yellow)
- Above 500 ppm is life-threatening. (Red)

Limited visibility is, *in itself*, assumed to be not life-threatening, and will lead to condition “yellow” that may last indefinitely as long as temperature and carbon monoxide level each remain below the lower safety limit.

In the further analysis, the following symbols are used:

Yellow due to poor visibility is assigned the symbol  $Y_{vis}$

Yellow due to high temperature is assigned the symbol  $Y_{temp}$

Yellow due to high CO level is assigned the symbol  $Y_{co}$

The interaction between the three factors is expressed in this analysis by applying the following rules:

- Exposure to a temperature  $> 50$  °C and for longer than 5 minutes leads to “red”:

$Y_{temp}$  and  $>5$  min = red

- Exposure to a CO level  $> 250$  ppm and for longer than 5 minutes leads to “red”:

$Y_{co}$  and  $>5$  min = red

- Combined exposure leads to “red” immediately:

$Y_{temp}$  and  $Y_{co}$  = red

The reason for this rule is that the extra effect of exertion and stress while trying to find an exit in combination with either heat or carbon monoxide is supposed to be life-threatening.

- Visibility of less than 10 m in combination with either  $Y_{co}$  or  $Y_{temp}$  leads to “red” immediately:

$Y_{vis}$  and  $Y_{co}$  = red

$Y_{vis}$  and  $Y_{temp}$  = red

Our analysis was done using the following procedure.

From the data collected and the criteria given above, it was determined when and for how long each situation “Red” and “Yellow” lasted in each test and at each measurement location.

Also, it is indicated for each situation if high temperature or CO is the primary threat.

4.9.3 Evaluation of verification test 1

VERIFICATION TEST 13-12-2007				
Occurrence and timing life-threatening conditions (LTC)				at
20 m, 40 m, 100m and 300 m downwind of the fire.				
Distance from fire	20	40	100	300
Moderate danger starts ...s after ignition	110	200	220	400
Acute danger starts ...s after ignition	240	210	510	1110
Acute danger ends ...s after ignition	380	870	1200	1500
Moderate danger ends ...s after ignition	1180	1200	1210	1710

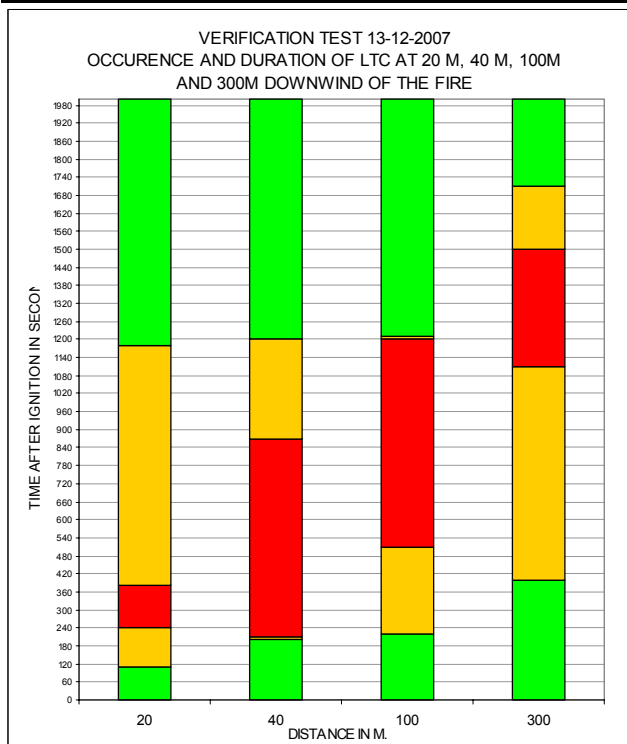


Figure 4.49. The water mist system was activated 335 s after ignition.

The fire load was a small lorry load of pallets, with a maximum RHR of 50 MW. The extinguishing medium was water with 1% AFFF added. The water mist-system was able to control and suppress the fire within a few minutes.

Tenability-factors:

- Close to the fire, high temperatures are the decisive threat, but as the smoke cools only carbon monoxide remains as a threat: at 20 m the high temperatures last only for about 2 minutes, but visibility remains poor (< 10 m) for 20 minutes. No CO data are available.
- At 40-50 m the high temperatures last for about 5 minutes until about 300 s. CO concentrations are high from 5 until 10 minutes after ignition, and visibility is again poor over the entire first 20 minutes.
- At 100 m, the CO concentration is dangerous between 6 and 20 minutes. Visibility is again poor over the entire first 20 minutes.
- At 300 m, the CO-peak occurs from 8 minutes to 25 minutes, and visibility is poor over the first 15 minutes.
- Both carbon monoxide and high temperature are significant threats, and the long duration of poor visibility (initially caused by smoke and later on by clouds of water droplets) worsens the effects of the two primary factors.

4.9.4 Evaluation of verification test 2

VERIFICATION TEST 19-12-2007				
Occurrence and timing life-threatening conditions (LTC) at m, 40 m, 100m and 300 m downwind of the fire.				20
Distance from fire	20	40	100	300
Moderate danger starts ...s after ignition	20	20	40	100
Acute danger starts ...s after ignition	40	30	211	120
Acute danger ends ...s after ignition	150	140	300	120
Moderate danger ends ...s after ignition	610	610	721	247

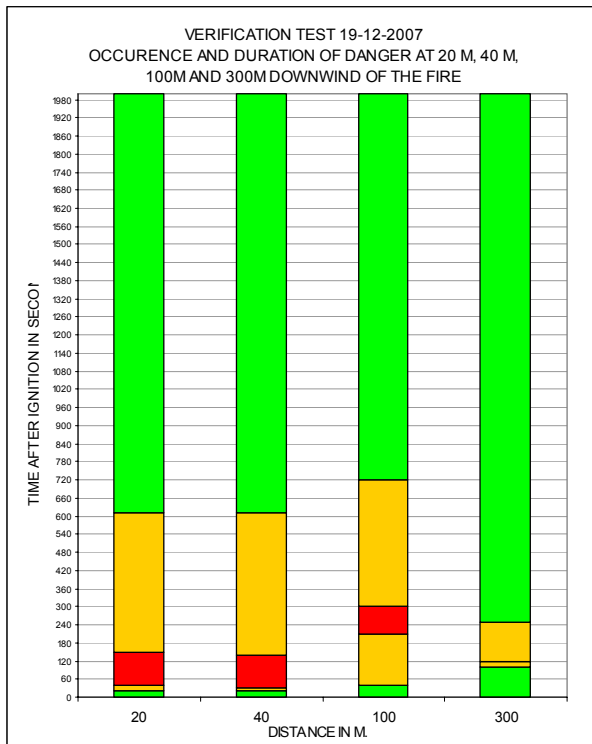


Figure 4.50 The water mist system was activated 96 s after ignition.

The fire load was a large pool fire, and the extinguishing medium was water with 1% AFFF added.

Tenability-factors:

- At 20 m and at 40-50 m the peak in temperatures (up to 600 deg C) coincided with the peak in CO-levels during 0 to 2.5 minutes. Visibility remained poor for about 5 minutes.
- At 100m and at 300 m, the carbon monoxide concentration remained at safe levels. No reliable temperature data are available at 100 m or at 300 m. Extrapolating from the temperatures at 40 m, it is likely that these will have led to condition “yellow” at 100 m at least. Combined with the poor visibility during the first 4 minutes, this leads to the conditions as shown in the figure.



4.9.5 Evaluation of performance test 1

PERFORMANCE TEST 9-1-2008				
Occurrence and timing life-threatening conditions (LTC) at 20 m, 40 m, 100m and 300 m downwind of the fire.				
Distance from fire	20	40	100	300
Moderate danger starts ...s after ignition	50	50	50	80
Acute danger starts ...s after ignition	60	60	130	160
Acute danger ends ...s after ignition	190	250	220	280
Moderate danger ends ...s after ignition	200	260	700	600

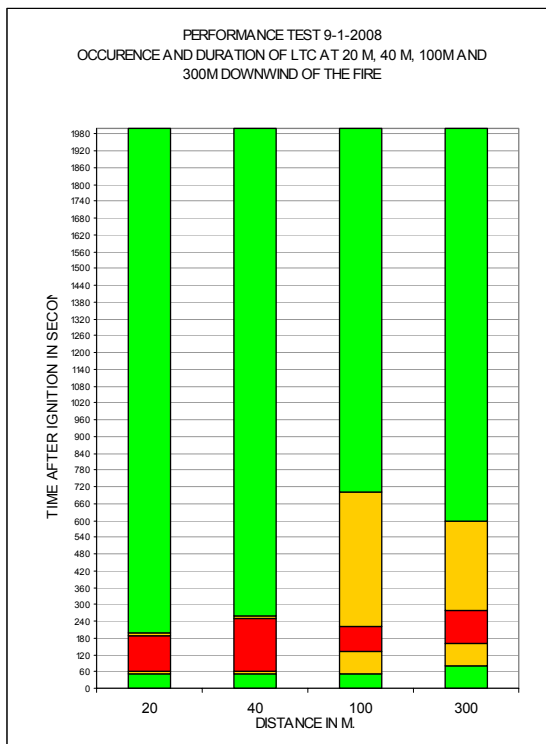


Figure 4.51 The water mist system was activated 125 s after ignition.

The fire load was the large pool fire, and the extinguishing medium was pure water (no additives).

The duration of the threat runs from 2.5 minutes at 20 m to 4.5 minutes at 300 m. The “red periods” are longer than during the test on 19-12-2007, indicating that pure water seems less effective in controlling and suppressing the fire than water with AFFF added.

Tenability-factors:

- At 20 m, the heat pulse from the fire lasts about 3 minutes and has a peak of more than 800 degrees C. At 50m, the pulse lasts for about 4 minutes with a slightly lower temperature.
- At 100m there are no reliable temperature data, but the CO-pulse of more than 1200 ppm lasts for about 4 minutes, and there is poor visibility during 12 minutes after ignition.
- At 300 m, the CO concentration stays just below 1000 ppm, and visibility is slightly better, resulting in a shorter “yellow” period.

4.9.6 Evaluation of performance test 2

PERFORMANCE TEST 14-1-2008				
Occurrence and timing life-threatening conditions (LTC) at 20 m, 40 m, 100m and 300 m downwind of the fire.				
Distance from fire	20	40	100	300
Moderate danger starts ...s after ignition	50	60	60	90
Acute danger starts ...s after ignition	70	60	70	120
Acute danger ends ...s after ignition	250	270	240	300
Moderate danger ends ...s after ignition	1500	1500	260	400

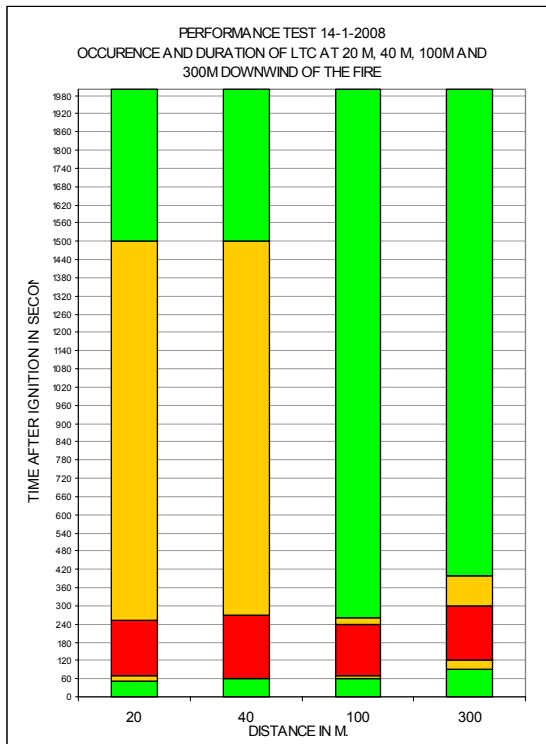


Figure 4.52 The water mist system was activated 160 s after ignition.

The fire load was a large pool fire, and the extinguishing medium was water with 1% Bioversal added.

The duration of the threat runs from 1 to about 5 minutes. The “red “periods are, if anything, longer than during the test on 9 January 2008, indicating that using water with a biodegradable AFFF seems certainly not more effective in controlling and suppressing the fire than using pure water.

Tenability-factors:

- At 20 m the heat pulse with a maximum temperature of > 900 deg. C lasts about 4 minutes. Visibility stays poor for a longer time due to effects of the WMS.
- At 40-50 m the situation is similar, with slightly lower temperatures of about 700 deg C.
- At 100 m, the pulse of heat (at 550 deg C maximum), high CO-concentration and poor visibility occur in the same time interval of about 5 minutes after ignition.
- Also at 300m, the heat pulse, the poor visibility and the high CO concentration last for about 6 minutes.

4.9.7 Evaluation of performance test 3

PERFORMANCE TEST 17-1-2008				
Occurrence and timing life-threatening conditions (LTC) at 20 m, 40 m, 100m and 300 m downwind of the fire.				
Distance from fire	20	40	100	300
Moderate danger starts ...s after ignition	150	130	220	260
Acute danger starts ...s after ignition	220	150	230	270
Acute danger ends ...s after ignition	1560	1570	2000	2000
Moderate danger ends at ...s after ignition	2000	2000	2000	2000

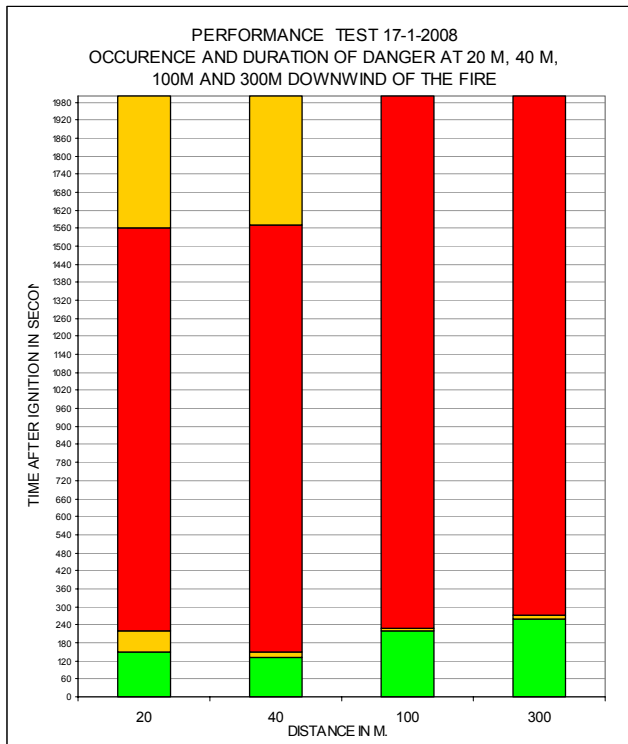


Figure 4.53 The water mist system was activated 439 s after ignition.

The fire load was a large lorry load of 720 pallets, with a maximum RHR of approximately 200 MW. The extinguishing medium was water without additives. The water mist-system was marginally able to control and suppress the fire.

- At 20 m, the temperature rose to lethal levels between 3 min and 22 min after ignition.
- At 40-50 m, conditions and times were similar. Visibility was poor for about 35 minutes after ignition.
- At 100m, high temperatures lasted until 22 minutes, but lethal CO concentrations and poor visibility persisted until 35 minutes. Similar conditions were found at 300 m.

#### **4.10 Conclusions**

Threats to human safety and health do occur during these tests in the region between the fire and 300 m downwind, and possibly much further. It is a dangerous place to be indeed.

In the tests described here, the dangers presented by high temperatures and by carbon monoxide were both serious, and they occurred more or less simultaneously. A fundamental difference between the two is the effect of distance from the fire. At longer distances from the fire, the gases flowing through the tunnel will have cooled, and beyond a certain point their temperature will no longer present a risk. However, the carbon monoxide content of the gases flowing through the tunnel is not significantly reduced, and will continue to present a real risk to human beings much further downstream.

The mitigating effect of the water mist-system on the dangerous conditions is quite clear: the pool fires were of short duration, in the order of a few minutes, and the high temperatures and dangerous CO concentrations vanished within minutes after the fire was extinguished. The pallet fires took much longer to extinguish, in particular the last test-fire, and the conditions downwind remained untenable for the duration of the fire.


No special negative effects of the water mist system were observed beside the reduced visibility downwind of the fire during operation. The test fires had a large rate of heat release and produced significant circulation and mixing of hot smoke and cool air. Additional disruption of stratification by the suppression system may have occurred, but the tests were not designed to investigate this disruption. The relative humidity in the tunnel downwind of the fire will rise as an effect of activating the water mist system. In addition, a hydrocarbon fire or a carbohydrate (wood) fire itself will also produce a significant amount of water (about 5 kg/s for a 100 MW fire). It is estimated that the possibly negative effect of higher humidity is small compared to the direct positive effect of suppressing the fire.

To summarize: The reduction in fire size and duration that is achieved with a suppression system has a strong overall beneficial effect on the duration of untenable conditions downwind of a tunnel fire, especially for pool fires.

#### **4.11 Recommendations**

The tests show that early detection of the fire and a quick response of the suppression system will lead to a reduction of the fire size and therefore drastically improved conditions downstream. This knowledge should be incorporated in future designs of suppression systems in tunnels

From the results of the tests it appears that staying inside a stationary car downstream of a tunnel fire that is being extinguished may be a suitable strategy under specific circumstances, because of the short duration of the untenable conditions. It should therefore be investigated if it is always good advice to leave the car as soon as possible.



Ir. V.J.A. Meeussen



Ir. A.D. Lemaire

This report is issued by Efectis Nederland BV (previously TNO Centre for Fire Research). Efectis Nederland BV and her sister company Efectis France are full subsidiaries of Efectis Holding SAS since 1 January 2008, in which the Dutch TNO and the French CTICM participate. The activities of the TNO Centre for Fire Research were privatized in Efectis Nederland BV since 1<sup>st</sup> July 2006. This is in response to international developments and requests by customers. In order to be able to give a better answer to the customer's request and offer a more comprehensive service of high quality and a wider range of facilities, the international collaboration has been further expanded. This is done with highly experienced partners in fire safety in Norway (Sintef-NBL), Spain (Afiti-Licof), Germany (IFT), USA (South West Research Institute) and China (TFRI). Further information can be found on our website.

## 5 References

- [1] Van Schepdael L, P. Globevink. “Rijkswaterstaat Steunpunt tunnelveiligheid, Explosie tankauto’s, Fase 1”, Verslag Solico nr r\_597-1 rev.-, 6 december 2005
- [2] Van Schepdael L, P. Globevink. “Rijkswaterstaat Steunpunt tunnelveiligheid, Explosie tankauto’s, Fase 2: analyse tankauto LPG”, Rapport Solico nr r\_597-2 rev.1, 3 juli 2006
- [3] Draft Report SINTEF NBL, to be published
- [4] Lemaire A.D, V.J.A. Meeussen, “Methodiek globale beoordeling BLEVE risico op basis van volle schaal brandproeven in een tunnel met een watermist systeem”, Efectis rapport nr. 2007-Efectis-R0841, november 2007
- [5] L. Haffmans, “Menselijk gedrag bij brand”, SBR-rapport nr. BI 83-33, mei 1983

## 6 Acknowledgements

The authors wish to thank the following persons:

Our colleagues Arjo Lock and Ton Eekhout for their hard work, inventiveness and for their enthusiasm during preparation in Rijswijk and during the tests in Andalsnes.

Also Lea Tiwon who was always quick to sort out all complicated arrangements for travel and accommodation.

Rik van Bragt and Sandra Maijer who managed to source and buy all the technical equipment in time, and took very good care of the shipment to Norway.

Finally, we want to thank Per Fiva of Statens Vegvesen for his hospitality on the test site, for organizing all subcontracting on site for us, and of course for the coffee.

## **A Technical information measurement equipment**

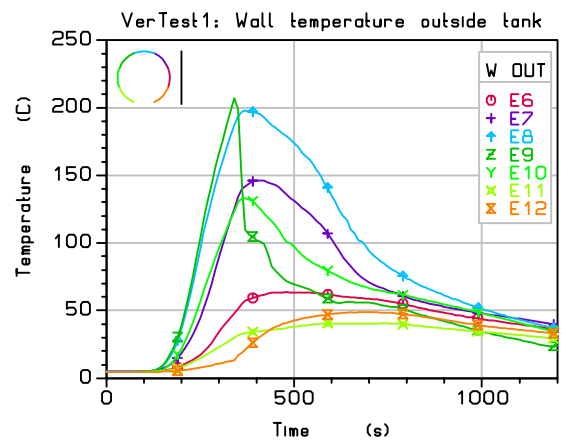
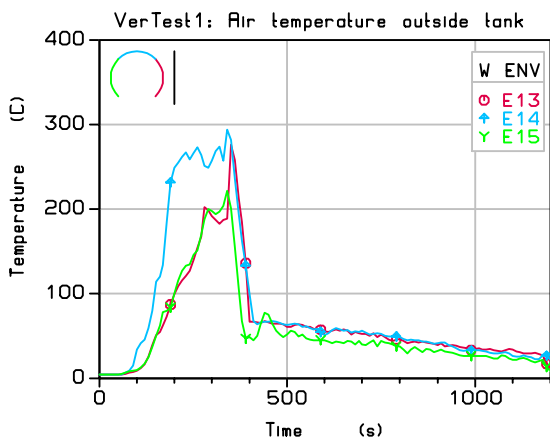
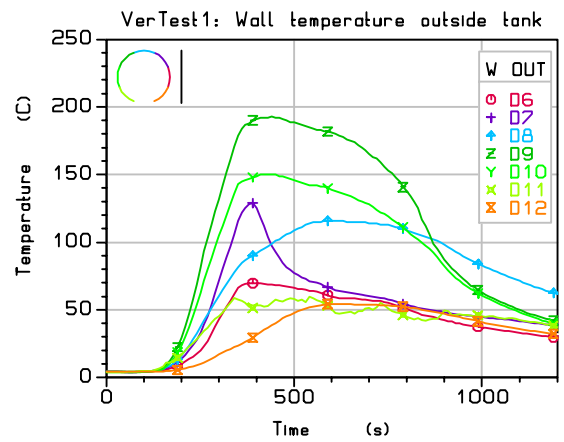
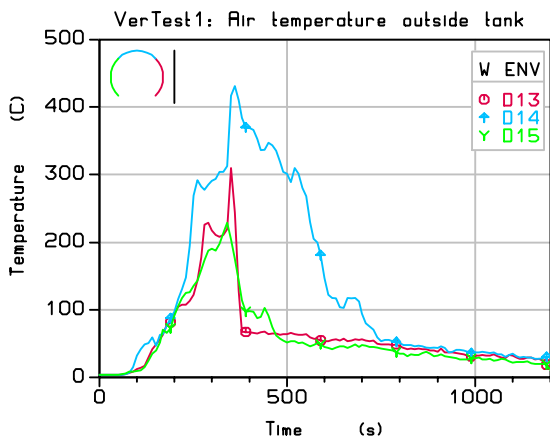
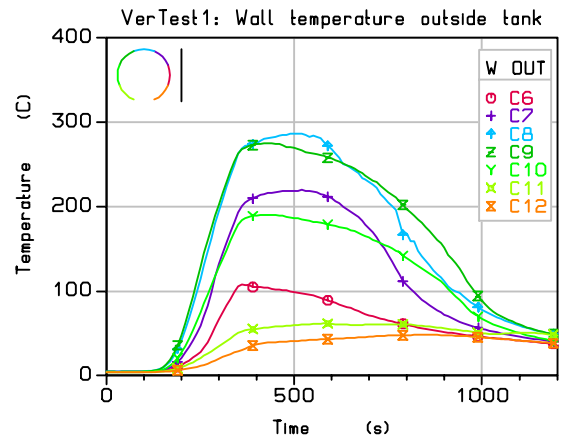
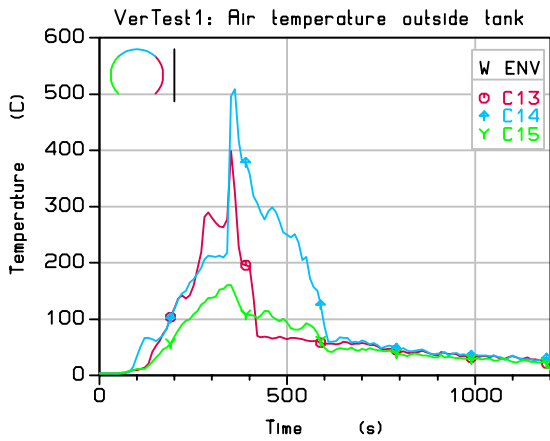
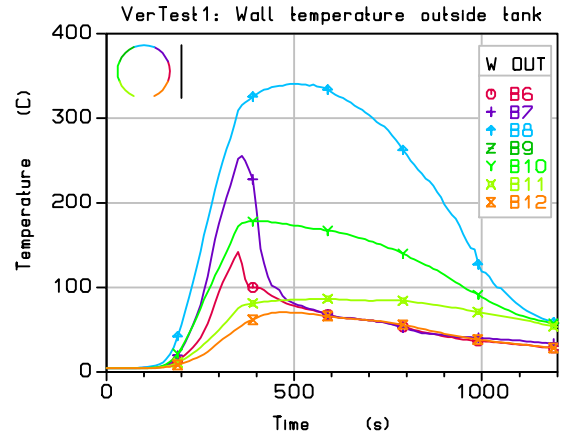
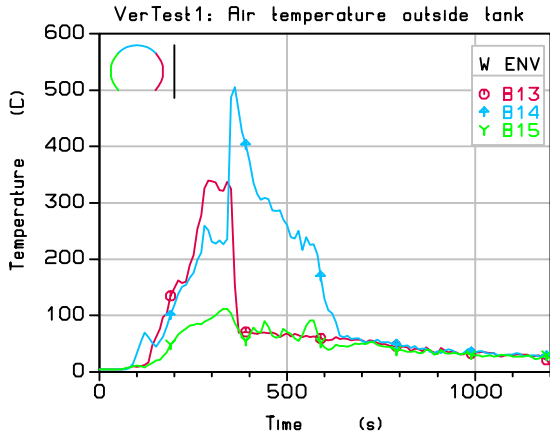
All temperatures were measured with Type K thermocouple wires with a diameter of 1.5 mm and a temperature range up to 1250 °C.

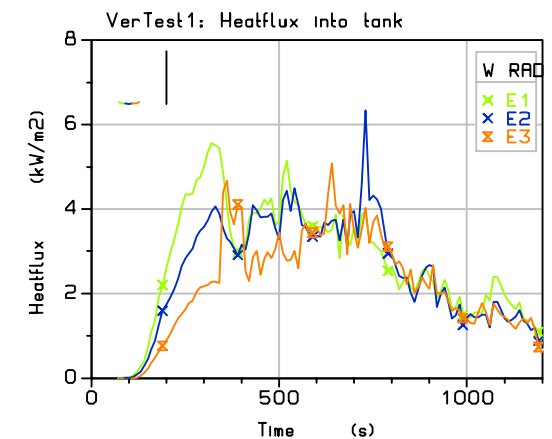
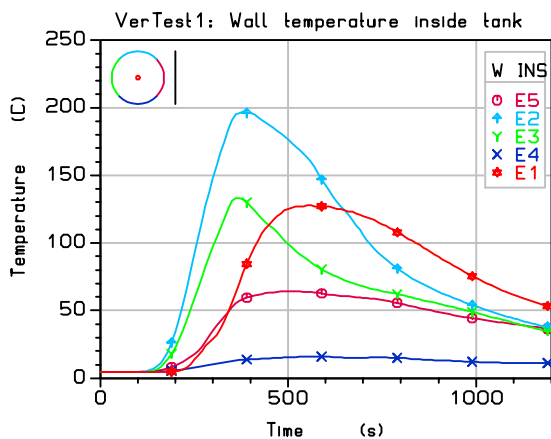
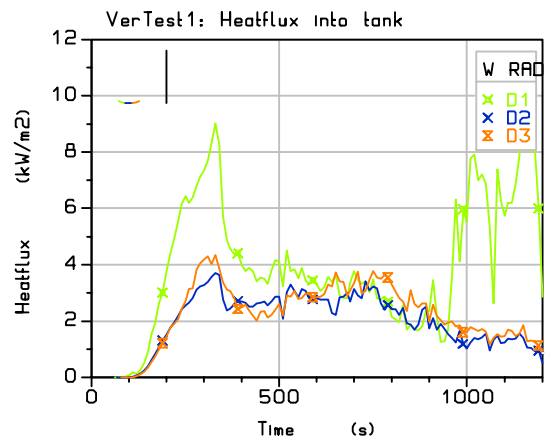
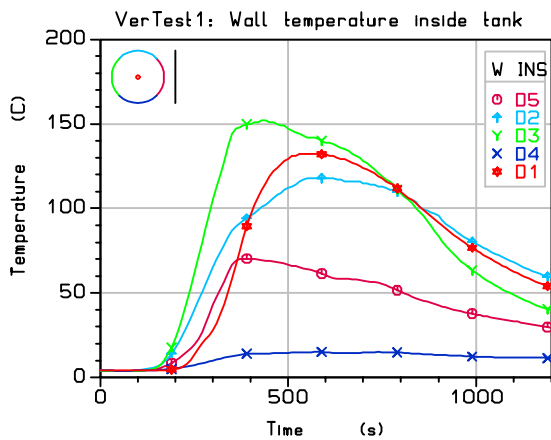
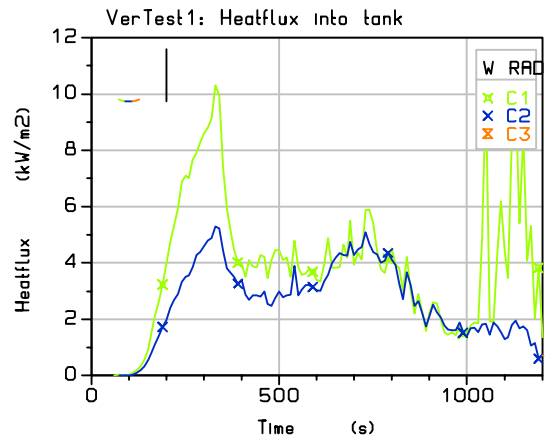
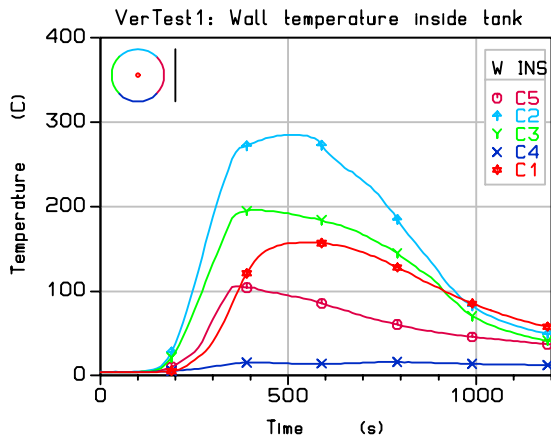
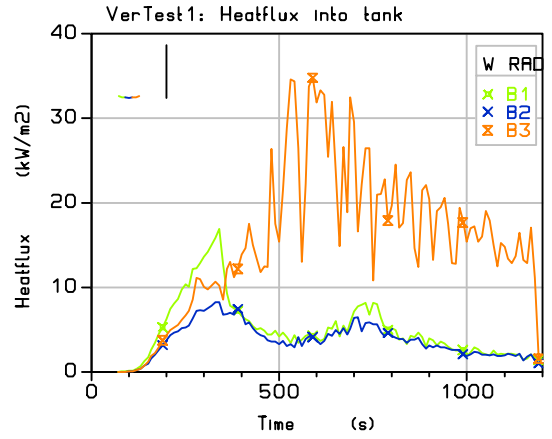
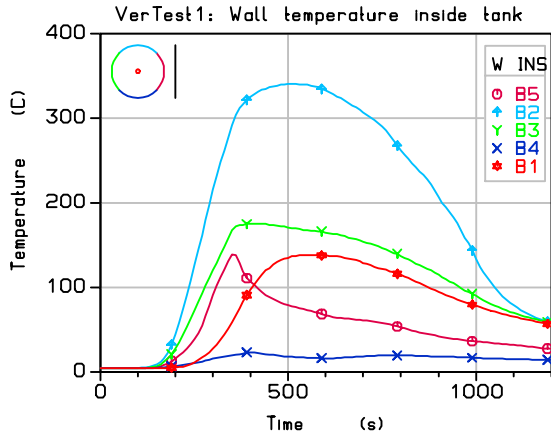
The radiation heat flux from the fire was measured with Schmidt-Boelter type water cooled heat flux meters from MedTherm. The measuring range of the sensors varied from 0 – 20 kW/m<sup>2</sup> up to 0 - 200 kW/m<sup>2</sup> dependent on the location and test performed. In some tests the measured heat flux exceeded the specified range of the sensor. When that occurred the sensor was replaced after the test and recalibrated at Efectis including the measured heat flux range. The errors due to the exceeding of the specified range turned out to be less than 10 %. As general known, the deviations are relatively small because of the nature and measuring principle of the sensor. No corrections were therefore made in the final processing of the heat flux data.

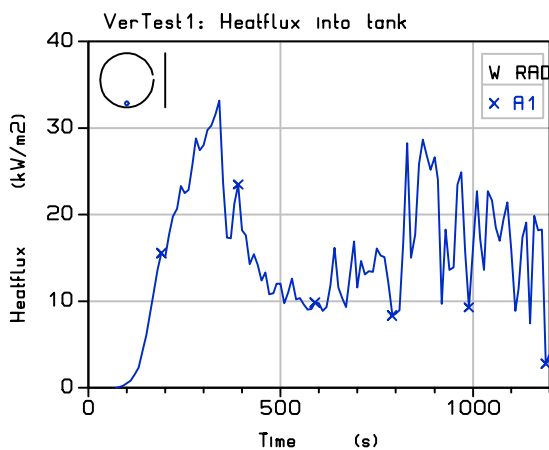
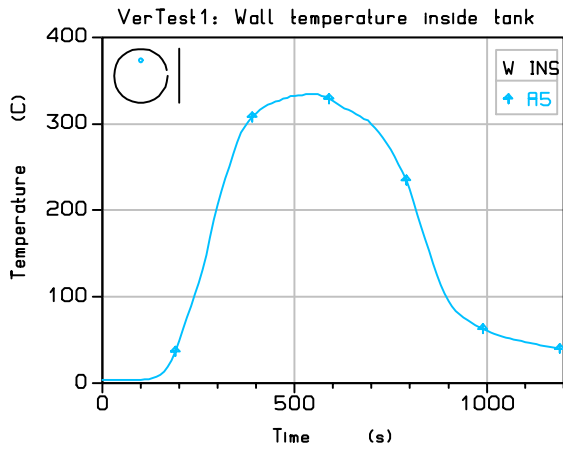
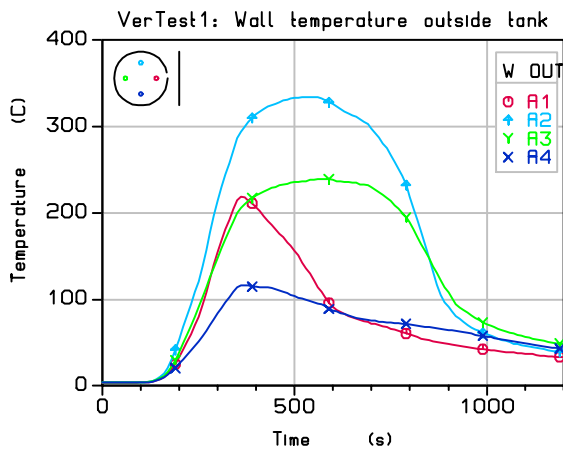
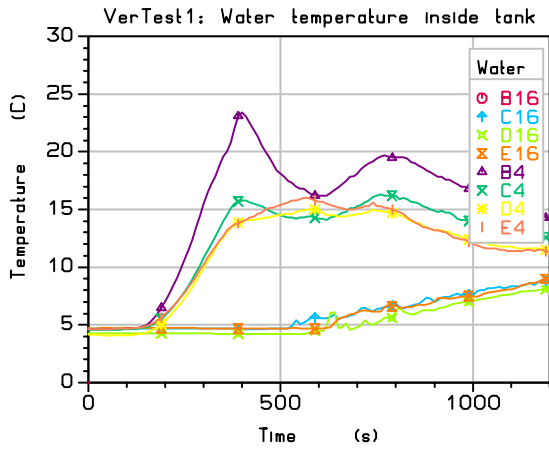
The sensor signals were measured and converted by 2 Agilent HP-3970 data loggers. Each data logger was connected to a ASUS laptop with a USB 2.0 GPIB interface in conjunction with a PCMIA USB connector. Agilent IO libraries suite 14.2 and Agilent 82357B drives were installed for the GPIB interface. The data loggers were labelled data logger A and data logger B. Data logger A measured the signals of all heat flux meters and thermocouples on section A, C and E on the tank wall surface. The remaining heat flux meters and thermocouples were connected to data logger B. In this way sufficient data would remain in case of a failure of one of the data logging systems.

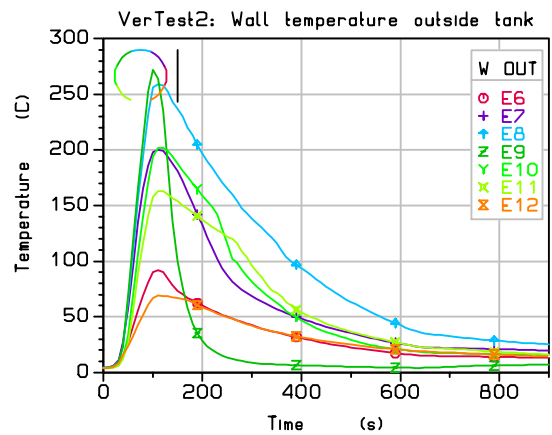
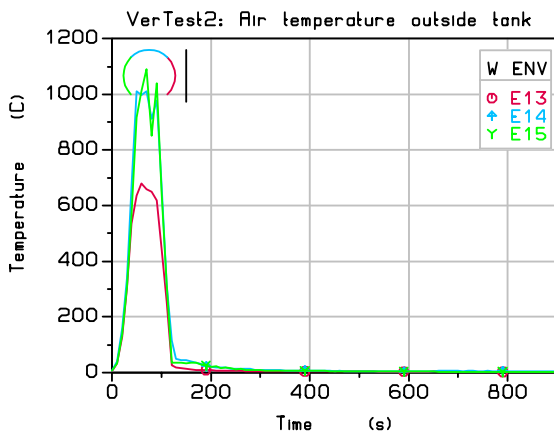
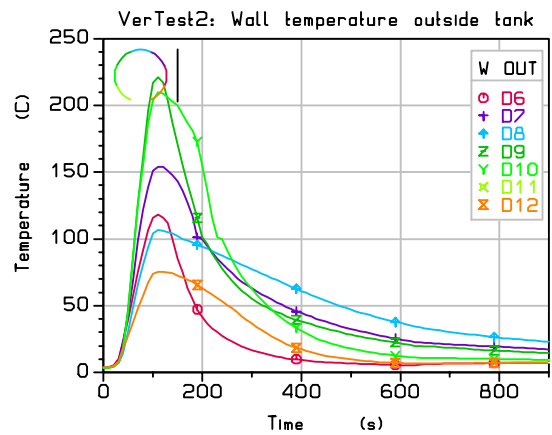
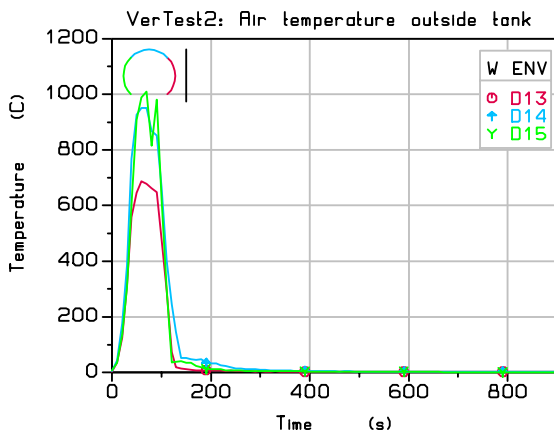
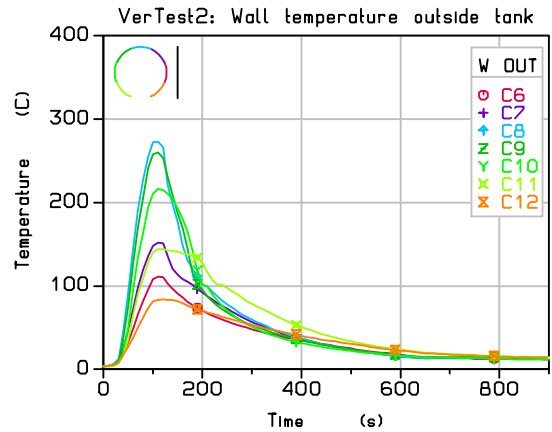
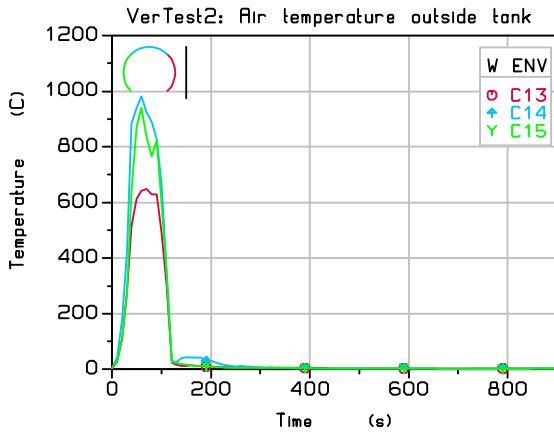
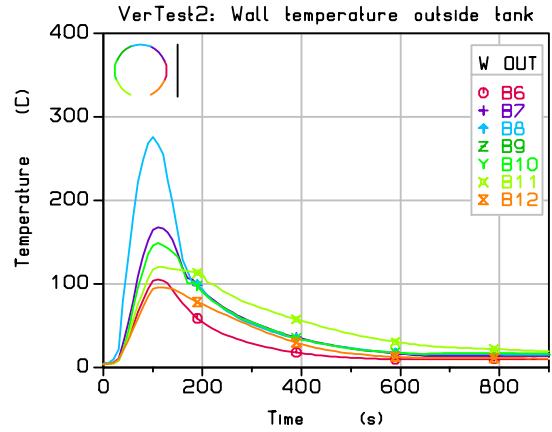
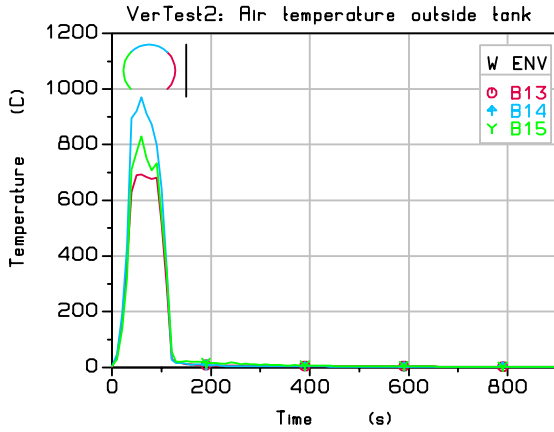


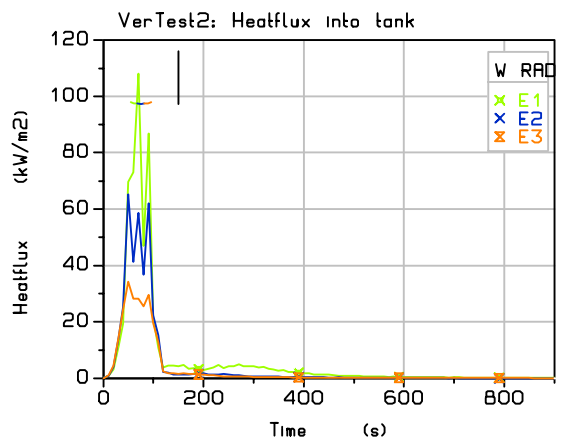
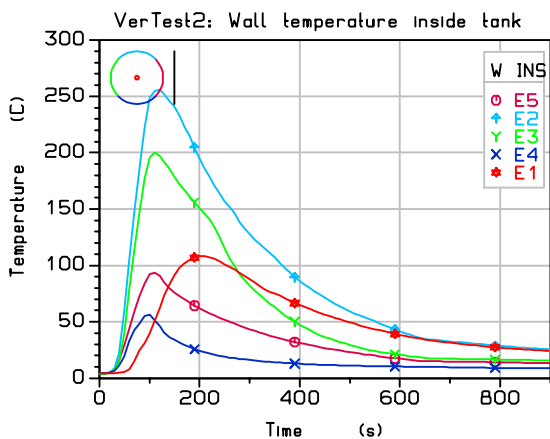
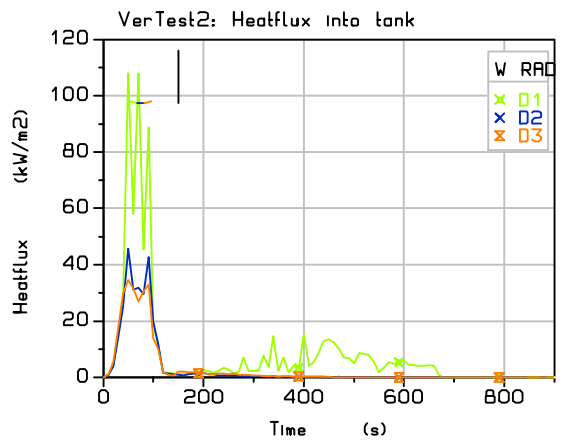
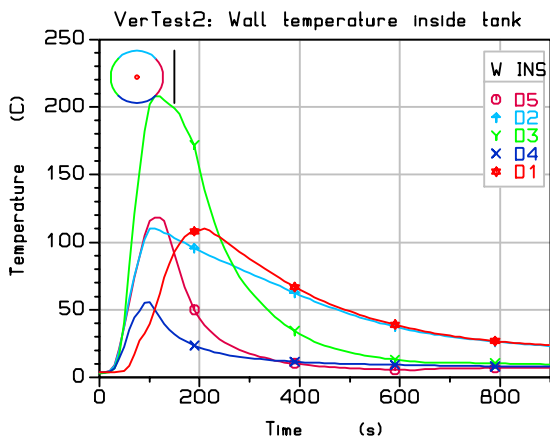
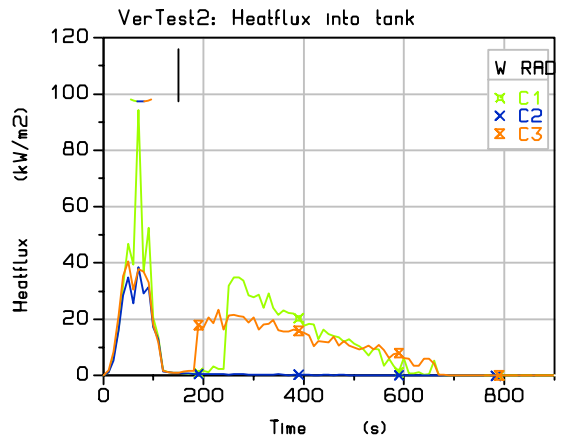
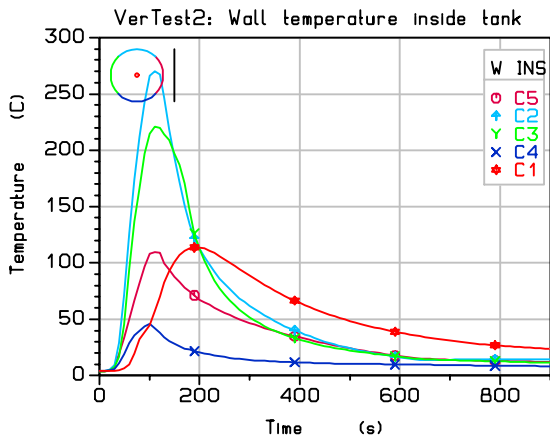
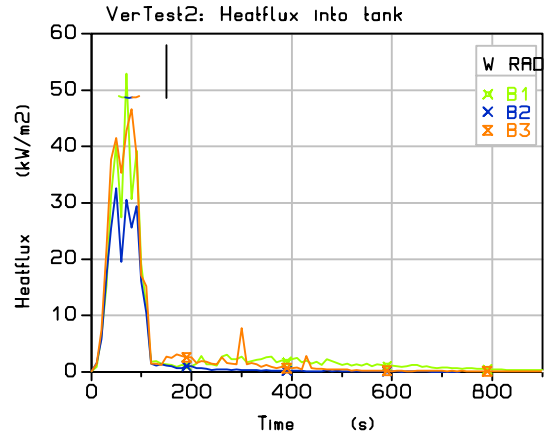
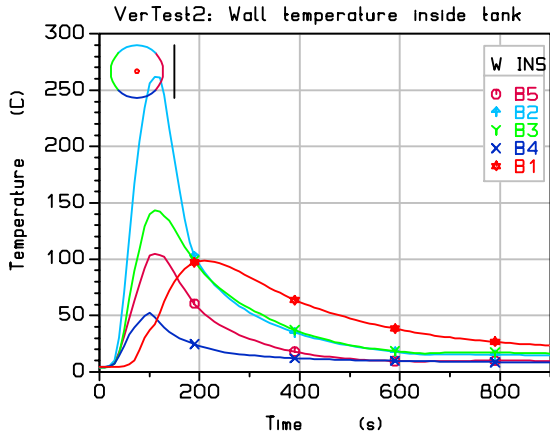
## **B Presentation of measured data on the test tank**

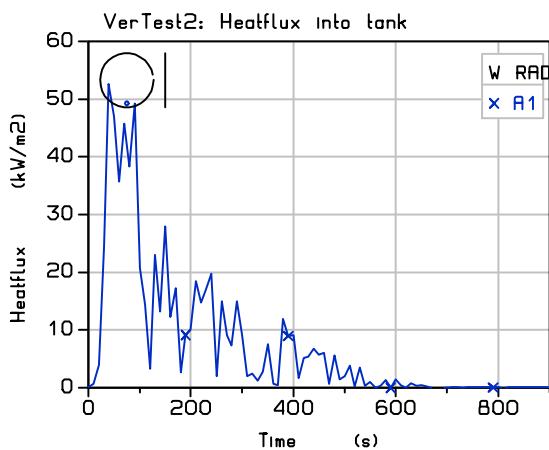
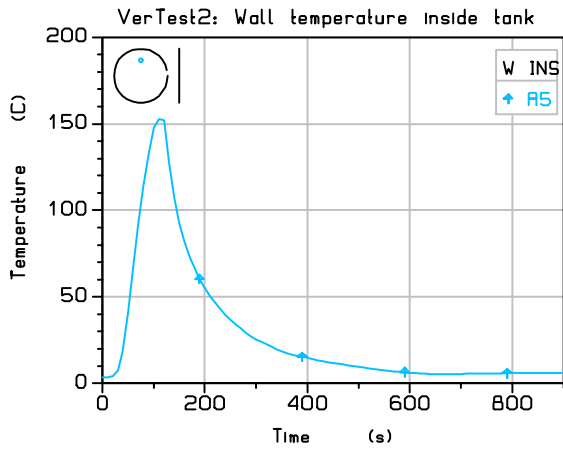
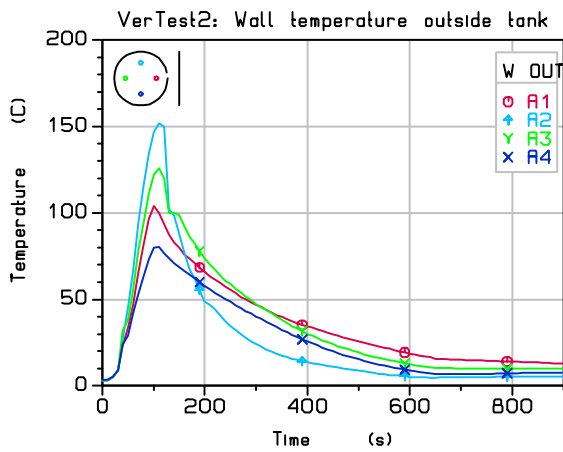
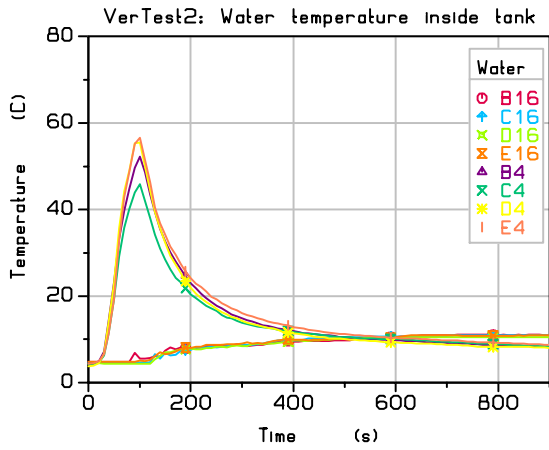


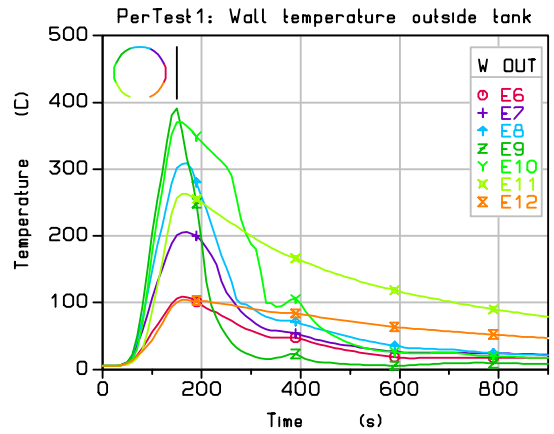
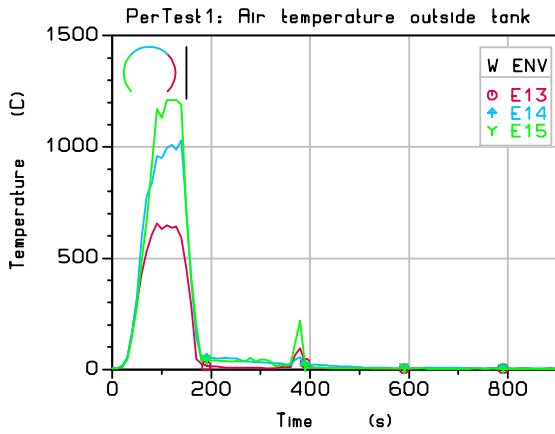
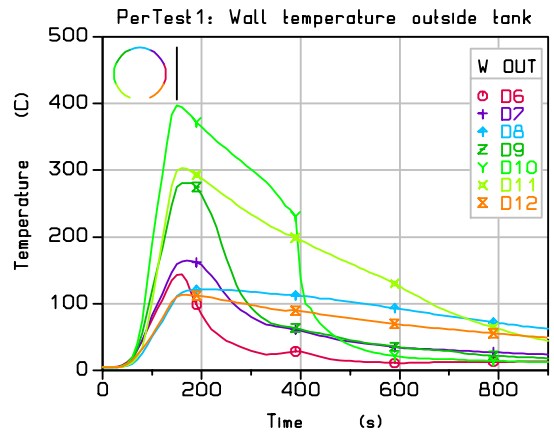
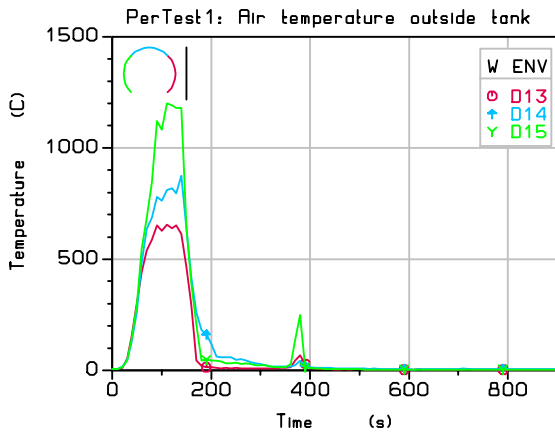
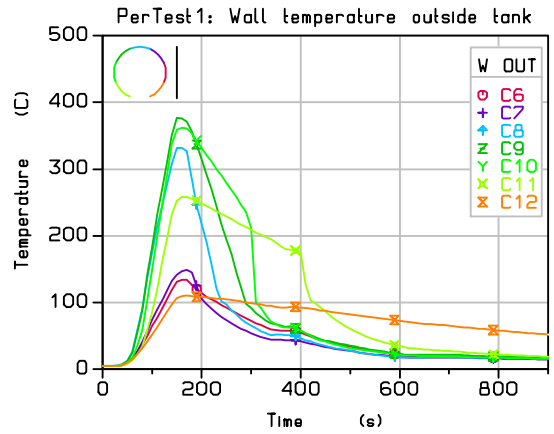
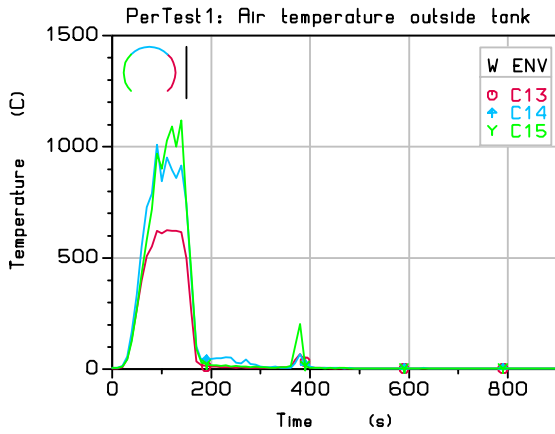
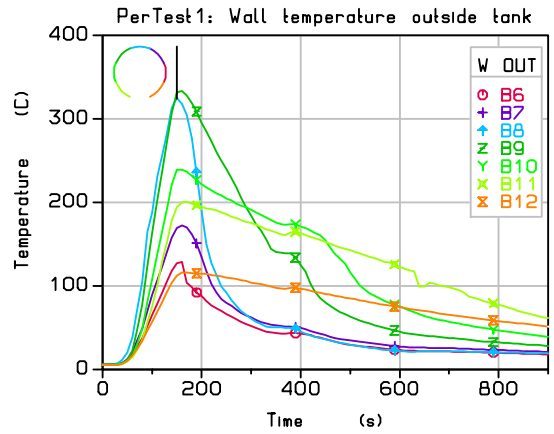
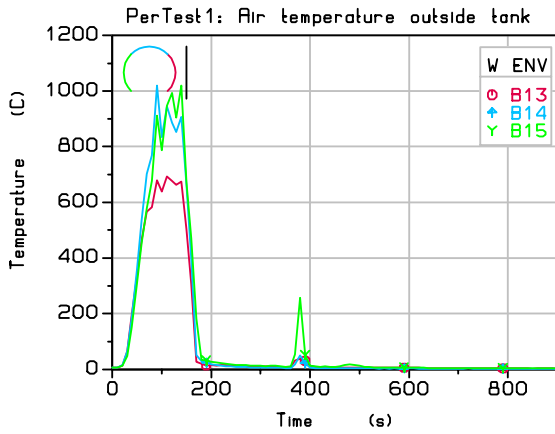




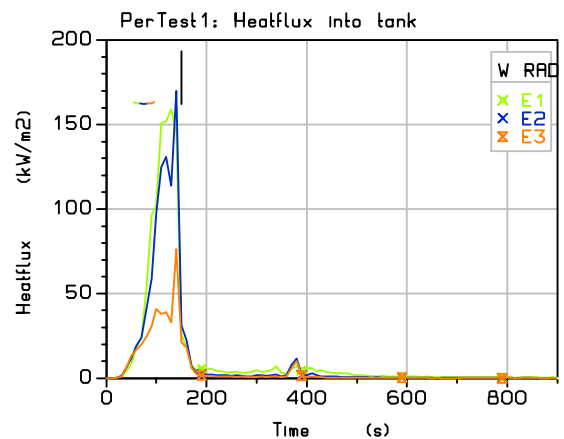
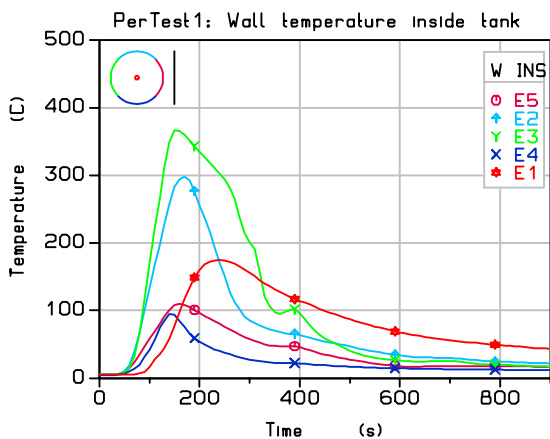
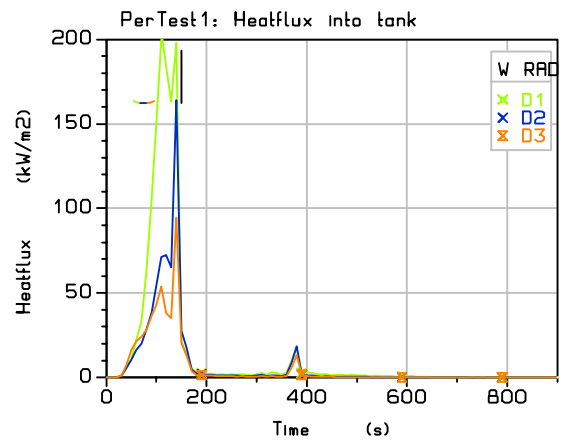
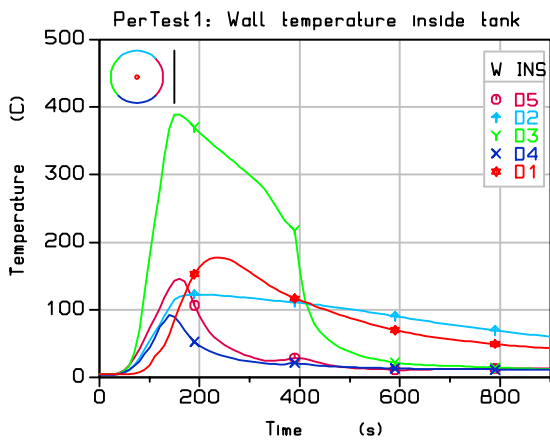
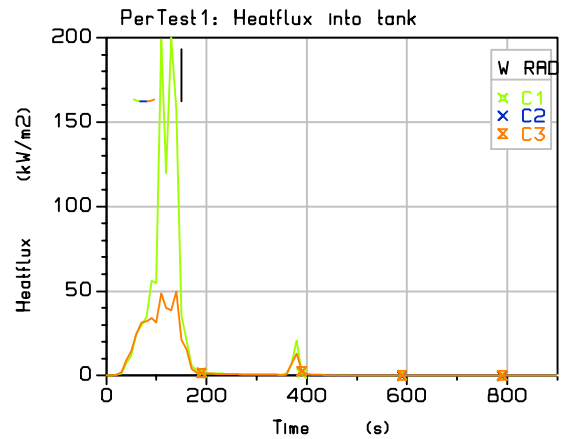
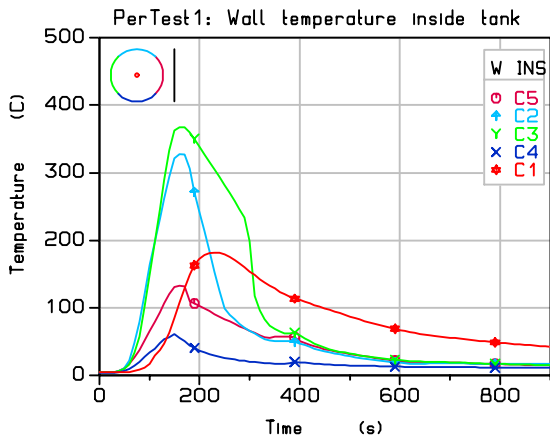
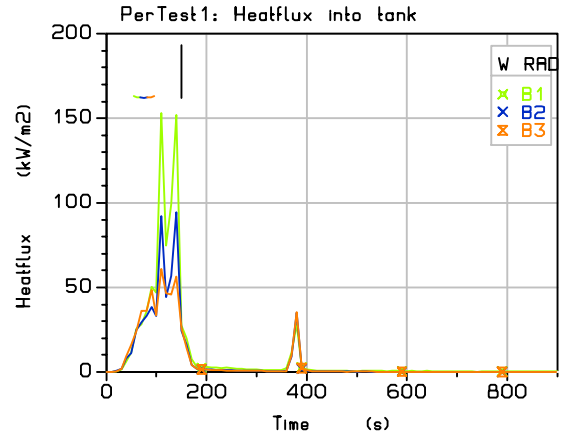
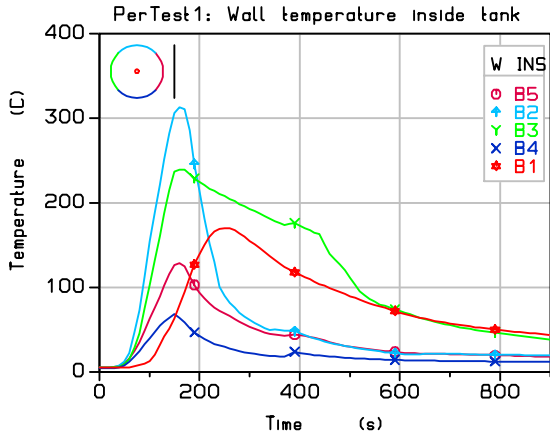


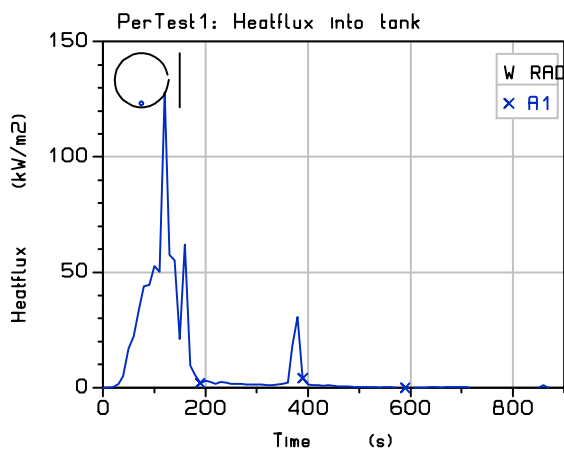
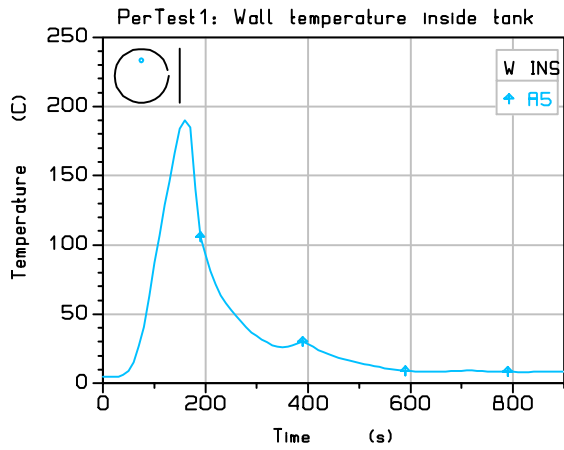
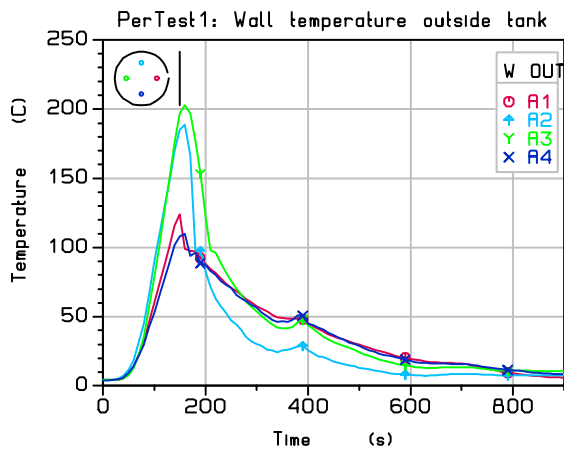
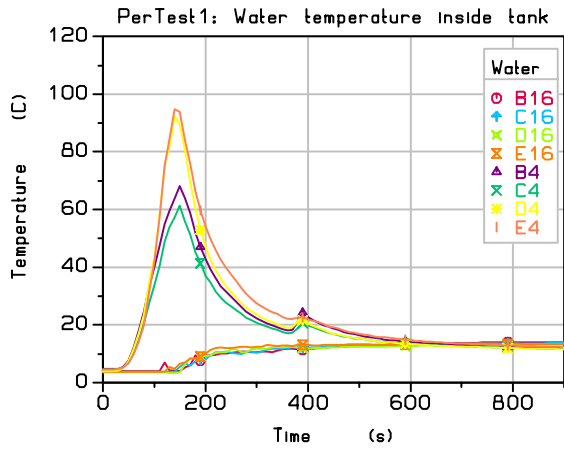


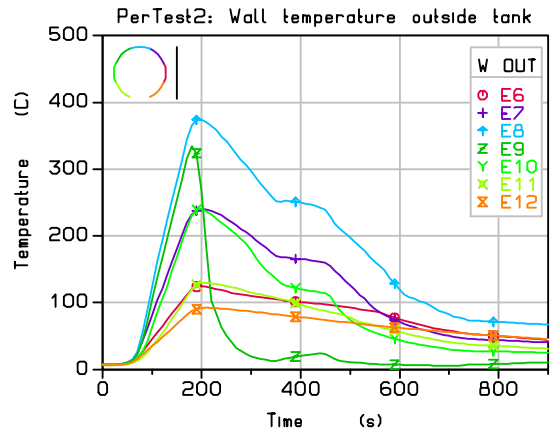
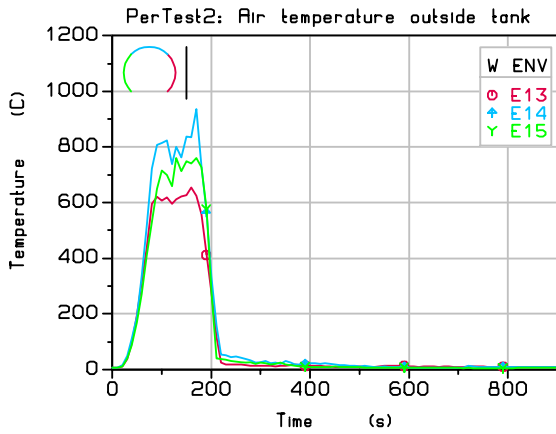
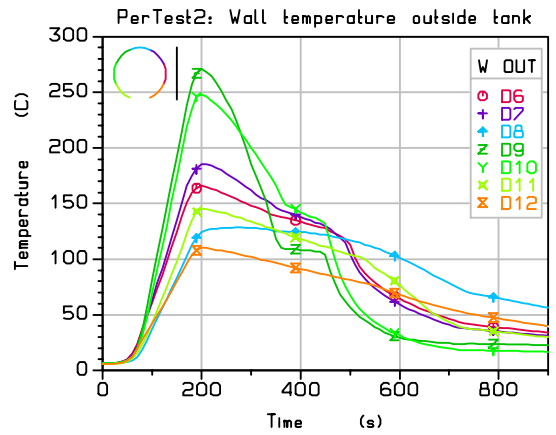
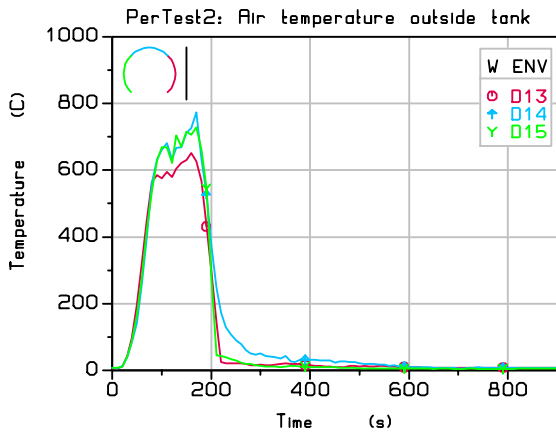
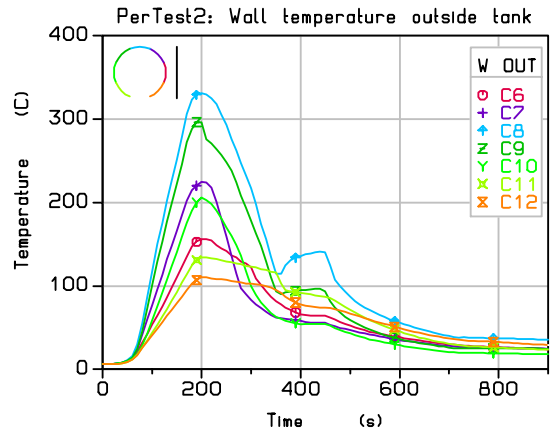
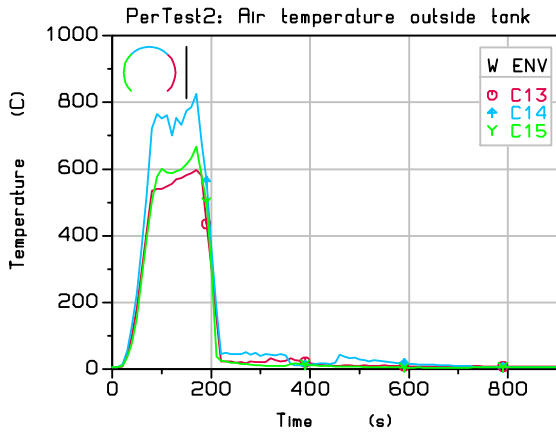
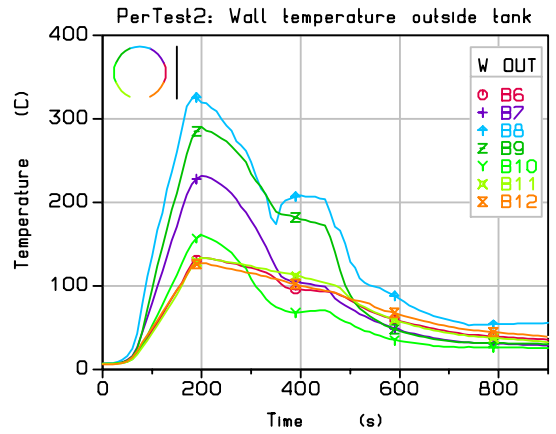
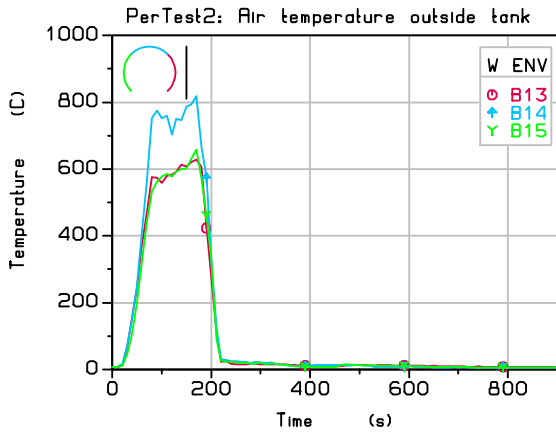


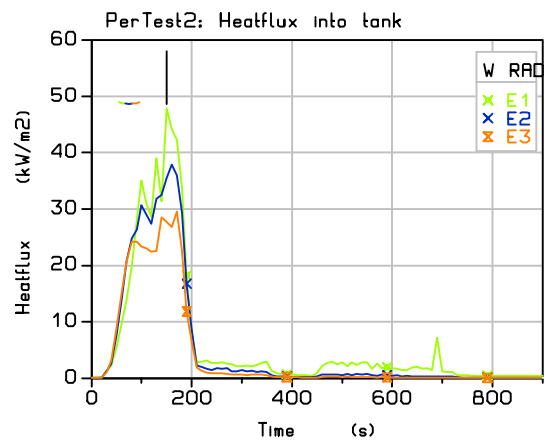
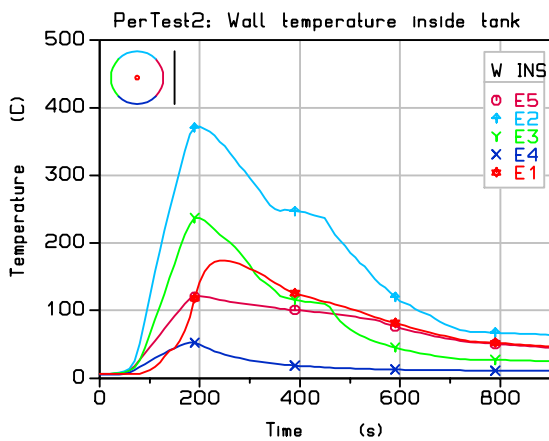
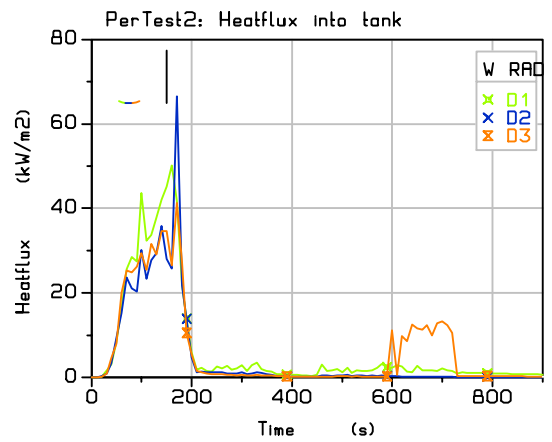
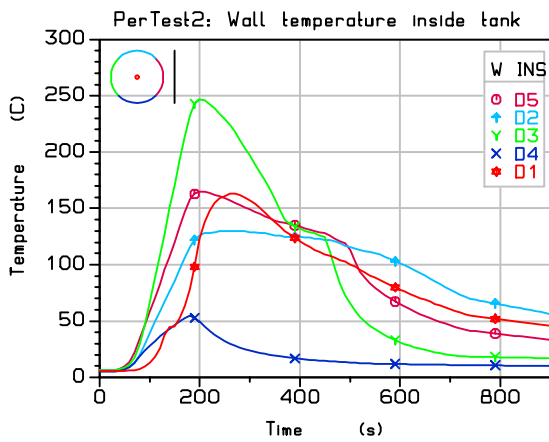
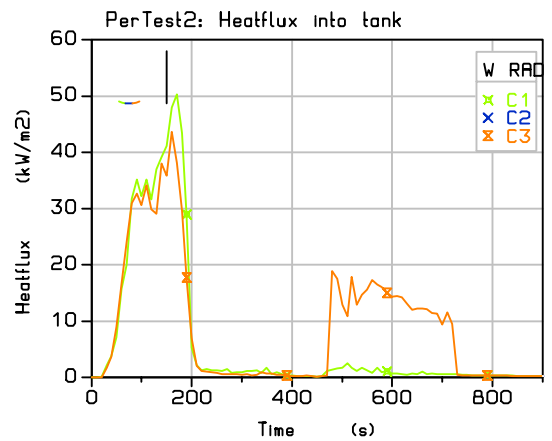
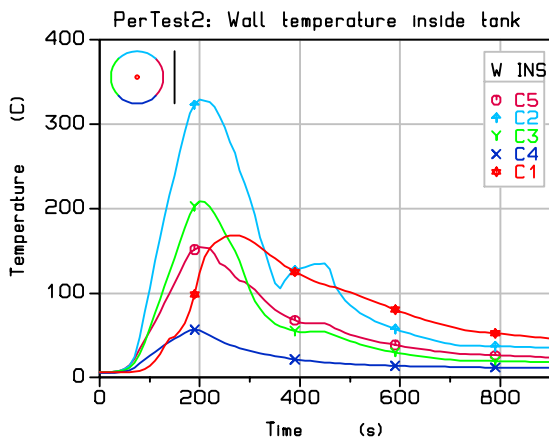
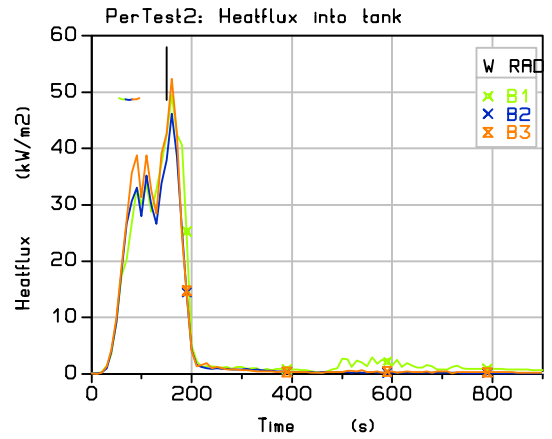
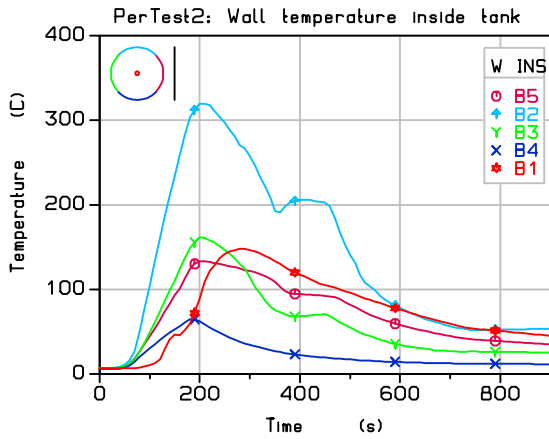


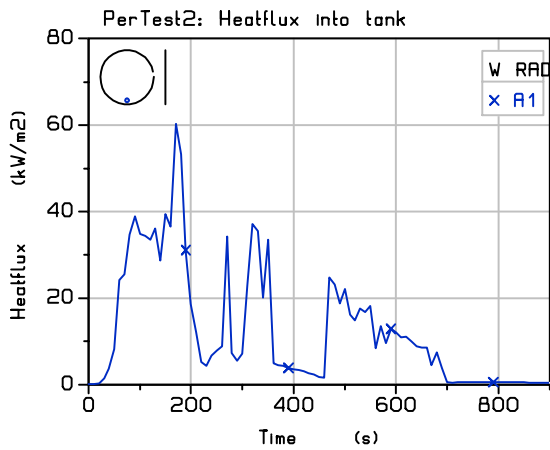
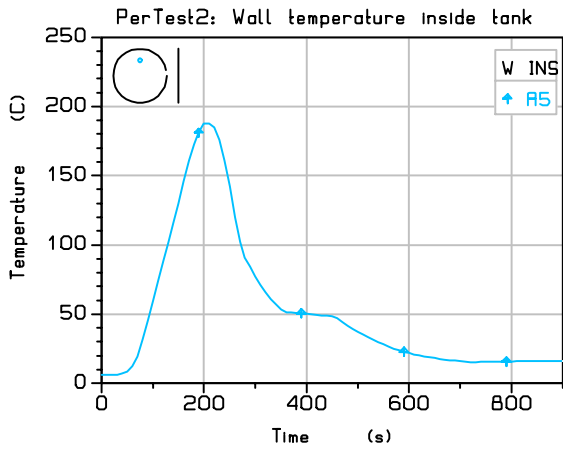
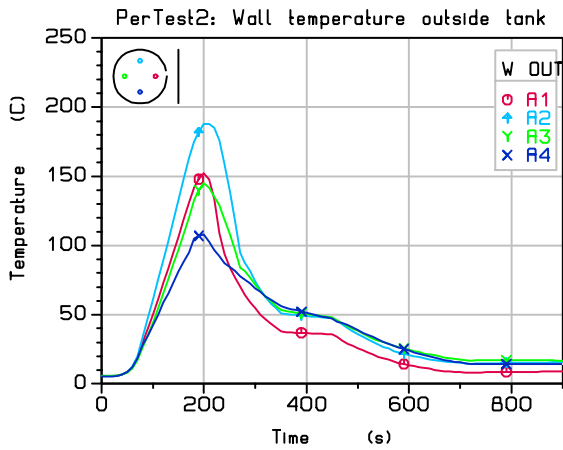
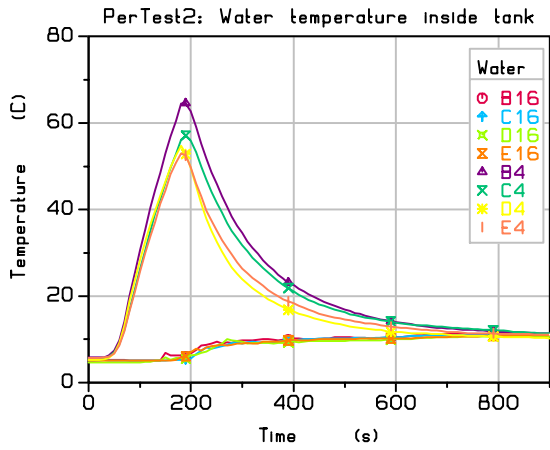


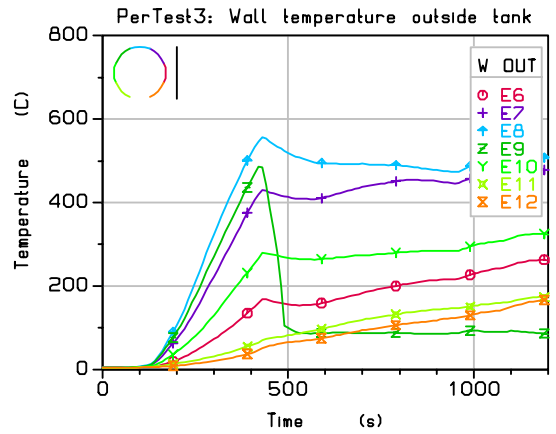
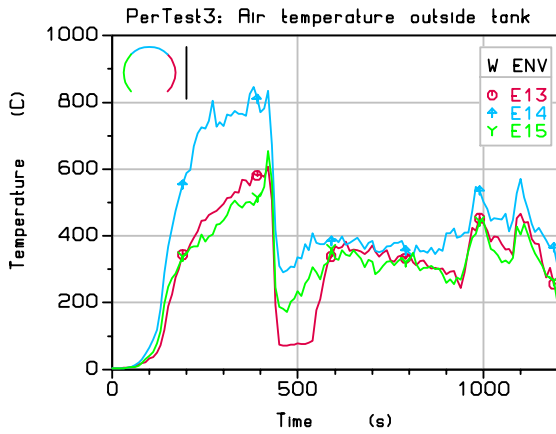
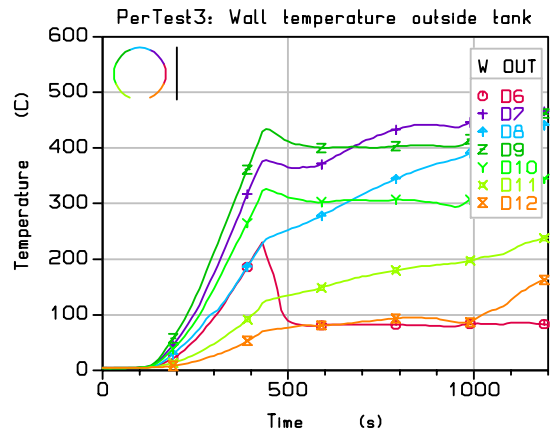
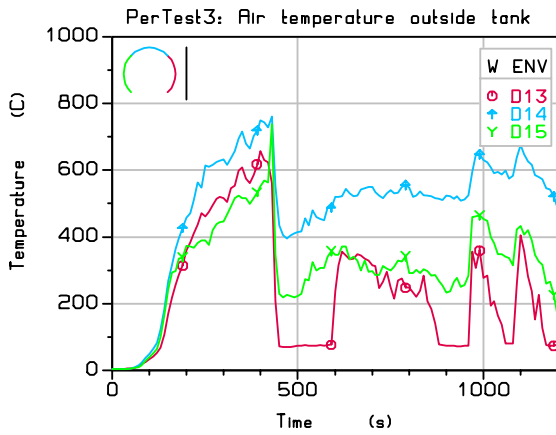
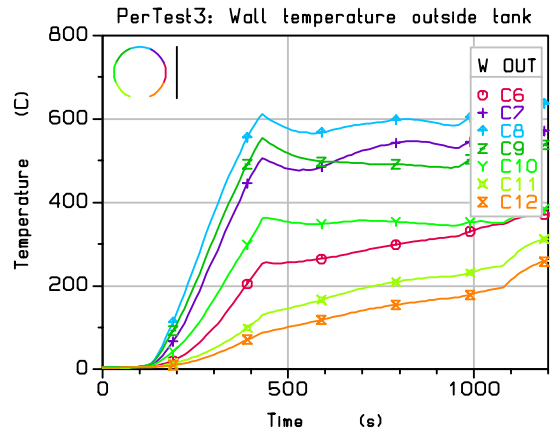
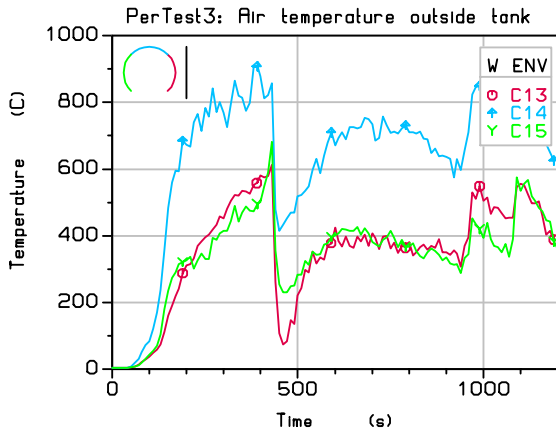
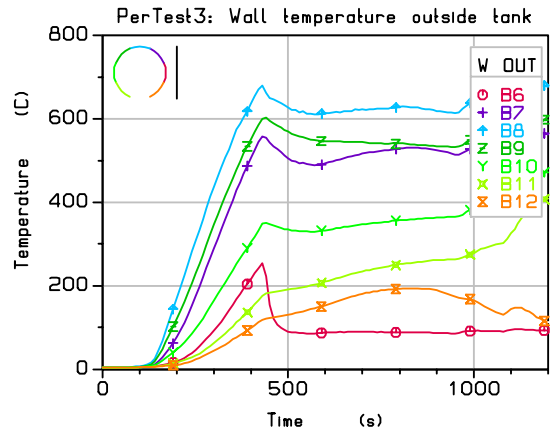
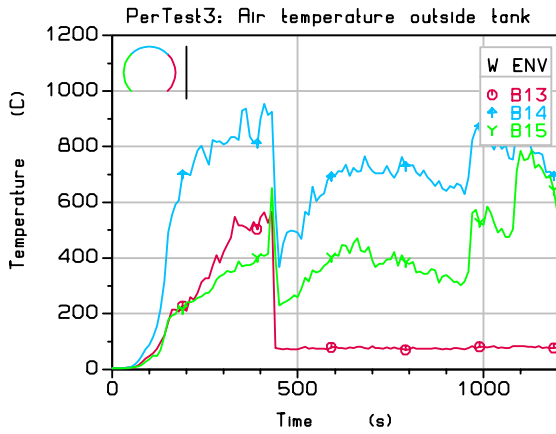


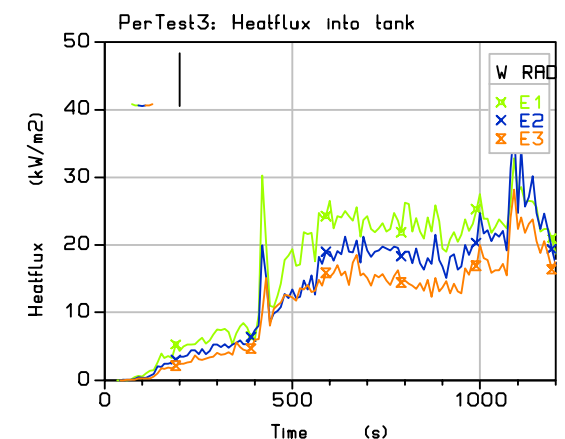
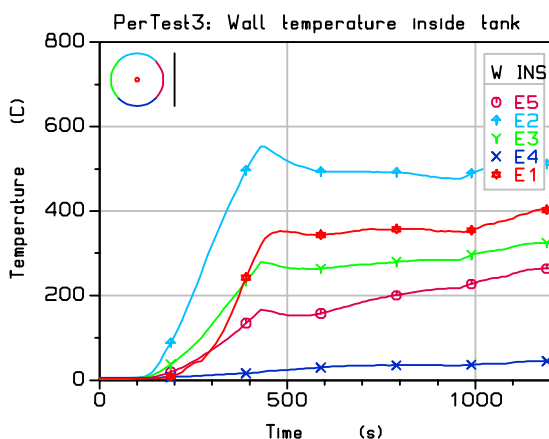
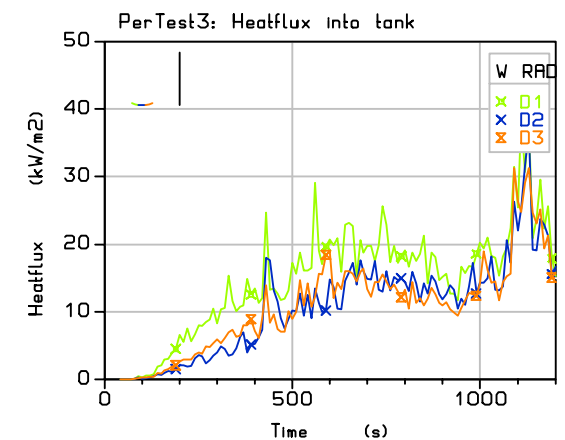
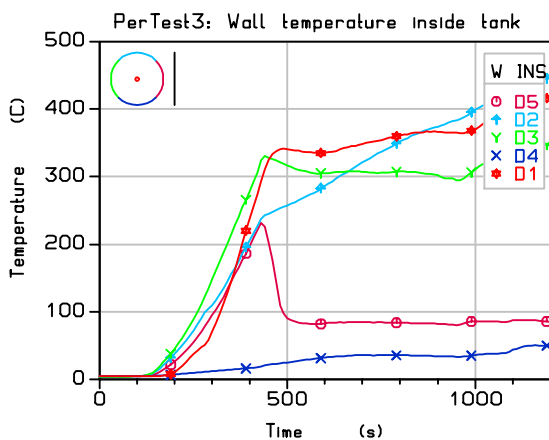
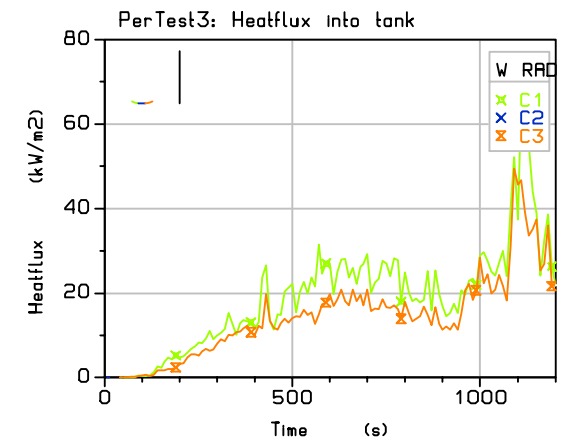
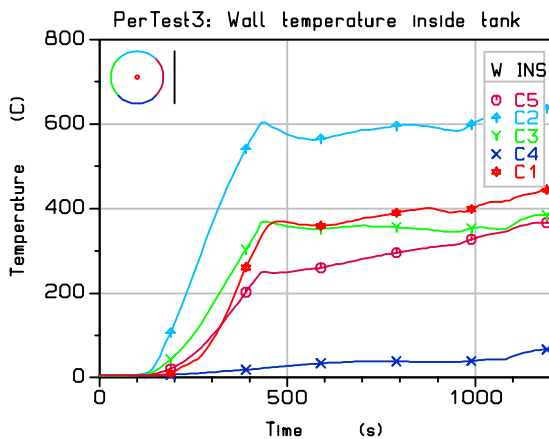
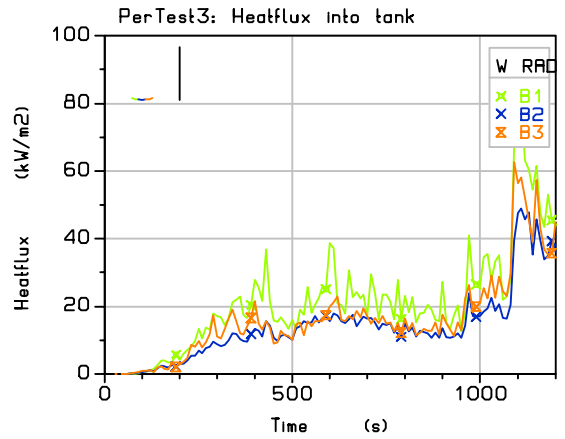
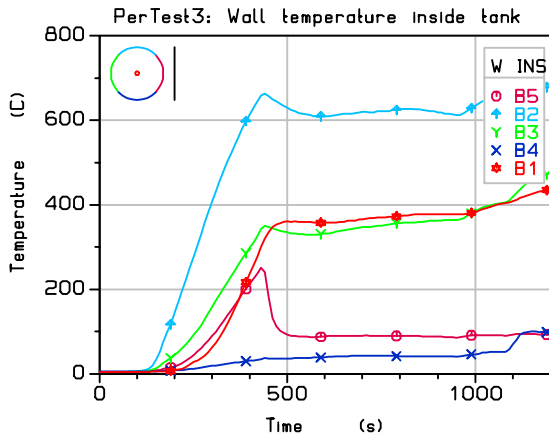


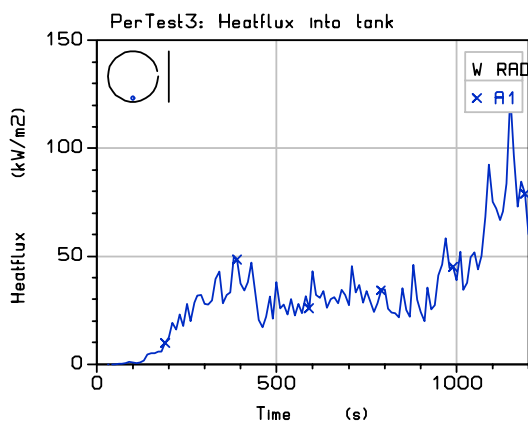
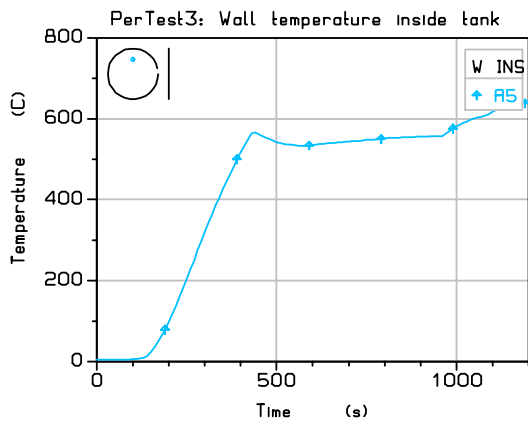
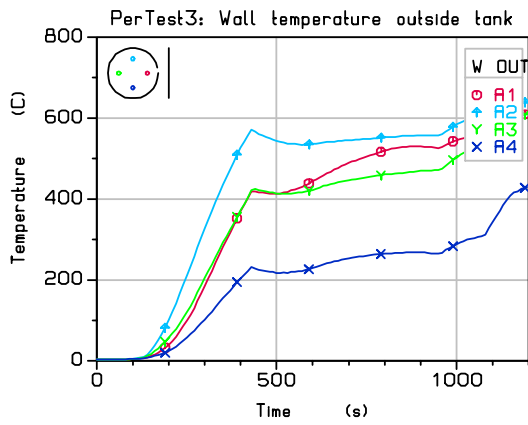
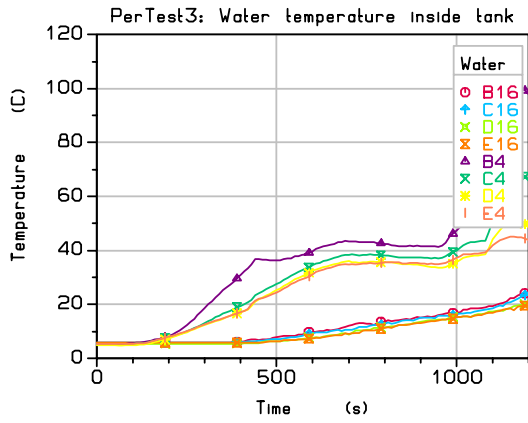






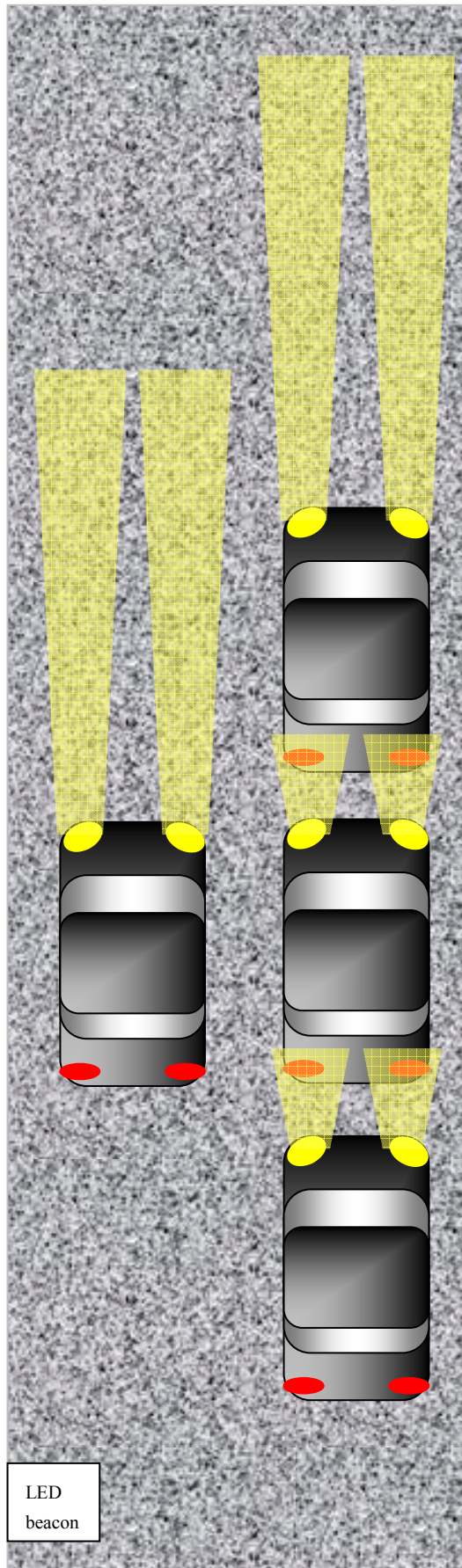








## C Indicative measurement of vision distance in “cold” test



A test to determine vision distance was carried out on 15 January 2008.

Four cars were placed in the tunnel underneath sections 2 and 3 of the water mist system, all headlights pointing in the downwind direction. The lights of all cars were switched on, and the headlamps were set at dipped beam.

The water mist system was activated during 3 minutes, and three persons dressed in waterproof clothing tried to find their way from the car in the middle around the other cars and towards the beacon on foot. They noted the visibility of the cars, of the surroundings and of the LED beacon.

In addition, a video was made from the car in the middle to obtain an impression of an incident from the driver's point of view.

No other lighting was used during this test.

The ventilation velocity was 2 m/s.

The reports from the pedestrians show that the intensity of the water mist system can be compared to a very heavy tropical downpour, and that visibility of objects that do not emit light themselves was very poor under the test-conditions. However, the headlights, rear lights and the LED beacon were visible from a distance. The table below shows the results.

Source	Visible from ... m away
Dipped headlight	29
Rear light	19
LED beacon	19

Five stills from the video taken inside the car during the test. Visibility is generally poor (at most a few metres), but the rear lights of the car in front, about 5 m away, are clearly visible.

